A POINT MODEL OF AQUIFER CLEANUP
WITH A DISTRIBUTION OF
FIRST-ORDER RATE PARAMETERS

THESIS

Jon E. Hodge, Captain, USAF

AFIT/GAP/ENP/95D-08

DEPARTMENT OF THE AIR FORCE
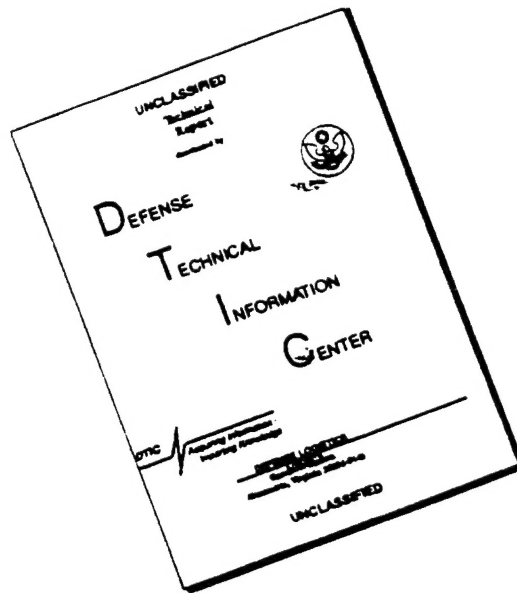**AIR UNIVERSITY**
AIR FORCE INSTITUTE OF TECHNOLOGY

Wright-Patterson Air Force Base, Ohio

DISCLAIMER NOTICE

UNCLASSIFIED
Technical
Report

DEFENSE

TECHNICAL

INFORMATION

CENTER

DTIC

UNCLASSIFIED

THIS DOCUMENT IS BEST QUALITY AVAILABLE. THE COPY FURNISHED TO DTIC CONTAINED A SIGNIFICANT NUMBER OF PAGES WHICH DO NOT REPRODUCE LEGIBLY.

A POINT MODEL OF AQUIFER CLEANUP WITH A DISTRIBUTION OF FIRST-ORDER RATE PARAMETERS

THESIS

Jon E. Hodge, Captain, USAF

AFIT/GAP/ENP/95D-08

19960402 081

Disclaimer

The views expressed in this thesis are those of the author and do not reflect the official policy or position of the Department of Defense or the U. S. Government

AFIT/GAP/ENP/95D-08

A POINT MODEL OF AQUIFER CLEANUP WITH A DISTRIBUTION OF

FIRST-ORDER RATE PARAMETERS

THESIS

Presented to the Faculty of the Graduate School of Engineering of the

Air Force Institute of Technology

Air Education and Training Command

In Partial Fulfillment of the Requirements for the Degree of

Master of Science

Jon E. Hodge

Captain, USAF

December 1995

AFIT/GAP/ENP/95D-08

A POINT MODEL OF AQUIFER CLEANUP WITH A DISTRIBUTION OF

FIRST-ORDER RATE PARAMETERS

Jon E. Hodge, B. S.

Captain, USAF

Approved:

Kirk A. Mathews   4 Dec 1995

Dr. Kirk A. Mathews, Advisor

Edward Heyse   4 DEC 95

Maj. Edward Heyse

William P. Baker   4 Dec 95

Dr. William P. Baker

Jeffrey B. Martin   4 Dec 95

Capt. Jeffrey Martin

Preface

I hope this work will prove useful to future sorption modeling and groundwater cleanup efforts. The task is indeed ominous, and understanding all of its nuances is far from my grasp. The patient instruction of Maj. Edward Heyse and much study yielded the understanding I have gained. My indebtedness in groundwater and contaminant transport topics is entirely to him. Dr. William P. Baker gave excellent tutoring early on in the area of differential and integral equations. The foundation of my limited knowledge of numerical analysis was laid by Maj. Dave L. Coulliette, but the tough task of raising me to the level of understanding in this area necessary for this work was expertly accomplished by my advisor, Dr. Kirk A. Mathews. He posed the problem, roughly formulated the model, proposed the Volterra integral equation solution approach, and suggested the trapezoidal algorithm, not to mention all the timely advice, help and direction he gave along the way. I thank my wife, Corina for enduring this time-rigorous process. I thank my daughter Kira for her many smiles, giggles and self control in not consuming this work, though her appetite for paper products is still quite strong. Lastly and most importantly, God has been very gracious to me all of my life. This was surely the case during this work. Seeing that He "...giveth to all life, and breath, and all things..." (Acts 17:25), all glory for any good that comes of this work is due Him, because I have only done that which is my duty to do towards Him (Luke 17:5-10, Colossians 3:22-25). Without the Lord Jesus Christ, we can do nothing (John 15:5). I owe Him all.

iii

Table of Contents

List of Figures

List of Tables

x

List of Symbols

A [M]	Contaminant mass stored in elementary volume
A_{im} [M]	Contaminant mass stored in immobile zone
b [L]	Mean radius of spherical aggregates
$c_1, \dots, c_4$	Constants used in defining analytic, one-parameter solution
C [M/L^3]	Generally, concentration in units of mass per volume of fluid
C_0 [M/L^3]	In-flowing contaminant aqueous concentration
C_{im} [M/L^3]	Immobile region concentration(s)
C_m [M/L^3]	Mobile region concentration
C_r [M/L^3]	Reference concentration used to non-dimensionalize
d_1	Proportion of a bimodal distribution found in the first mode
D_m [L^2/T]	An effective dispersion coefficient
EI	An exponential integral defined by Equation 4.16
$\tilde{f}$	Shape factor to convert diffusion model to first-order rate model
f	Non-dimensional distribution function
f_1, f_2	Two modes of bimodal, non-dimensional distribution

F	Proportion of equilibrium-controlled sites
F'	Proportion of sorbed solid in contact with mobile water
g	Non-normalized distribution of immobile zone water content
h	Step size for numerical methods (non-dimensional time)
H	Function used in numerical methods section
j	Function used in solution approaches section
J	Integral function of j used in solution approaches section
k [1/T]	First-order rate parameter for concentration differences
k' [1/T]	Same as k, but not including θ_{im}
$\tilde{k}$ [1/T]	Same as k, only for mass differences
$k_r, \tilde{k}_r$ [1/T]	Reference rate parameters used to non-dimensionalize
K_d [L^3/M]	Distribution coefficient for linear sorption
K_F [L^3/M]	Freundlich equilibrium sorption partition coefficient
n_{im}	Porosity of immobile region(s) [Vol. of Immobile voids/Vol. total]
n_m	Porosity of mobile region [Vol. of Mobile voids/Vol. total]
p	Non-dimensional pump rate parameter
q	Constant used in solution approach section
Q [L^3/T]	Pump rate
s	Integration dummy variable

s'	Integration dummy variable
S	Sorbed mass/total mass in soil
S_1, S_2	S for equilibrium and kinetic sorption sites respectively
S_{im}	Sorbed mass in immobile region(s)/total mass in soil
S_m	Sorbed mass in mobile region(s)/total mass in soil
t	Non-dimensional time
$\tilde{t}$ [T]	Time
V_m [L^3]	Total volume of mobile fluid
V [L^3]	Total volume of region of interest
w	Function used in solution approaches section
W	Integral function of w used in solution approaches section
x	Non-dimensional mobile region concentration
x_0	Starting mobile region concentration, $x(0)$
y	Non-dimensional immobile region concentration(s)
y_0	Starting immobile region concentration(s), $y(\lambda, 0)$
z	Function used in analytic, one rate solution and numerical methods (also unspecified spatial dimension in Model Development section)
Z	Approximate value of z in numerical method
α	Adjustable shape parameter for Gamma distribution function

β	Adjustable position parameter for Gamma distribution function
δ	Dirac delta function
γ	Three-parameter Gamma distribution adjustable minimum value
Γ	Gamma function
λ	Non-dimensional rate parameter
μ	Mean of a given distribution, also used as rate parameter
ν	$(\theta_{im})_{total}/\theta_m$ (alternately defined for chemical model)
θ	Volumetric water content [Vol. water/Vol. total]
θ_{im}	Volumetric water content of immobile region(s) [Vol. immobile water/Vol. total]
θ_m	Volumetric water content of mobile region [Vol. mobile water/Vol. total]
ρ $[M/L^3]$	Bulk solids density [Mass of solids/Vol. total]
σ	Standard deviation of a given distribution
τ	(t-s) in solution approaches section

Abstract

Many try modeling groundwater contaminant transport to predict it. Is this possible with rate-limited processes, and under what conditions? On occasion, cleanups go slower than predicted (tailing) and hazardous concentrations reappear after cleanup is thought complete (rebound). Rate-limited transport is blamed by many. When immobile water is present, diffusion from varied sizes and shapes of immobile regions can cause varied rate limitations (due to varied diffusion path lengths). Although known, most modelers represent these varied rate-limiting processes with a single "representative" rate-parameter. This can yield poor predictions for long-term experiments, and the parameter is generally time and pump-rate dependent. This model employs a distribution of first-order rate parameters to investigate the effects of using a single rate-parameter. Spatial effects are ignored by using volume-averaged concentrations (a point, well-mixed model) and dilutive pumping and rate-limited transport are modeled to isolate rate-limited transport for study. A three-parameter Gamma distribution defines the rate parameter continuum. A clean flow approximation is used extensively, and pulsed pumping is examined briefly. An effective time and pump-rate dependence is seen in the average rate. Long-term soil and contaminant transport characteristics along with uptake history or good experimentally-derived initial contaminant presence are concluded as necessary for accurate predictions.

A POINT MODEL OF AQUIFER CLEANUP WITH A DISTRIBUTION OF FIRST-ORDER RATE PARAMETERS

I. Introduction

Groundwater Crucial

To Mankind. Our groundwater is a precious commodity. It provided drinking water for 53 percent of our nation's population in 1991 (Masters, 1991:104; Claborn and Rainwater, 1991:1290) and is used extensively in crop irrigation, affecting all of our diets. Preventing and reducing the contamination of our groundwater and improving our cleanup efforts are therefore of dire importance to all of us.

To the USAF. Department of Defense (DOD) installations are responsible for a significant amount of accidental groundwater contamination, and cleaning up these sites is, therefore, the responsibility of the DOD. The US Air Force alone will spend an estimated $7-10 billion on Installation Restoration Program (IRP) cleanups from 1992-2002, and a "substantial portion of these costs will be associated with groundwater contamination remediation," (Adams and Viramontes, 1993:1-2; Vest, 1992). Seeking to improve the effectiveness and efficiency of cleanup efforts is very much an Air Force problem, and one which can be given significant attention without apology to the public at large.

Problem Statement

At present, the most common method for cleaning up a contaminated site is to sink extraction wells at various locations, pump out the contaminated groundwater until the concentration in the ground is deemed safe, treat the extracted water to remove or make safe the contaminant, and return it to the environment (Adams and Viramontes, 1993). Models are used to predict cleanup times and costs, but often they fail at this task (Travis and Doty, 1990:1465). *Pulsed pumping* is a technique being increasingly investigated as an improvement to the standard pump and treat technique. It involves turning the pumps on and off at calculated intervals to increase the average concentration being extracted from wells, thereby increasing treatment efficiency (Hartman, 1994). The pump-off period will hereafter be called the *soak* phase. Improved predictions for pump scheduling could be critical to the success of this newer technique.

Any given failure of a model to predict could have many different causes. Two behaviors that occur often and are difficult if not impossible to predict are *tailing* and *rebound* (Olsen and Kavanaugh, 1993:44). Tailing is defined as a slower than predicted decrease in the concentration of contaminated water streaming from the extraction well, especially at later time intervals. This obviously involves longer than predicted cleanup times and higher than predicted costs. Rebound is defined as contaminant concentration rising significantly from the level it was at when pumps were turned off. On occasion, cleanups have been declared complete (with well heads even removed, etc.), only to rebound years later to unexpectedly high (and hazardous) contaminant concentrations.

This is frustrating for modelers and those tasked with cleanup, but it is more importantly dangerous for groundwater consumers. The cause of these two behaviors is not known for certain, but rate-limited transport is frequently suggested (Adams and Viramontes, 1993:1-4). Present one-parameter rate-limited models do predict some of the long-term tailing and rebound, but not all of it.

Tailing and rebound both could be generalized as inaccurate predictions of concentration versus time. For this work, inaccurate is defined as causing significant schedule deviations, significant cost overruns, or the unpredicted reappearance of hazardous concentrations. The first major question is: Are accurate predictions even possible? The second is: If accurate predictions are possible, what conditions and tools will facilitate accurate predictions and are these predictions worth the effort?

There is another baffling behavior that will be investigated. Experiments to determine "representative" rate parameters have found them to be time and pump-rate dependent (Brusseau and Rao, 1989:56). This is clearly related to the inadequate modeling of tailing and rebound described earlier. What is the cause of these dependencies? Is there only a single rate-limiting process, but one which is time and pump-rate dependent? Could the presence of multiple rate-limiting processes cause this behavior?

Research Objectives and Limitations

The first major objective of this work is to investigate the predictability of rate-limited contaminant transport if a range of different rate limitations are in fact present,

represented by a distribution of rate-parameters (instead of the common, single "representative" rate-parameter). To do this, a model is built to focus purely on rate-limited transport and to compare the behavior of a one-parameter case to that of a case assuming a continuum of rate parameters, defined by a continuous distribution function. Also, comparisons will be made between the behaviors observed for various distributions, including a bimodal. Assumptions concerning every other possible process will be made in order to ensure that only rate-limited transport and simple dilution cause the observed behavior.

The second and final major objective is to investigate the solutions obtained by using a distribution of rate parameters in order to determine whether the presence of multiple rate-limiting processes is a possible explanation for difficult to predict effects such as tailing, rebound and the variability of "representative" rate parameters with time and pump rate.

Others have used a distribution of first-order rate parameters. Connaughton (et al, 1993) modeled mass transfer using a multi-site (multi-rate, distributed) model where sites were in parallel, but did not compare the resulting solution to that of a one-parameter model. Heyse (1994) modeled mass transfer in a continuously-stirred flow cell with two different distributed models, one like that of Connaughton's and another where the sites were in series. Although a one-parameter model was compared to the distributed models in his work, experiments were limited in duration. Well before both of these researchers, Villermaux (1974) modeled mass transfer in a chromatographic column using what

appeared to be a distributed model with sites in parallel, but as with Connaughton's work, his solutions were not compared to a one-parameter solution.

In summary, the effects (especially long-term effects) of using multiple rate parameters instead of one representative parameter was not clear in the literature to this author. The overall goal of this work is to investigate these effects.

Overview

First, an overview of general soil characteristics important to this work, groundwater contaminant storage and transport concepts, and modeling will be given in the *Background* section. In addition to a brief overview of concepts discussed and used in following sections, a theoretical justification for using multiple rate parameters is sought. In the *Model Development* section, governing equations for two contaminant transport models will be constructed based on stated assumptions for a mobile/immobile zone conceptualization and for a chemical conceptualization, using three different rate parameter cases:

1. The unimodal (distribution of rate parameters) case,

2. The bimodal (distribution of rate parameters) case, and

3. The one-parameter case, (i.e. the case for most present rate-limited sorption models)

with an overview and analysis of distribution function choices. In the *Solution Approaches* section, various approaches to solving the three cases are examined, including a discussion of a clean flow approximation, pump rate changes, a soaking phase, and solution uniqueness. In general, this analysis yields either a Volterra integro-differential governing equation, or a Volterra (second kind) integral governing equation.

The *Numerical Methods* section examines three different classes of numerical methods for both the Volterra integro-differential type and Volterra (Second Kind) type governing equations. Error estimation, pump rate changes, soaking and reinitialization are discussed there, along with a justification for the method of choice. In the *Applications* section, the developed tools are used to examine various solution behaviors, leading to the fulfillment of stated objectives. Finally, *Conclusions and Recommendations* are given, along with perceived areas of uncompleted, related work.

II. Background

Soil Characteristics and Groundwater Contaminant Transport Concepts

Generally, many soil characteristics can affect contaminant transport, and hence, cleanup operations. Porosity, n, is the ratio of void volume to total volume. Saturation, S, is the ratio of water volume to void volume. Volumetric water content, θ, is the product of porosity and saturation, or the ratio of water volume to total volume. Properties of soils are stated on the basis of the scale over which they are possibly variant or invariant: microscopic, macroscopic and megascopic. For example, porosity may appear invariant on the macroscopic scale (sometimes called the Darcy scale), while varying significantly on the microscopic and megascopic scales. Finally, the chemical/elemental constituents, surface properties, and distribution of solids in soil can be important.

Typically, aqueous phase contaminants are easily cleaned up by the process of *advection*. Advection is the movement of contaminant due solely to the mean flow of water (Domenico and Schwartz, 1990:358). Cleanup operations usually involve pumping groundwater out of contaminated sites at flow rates that allow uncontaminated water from surrounding regions to flow through the site and evacuate a great majority of originally present mobile water in a relatively short time (Adams and Viramontes, 1993). In laboratory work, contaminated water is typically drawn into the experimental soil section, and the concentration exiting the opposite end of the experimental section is analyzed.

2.1

Both in laboratory experiments and in field work, when concentration versus time is plotted, *breakthrough curves* (or BTC's) are said to be generated.

The term breakthrough is used both in field and lab work. This is because contaminant concentration typically stays nearly constant for a period of time. In the lab, this time period is the time required for the first contaminated effluent to arrive at sensors. In the field, this period is that required for cleaner flow from surrounding uncontaminated sites to break through the contaminated region of interest, arriving at well-heads/sensors. Once this period is over, sharp increases (in lab work) or sharp decreases (in field work) in contaminant concentration follow.

In addition to advection, *dispersion* and *diffusion* within the mobile region can effect the shape of BTC's. Diffusion involves the movement of contaminant opposite concentration gradients, and dispersion involves the spreading of contaminant due to local variations in fluid flow velocities. The effects of advection, dispersion, and diffusion, at least in the mobile region, are usually dominant in the short term as compared to rate-limited sorption. This is evident in the tailing which occurs when models do not account for rate-limited sorption: advection, dispersion and mobile region diffusion are being modeled successfully, but rate-limited sorption does not begin to dominate until the tailing appears in the longer term.

As we shall see in greater detail, a well-mixed situation as will be used, ignores dispersion and diffusion in the mobile region, and reduces advective processes to simple dilution. Because of this, the short-term regions of BTC's generated by this work's

models are not intended to be accurate and are not important to the work. It will be the longer term that will be of interest, due to rate-limited transport domination there.

The contaminants that often pose real cleanup problems are those in the solid phase (sorbed included). Solids typically do not move with natural groundwater flow or during pumping operations. They continue to supply contaminant to the mobile region to allow removal, but at much slower rates due to the following processes.

Contaminant Storage

Contaminants are introduced into groundwater in a variety of ways and on a variety of schedules. Sometimes exposures are short and highly concentrated, while other times they trickle in over long, continuous periods of low concentration exposure. Contaminants can enter the ground in various phases and change phase as they are deposited or transported. Although this work is primarily focusing upon cleanup behavior, adsorption behavior during deposition for a reversible process is clearly in view also. It is this process which ultimately determines valid initial contaminant levels for cleanup efforts. For reversible processes, conclusions about desorption behavior can be equally applied to adsorption behavior.

Sorption and Immobile Regions. In general, we will investigate two possible rate-limiting processes which could cause some of the inaccuracies in present modeling techniques. Rate-limited refers to processes which limit the possible rate at which contaminant can be removed from storage in the ground. This work is primarily concerned with contaminant storage by two basic processes: *adsorption* and diffusion into immobile regions. Adsorption is the process by which contaminant bonds to solid

2.3

soil surfaces, and *desorption* is the breaking of these bonds. Although absorption is normally included in the term, *sorption* in this work will be primarily referring to adsorption. Adsorption bonds fall into three basic categories, with some subcategorizes based upon slight variance in bond type:

1. Chemical, or chemisorption
   a. Covalent
   b. Hydrogen Bond

2. Electrostatic
   a. Ion-Ion
   b. Ion-Dipole

3. Physical
   a. Dipole-Dipole/Coulombic
   b. Keesom energy
   c. Dipole-Induced Dipole/Debye energy
   d. Instantaneous Dipole-Induced Dipole/London dispersive energy

(Weber et al, 1991:501).

The strength of a given adsorption bond as well as the conditions under which it will form or be broken is a function of contaminant type/phase, sorption site, and temperature (Treybal, 1980). I suspect that pore water velocity can effect the bonding process also. These bond types are presented as evidence of the fact that different types and strengths of adsorption bonds are indeed possible for some contaminants.

Immobile regions are defined as regions of immobile but connected water. If these immobile regions are indeed present, it is assumed that contaminant diffuses into these regions. Thus, removal of contaminant from these regions can be rate-limited due

to the diffusive process required. The existence and importance of immobile regions to many cases is well established (Brusseau and Rao, 1989).

Equilibrium Sorption. If water with a given concentration of contaminant is kept in stagnant contact with sorptive surfaces for a long enough time, an equilibrium relationship is established. That is, the amount of sorbed contaminant eventually reaches a constant value, at which time adsorption and desorption are in balance. The sorption reaction rate determines the time required for equilibrium to be sufficiently established. If sorbed mass , S, is plotted versus contaminant concentration, *sorption isotherms* are the result (constant temperature is assumed). Most isotherms can be expressed by the following:

$$S = K_F C^n \tag{2.1}$$

(Weber et al, 1991:506). This form defines a linear isotherm when $n=1$, an approximate Langmuir isotherm when n is appropriately less than one, and a Freundlich isotherm generally. If this relation holds (with a constant n and K) for both adsorption and desorption, the process is said to be *singular*. If isotherms are non-singular, or *hysteretic*, some contaminant bonds permanently to the soil, rendering desorption impossible (usually due to a chemical reaction). Finally, most isotherms are generated under *equilibrium* conditions, eliminating rate-limiting effects. Isotherms which are linear, singular, reversible, and produced under equilibrium conditions are said to be *ideal*. In this work, isotherms are assumed rate-limited, but otherwise ideal.

Non-equilibrium, Kinetic, or Rate-limited Sorption. For a given laboratory or field situation, some conditions of flow for a given contaminant and soil do not allow time for equilibration. Much laboratory and field investigation has proven many cases to be rate-limited (Brusseau and Rao, 1989:41). Now we will summarize how these processes are presently modeled, and how these models are used.

Model Construction and Usage

As was previously mentioned, models are typically built to produce accurate BTC predictions for the purpose of cleanup scheduling, budgeting, and safety considerations. Laboratory work also normally involves model construction for improved understanding of the behavior being investigated. It is not the point of this work to argue for or against the need for more accurate modeling. The possible importance of it is briefly mentioned in the introduction and in this section. If it is found necessary to build more accurate models, this work suggests one possible means of improvement. Since it is clear that many situations prohibit the assumption of equilibrium (Brusseau and Rao, 1989:41), non-equilibrium will be the primary focus of this work. But to better understand non-equilibrium, a brief overview of how some past and present modelers have assumed equilibrium is given.

Local Equilibrium Assumption (LEA). This assumption is made by many modelers in building their solute-transport equation because of its simplifying effects (Adams and Viramontes, 1993). Specifically, it involves assuming equilibrium is reached "locally," meaning in the discretized spatial regions of three dimensional transport models. Often, isotherms of the form given in Equation 2.1 are used with $n=1$ (linear).

2.6

Whenever it is valid, it greatly simplifies modeling without any noticeable accuracy losses.

> In order for the LEA to be valid, the rate of the sorption process must be fast relative to the other processes affecting solute concentration (e.g., advection, hydrodynamic dispersion) so that equilibrium may be established between the sorbent and the pore fluid (Brusseau and Rao, 1989:41).

Most if not all contaminants follow a pattern of a short, initially fast period of adsorption (due to *fast* sites which might allow local equilibrium) followed by an extended period of slow adsorption (presumably due to *slow* sites for which the LEA is invalid) (Wu, 1986:725). If the process is reversible, this pattern is duplicated during the desorption process. Fast and slow here refer to the rate of kinetic sorption relative to advection, primarily.

During laboratory experiments, when contaminant is introduced into columns or cells of soil by sending it through in the aqueous phase, resulting BTC's are either symmetric or asymmetric (Brusseau and Rao, 1989). Asymmetries are almost always caused by rate-limited sorption, the rare exception to this being when they are due exclusively to hydrodynamic dispersion (Brusseau and Rao, 1989). Rate limitations in the laboratory evidenced by asymmetric BTC's are very common, and with "tailing" and "rebound" in the field, attest to the widespread importance of rate-limiting effects to sorption modeling.

The frequent reality of rate-limited sorption means the frequent sacrifice of accuracy in sorption modeling whenever the LEA is made. This sacrifice may or may not be called for, depending upon the relative importance of sorption compared to other

processes and upon the level of accuracy required. Valocchi (1986:1699) demonstrated that with inward radial flow, there is a range outside of which the LEA is valid, due to slower fluid velocities. If a three-dimensional flow field is used in any given model, knowing where the LEA could safely be made would save unnecessary complexity and possibly computing time. If accurate sorption modeling is required, non-equilibrium, or rate-limited sorption should be the starting point and the LEA made only when and where it is carefully proven valid. Many researchers are going to great lengths to follow this very advice, several of which have already been cited.

Rate-Limited Transport. There is not just one accepted way to mathematically or conceptually deal with rate-limited sorption/transport. Non-equilibrium models can be divided into two basic categories: chemical and physical (Brusseau and Rao, 1989).

Chemical. This class of models involves the hypothesis that sorption sites themselves can be rate-limited, without assuming the presence of any rate-limiting diffusion processes occurring in immobile regions (Brusseau and Rao, 1989). Most assume two classes of sorption site: one rate-limited and the other at equilibrium (Nkedi-Kizza et al, 1984:1124). The differences between sites are attributed to different chemical/bonding interactions for one predominant soil content or sorption surface feature (say limestone) versus another (say organic material). Here, the rate-limited sites are typically represented by a single rate-parameter, $\tilde{k}$, as in the following expression for a sorbed mass balance:

$$\frac{\partial S(\tilde{t})}{\partial \tilde{t}} = \tilde{k}\left[(1-F)K_d C_m(\tilde{t}) - S(\tilde{t})\right] \qquad (2.2)$$

2.8

(Nkedi-Kizza et al, 1984:1124,1129). Here, S is the total sorbed mass for a given class of sites per total mass in soil, F is the percentage of equilibrium-controlled sites, and K_d is the distribution coefficient for linear adsorption. This rate parameter for chemical models is not derived from first principles using known physical or chemical constants (for the contaminant, soil or solvent) but purely by curve-fitting experimental data (Brusseau and Rao, 1989). Tildes are used here and in following equations for dimensional variables because most of this work will be done in non-dimensional variables. This reduces presentational complexity throughout.

Physical. With this type of model, mass transfer is hypothesized to be rate-limited due to the presence of immobile zones (Brusseau and Rao, 1989). The sorption sites in both the mobile and immobile regions are assumed to be at equilibrium, but mass transfer from immobile to mobile zones is assumed to be a diffusive process (Brusseau and Rao, 1989). This diffusive process is modeled using three basic techniques:

1. Explicitly with Fick's law (second order),

2. Explicitly using a semi-empirical first-order mass-transfer expression to approximate Fickian diffusion (semi- because this first order rate parameter has been successfully estimated from first principles using the diffusion coefficient and an assumed geometry), and

3. Implicitly with the use of an effective or lumped dispersion coefficient that includes the effects of sink/source diffusion, as well as hydrodynamic dispersion and axial diffusion

(Brusseau and Rao, 1989:46).

2.9

Although surface diffusion is possibly important, it is not investigated in this work. Instead, diffusion through the immobile zone water is focused upon. The various sizes and shapes of immobile zones are typically modeled by a single representative (mean) size and shape. This technique, at least in the time frames experimentally tested, seems to have stronger justification than the chemical model for a majority of contaminants and soils (Nkedi-Kizza et al, 1982:475).

One advantage of this conceptual approach, as previously mentioned, is that rate parameters can sometimes be reasonably estimated using a first-principles approach, starting from known contaminant and solvent diffusion properties and assumed geometries. The real advantage here is gained if laboratory experiments (especially long-term) become unnecessary. Unfortunately, the approach has proven inapplicable to some cases, and rate parameter estimates are not always accurate enough even when this conceptual approach is proven valid (Brusseau and Rao, 1989).

If immobile zones are found to be of importance for a given contaminant/soil, knowing their sizes and shapes would be helpful. Unfortunately, these sizes and shapes are quite illusive. If their sizes and shapes were exactly known, the most rigorous way to model the rate limitation would be to use a second-order, Fickian diffusion approach. The real range and distribution of mass transfer rates would be best analyzed with this approach using measured aggregate size and shape distributions. One researcher required ten aggregate size classes (all spherically shaped) for accurate modeling (Cooney et al, 1983).

The first-order technique described above was found to be the most common explicit technique used, but the general argument for the presence of many mass transfer rates based purely upon the presence of many different diffusion path lengths/geometries holds for either explicit technique. At this point it is noteworthy that the first-order chemical approach and the first-order physical diffusion approach are mathematically equivalent, while the physical meaning of variables is different (Nkedi-Kizza et al, 1984).

When sorption in the immobile region is ignored, the first-order kinetic model for physical diffusion yields the following immobile zone mass balance:

$$\theta_{im} \frac{\partial C_{im}(\tilde{t})}{\partial \tilde{t}} = k' \left[C_m(\tilde{t}) - C_{im}(\tilde{t}) \right]. \tag{2.3}$$

Once a given immobile zone geometry is assumed (spherical in this case), the effective diffusion coefficient and geometry combine to yield the following estimated first-order rate-parameter (termed the mass-transfer coefficient in the literature):

$$k' = \frac{D_m \theta_{im}}{b^2 \tilde{f}^2} \tag{2.4}$$

(Brusseau and Rao, 1989:56). Here, D is the effective diffusion coefficient, b is the mean spherical aggregate radius, and $\tilde{f}$ is the shape factor for transforming the spherical diffusion model to the kinetic model. Even though this equation is the product of a first-order kinetic model assumption, it is clear that both the diffusion coefficient and path length associated with a given geometry assumption significantly affect mass transfer rate. Large/thick aggregates cause slow diffusive transfer rates and small/thin ones cause fast diffusive transfer rates.

It is important to note here that the "representative" rate parameter is time and pump-rate dependent (Rao et al, 1980; Brusseau and Rao, 1989:56). This work will investigate this effect also. The lumped dispersion coefficient technique is not used in this work, so this completes our overview of physical (diffusion) modeling techniques.

Summary

If immobile zones are proven important or sorption sites with different kinetic reaction rates indeed exist for a given case, it immediately follows that different mass transfer rates do coexist. This work will investigate how much variation in mass transfer rates requires more than one rate parameter in the long-term modeling effort. It will also investigate the relationship that this variation has to tailing, rebound, and the time and pump rate dependence of the supposed "representative" rate parameter.

III. Model Development

<u>Goal/General Assumptions</u>

The goals of this model need to be very clear: investigate rate-limited transport, assume the presence of multiple rate-limiting processes, model these with varied mass transfer rates, and minimize complexity. Both chemical and physical diffusion models are used because these two models together include the widest range of contaminants. If this work was only applicable to a small minority of contaminants, its usefulness would be greatly diminished.

With the chemical model, rate-limited sites were assumed in parallel (rather than in series as some researchers have done: Heyse, 1994; Brusseau and Rao, 1989:43) to keep it similar to the physical diffusion model and to minimize complexity. The choice of approach with physical diffusion is more difficult.

It is doubtful that second-order diffusion effects are important to the basic premise of this work: simultaneously present rate-limiting processes causing multiple, simultaneously present mass transfer rates. In addition, second order Fickian diffusion is likely to inject significant complexity into the solution process. For these two reasons, a first-order mass transfer rate for both models was assumed.

Because one-parameter first-order models have failed to model tailing and rebound adequately in some cases, and because theory suggests the presence of multiple,

simultaneously-active rate-limiting processes for many cases, a continuum of possible rate parameters will be used.

Present Model-Building Techniques

Models that consider spatial effects typically involve using a spatial discretization (an elementary volume) which assumes soil parameters of interest are somewhat constant. This elementary volume is normally shrunk to differential size for the governing equations, becoming finite in size upon implementation of the chosen discretization scheme. All models involve doing a mass-balance on this elementary volume, setting the time rate of change of contaminant mass in the elementary volume, $\dfrac{\partial A}{\partial \tilde{t}}$, equal to the net losses and gains through the boundaries plus or minus any sources or sinks. This time rate of change of contaminant mass term is typically broken up into all the phases in which a contaminant could be stored: possibly multiple solid, liquid, aqueous and gaseous forms. For this work, there will be three storage phase possibilities: mobile aqueous phase, immobile aqueous phase, and adsorbed solid phase.

The other side of the mass balance (losses/gains through the boundaries and source/sinks) represents how mass moves between elementary volumes and whether or not mass could be effectively created or destroyed (an example of this would be if a contaminant becomes non-toxic upon undergoing a certain reaction, and we are only concerned about toxic forms). Keep in mind that this work is not about mobile region

3.2

contaminant transport, but primarilly transport of contaminant into and out of other storage regions. Sources/sinks are also excluded in this work.

After this mass balance is accomplished, it is usually restated in terms of concentration units. An example in the literature of this sort of model (without the multiple rate-parameters), which considers mobile region contaminant transport in detail is:

$$\theta_m \frac{\partial C_m}{\partial \tilde{t}} + F'\rho \frac{\partial S_m}{\partial \tilde{t}} + \theta_{im} \frac{\partial C_{im}}{\partial \tilde{t}} + (1-F')\rho \frac{\partial S_{im}}{\partial \tilde{t}} = \theta_m D_m \frac{\partial^2 C_m}{\partial z^2} - \theta_m v_m \frac{\partial C_m}{\partial z} \quad (3.1)$$

(Nkedi-Kizza et al, 1984:1123). Here, F' is the proportion of sorbed solid in contact with mobile water, D_m is the apparent diffusion coefficient, C_{im} is a volume-averaged immobile concentration, and v_m is the average mobile pore water velocity. This mass balance assumes F', θ and ρ to be constant with time (an assumption made in this work also), and θ_m and D_m to be independent of spatial position. The first two terms on the LHS represent the change in contaminant mass storage in the mobile region with time (allowing for aqueous and sorbed phases). The second two terms represent the change in contaminant mass storage in the immobile regions with time (again, allowing both aqueous and sorbed phases). The terms on the RHS represent dispersive/diffusive transport and advective transport respectively. Keep in mind that C here is a function of both time and spatial position.

Overall Assumptions

Since the main goal of this model is to single out rate-limited transport and prevent any other process from obscuring the clear observation of its effects, several unrealistic assumptions are made. First, a well-mixed cell assumption is made to eliminate all of the spatial dependencies. This means that once contaminant mass exits/enters immobile regions, desorbs from/adsorbs to a solid surface, or enters/exits the volume of interest by in-flow/out-flow of aqueous contaminant, it instantaneously mixes to cause an increase/decrease in contaminant concentration throughout the volume of interest. This assumption allows the elementary volume to encapsulate the entire region of interest, rather than just one small spatially-discretized portion of it. The mobile region is therefore represented by one volume-averaged concentration that is assumed to be only time-dependent. The immobile regions will be represented as in Equation 3.1, by volume averaged concentrations.

Second, the boundary conditions for the region of interest, having a mobile water volume of V_m, is that mobile water is being removed at a flow rate, Q, and water of a constant concentration is entering the region at the same rate. This assumption yields the following for the RHS of Equation 3.1:

$$\frac{MassFlowIn - MassFlowOut}{V} = \frac{Q}{V_m}\theta_m(C_0 - C_m), \qquad (3.2)$$

and for clean water flowing in from surrounding regions ($C_0=0$),

$$\frac{MassFlowIn - MassFlowOut}{V} = -\frac{Q}{V_m}\theta_m C_m. \qquad (3.3)$$

This will represent contaminant mass transport across the boundaries of the region of interest.

A First-Order, Physical Model

The Dimensional, One-Parameter Model. Since Equation 3.1 is a physical model, we will start with that type. The first-order rate, immobile zone mass balance is:

$$\theta_{im}\frac{\partial C_{im}}{\partial \tilde{t}} + (1 - F')\rho\frac{\partial S_{im}}{\partial \tilde{t}} = k'(C_m - C_{im}). \qquad (3.4)$$

Notice that in this form, the rate parameter, k', converts concentration difference units to units of time rate of change of contaminant mass stored in an immobile region per total volume of interest. The first assumption here is that since diffusion through immobile water is assumed to be the main rate-limiting process, there is assumed to be no sorption occurring in either mobile or immobile water (i.e. $S_m=0$ and $S_{im}=0$). This assumption is made to ensure that equilibrium type behavior is only observed due to immobile zones that could, in fact, be rate-limiting given the proper conditions.

This does minimize overall contaminant storage capacity, compared to sorptive possibilities, but it is the main rate-limiting process that we desire to focus upon. Note that after the completion of this work, it was realized that equilibrium sorption in the immobile zones effectively lowers each rate parameter, and depending on the contaminant, could slow mass transfer significantly. But, since our non-dimensionalization process will be designed to scale the model to show behaviors for any given average mass transfer rate, the initial ignorance of the effects of this assumption

3.5

should not effect any conclusions drawn from this model. It remains clear that equilibrium sorption in the mobile zone would only serve to mask rate-limiting effects.

You might recall from Equation 2.4 that k' includes θ_{im}, but for our usage we desire not to include it. This rate parameter without it will be denoted k. So, with the above stated assumptions the mass balances for immobile and mobile regions become (with dependencies shown):

$$\theta_{im} \frac{\partial C_{im}(\tilde{t})}{\partial \tilde{t}} = \theta_{im} k \left[C_m(\tilde{t}) - C_{im}(\tilde{t}) \right], \tag{3.5}$$

$$\theta_m \frac{\partial C_m(\tilde{t})}{\partial \tilde{t}} + \theta_{im} \frac{\partial C_{im}(\tilde{t})}{\partial \tilde{t}} = -\frac{Q(\tilde{t})}{V_m} \theta_m C_m(\tilde{t}). \tag{3.6}$$

This is the model that is to be used for the one-parameter case.

The Continuum of Rate Parameters/Immobile Zones. The first assumption for the case of a continuum of rate parameters is that the rate parameter, k, defines the class of immobile zone being described as well as θ_{im}. This means that water content is constant for all immobile zones with a given rate parameter. This is not overly restrictive in that the volume of immobile water is very likely to have some relation to the diffusion pathlength, assuming the same geometry is being compared.

The second assumption involves the definition of the distribution. If the overall mass balance for all immobile zones was to be written as a summation, it would be:

$$\frac{\partial A_{im}}{\partial \tilde{t}} = \sum_{i=0}^{\infty} (\theta_{im})_i \frac{\partial (C_{im})_i(\tilde{t})}{\partial \tilde{t}},$$

$$\sum_{i=0}^{\infty} (\theta_{im})_i = (\theta_{im})_{total} \quad . \tag{3.7}$$

3.6

Converting this to an integral yields:

$$\frac{\partial A_{im}}{\partial \tilde{t}} = \int_0^\infty g(k)\frac{\partial C_{im}(k,\tilde{t})}{\partial \tilde{t}}dk,$$

$$\int_0^\infty g(k)dk = (\theta_{im})_{total}.$$

(3.8)

Note that g here has units of θ per unit k. The bounds of integration here are the bounds of k, such that if upper and lower limits of k were to be set differently, so would these bounds. So to summarize, the overall mass balances for the distribution of rate parameters (unimodal) case become (with dependencies shown):

$$\theta_{im}(k)\frac{\partial C_{im}(k,\tilde{t})}{\partial \tilde{t}} = \theta_{im}(k)k\left[\left(C_m(\tilde{t}) - C_{im}(k,\tilde{t})\right)\right],$$

(3.9)

$$\theta_m\frac{\partial C_m(\tilde{t})}{\partial \tilde{t}} + \int_0^\infty g(k)\frac{\partial C_{im}(k,\tilde{t})}{\partial \tilde{t}}dk = -\frac{Q(\tilde{t})}{V_m}\theta_m C_m(\tilde{t}).$$

(3.10)

<u>Non-Dimensionalization.</u>   The following seven relations were used to non-dimensionalize the model:

$$x(t(\tilde{t})) = \frac{C_m(\tilde{t})}{C_r}, \qquad\qquad y(\lambda(k),t(\tilde{t})) = \frac{C_{im}(k,\tilde{t})}{C_r},$$

$$t(\tilde{t}) = k_r\tilde{t}, \qquad\qquad \lambda(k) = \frac{k}{k_r},$$

$$f(\lambda(k)) = \frac{1}{(\theta_{im})_{total}}g(k)\left|\frac{dk}{d\lambda}\right|, \qquad p(t(\tilde{t})) = \frac{Q(\tilde{t})}{V_m k_r},$$

$$v = \frac{(\theta_{im})_{total}}{\theta_m}.$$

(3.11)

3.7

Note that during this process, the non-dimensional distribution is now normalized

(i.e. $\int_0^\infty f(\lambda)d\lambda = 1$). The subscript, r, denotes a constant reference value for the given

variable. These reference values, when used to non-dimensionalize this linear set of

equations, accomplish a very useful purpose, as the following example demonstrates. If

x, y and λ are assumed equal to one, solutions can be explored for various values of p and

v (minimal set of independent parameters), and then reference concentrations and rate

constants can be chosen to scale all experiments to a given contaminant and set of initial

conditions. The appropriate variable substitutions and chain-rule derivatives result in the

following set of governing equations:

$$\dot{y}(\lambda,t) = \lambda\big[x(t) - y(\lambda,t)\big] \quad, \tag{3.12}$$

$$\dot{x}(t) = -p(t)x(t) - v\int_0^\infty f(\lambda)\dot{y}(\lambda,t)d\lambda \quad. \tag{3.13}$$

Dots above variables here represent the first derivative with respect to non-dimensional

time. These are the two governing equations on which this work is based. The identical

non-dimensionalization for the one-parameter case yields:

$$\dot{y}(t) = \mu\big[x(t) - y(t)\big], \tag{3.14}$$

$$\dot{x}(t) = -p(t)x(t) - v\,\dot{y}(t), \tag{3.15}$$

where μ here is used for λ because in our comparisons, the mean of the distribution of λ's

($f(\lambda)$) will be used for this case. This one-parameter case will be used not only to

illustrate the effects of the one-parameter assumption, but also as a benchmark problem

for testing numerical methods. It has an analytic solution and can be solved by the same

numerical techniques to be used for the distribution of rate-parameter cases which do not have analytic solutions.

A Chemical Model

Dimensional Form. A chemical model will now be built with very similar assumptions. From the same work as Equation 3.1, typical starting mobile water and sorbed mass balances for this model are:

$$\theta_m \frac{\partial C_m}{\partial \tilde{t}} + \rho \frac{\partial S_1}{\partial \tilde{t}} + \rho \frac{\partial S_2}{\partial \tilde{t}} = D_m \theta_m \frac{\partial^2 C_m}{\partial z^2} - v_m \theta_m \frac{\partial C_m}{\partial z}, \tag{3.16}$$

$$S_1 = FK_d C_m \text{ (equilibrium sites),} \tag{3.17}$$

$$\frac{\partial S_1}{\partial \tilde{t}} = FK_d \frac{\partial C_m}{\partial \tilde{t}}, \tag{3.18}$$

$$S_2 = (1 - F)K_d C_m \text{ (kinetic sites if equilibrated),} \tag{3.19}$$

$$\frac{\partial S_2}{\partial \tilde{t}} = \tilde{k}\left[(1 - F)K_d C_m - S_2\right] \text{(kinetic site first order rate law)} \tag{3.20}$$

(Nkedi-Kizza et al, 1984:1124). Here, S_1 is sorbed contaminant mass per total mass of solids in the volume of interest on sites that instantaneously equilibrate and S_2 is sorbed contaminant mass per total mass of solids in the volume of interest on kinetic sites. The fraction of instantaneously equilibrating sites is F. Notice that the first-order rate parameter here has different units than previously, and hence its symbol is different.

The same assumptions are made as previously about the RHS of Equation 3.16: a well-mixed cell, volume-averaged concentrations, a total pumping rate, Q, and clean

water flowing in. With these assumptions, and upon substituting Equation 3.18 into 3.16, the aqueous phase mass balance can now be written:

$$\left(\theta_m + \rho F K_d\right)\frac{\partial C_m}{\partial \tilde{t}} + \rho\frac{\partial S_2}{\partial \tilde{t}} = -\frac{Q}{V_m}\theta_m C_m. \qquad (3.21)$$

Non-Dimensional Form. With the following non-dimensional transformations and new definitions of v and p,

$$
\begin{aligned}
x(t) &= \frac{C_m\left(\tilde{t}(t)\right)}{C_r}, & y(t) &= \frac{S_2\left(\tilde{t}(t)\right)}{(1-F)K_d C_r}, \\
\lambda(\tilde{k}) &= \frac{\tilde{k}}{\tilde{k}_r}, & t(\tilde{t}) &= \tilde{t}\,\tilde{k}_r, & (3.22)\\
v &= \frac{\rho(1-F)K_d}{\theta_m + \rho F K_d}, & p(t) &= \frac{Q\left(\tilde{t}(t)\right)\theta_m}{V_m\tilde{k}_r\left(\theta_m + \rho F K_d\right)},
\end{aligned}
$$

Equations 3.14 and 3.15 are the result. This demonstrates for the one-parameter model, that a certain set of assumptions can be made to make a chemical model mathematically equivalent to a physical first-order rate model in their non-dimensional forms. Coefficients and variables have different meanings, but ultimately the actual behavior being modeled can be equivalently done with either conceptualization.

A Continuum of Rate Parameters. A slightly different distribution function definition is required for the chemical model. The simplest way to incorporate this continuum of rate parameters is to do so in the non-dimensional form. If $f(\lambda)$ is now defined as the portion of the total non-dimensional sorption rate ($(\dot{y})_{total}$) at kinetic sites with non-dimensional rate-parameter between λ and $\lambda+d\lambda$ per unit λ, Equations 3.12 and 3.13 are the result. So, we find at least for this given set of assumptions that these two

3.10

approaches, first-order chemical and physical, with an assumed continuum of mass transfer rates are mathematically equivalent in their non-dimensional forms. This demonstrates that this model is widely applicable because it accomodates the possibility of multiple mass-transfer rates for either the chemical or physical conceptualization.

Distribution Choices

Reality. Although theory and experimentation strongly suggest the simultaneous presence of multiple, rate-limiting processes, a "representative" rate parameter for each of these processes is evasive. If a continuum of rate-limitations is, in fact, present, the distribution is unknown for any contaminant for which it is applicable. No one has successfully measured the shape of a given contaminant's rate-parameter distribution (as far as this author knows), although Heyse (1995) is presently working on this.

The diffusion-based physical model suggests the usage of a distribution somehow related to the distribution of immobile zones and their associated diffusion lengths. Lognormal distributions are a good experimental approximation to the sizes of aggregates in many cases (Gilbert, 1987:152). It is therefore likely that the lognormal distribution is somehow linked to the actual distribution of mass-transfer rates for cases where diffusion in and out of aggregates filled with immobile water is a rate-limiting process of importance.

For the chemical model, multiple discrete mass transfer rates makes better theoretical sense than a continuum. In spite of this, conclusions associated with an unknown continuous distribution should be equally applicable to an unknown discrete

distribution. Also, most if not all conclusions associated with using a single parameter to represent multiple mass transfer rates can be based on the behavior of models that use either a discrete or a continuous distribution of rates.

Practicality. One general quality of the distribution function to be chosen determines its practicality for this usage: integrability in closed form of various moments of it. The Gamma distribution was found very practical, because all desired integrals were found analytically, and in closed-form in most every case.

Flexibility. One additional criterion for this choice was that the distribution's shape, including its mean, standard deviation, and minimum values, be flexible in enabling desired variations. The three-parameter Gamma distribution has the desired flexibility and closed-form integrability. It also can approximate the lognormal distribution with the appropriate choice of parameters. Figure 3.1 illustrates the distributions mentioned.

The Gamma Distribution (Three-parameter). This distribution is of the form:

$$f(\lambda) = \begin{cases} \dfrac{1}{\beta\Gamma(\alpha)}\left(\dfrac{\lambda-\gamma}{\beta}\right)^{\alpha-1}\exp\left[\dfrac{-(\lambda-\gamma)}{\beta}\right] & (\lambda > \gamma) \\ 0 & (\lambda < \gamma) \end{cases}, \qquad (3.23)$$

where $-\infty < \gamma < \infty,\quad \alpha > 0,\quad \beta > 0,$ and

$$\Gamma(\alpha) = \int_0^\infty \varphi^{\alpha-1} e^{-\varphi}\, d\varphi \quad \text{(Gamma function, normalization constant). (3.24)}$$

Sometimes β here is defined differently (as the inverse of this parameter: compare Connaughton, 1993:2399 to Gilbert,1987:157). This distribution's mean is $\mu=\alpha\beta+\gamma$, and

3.12
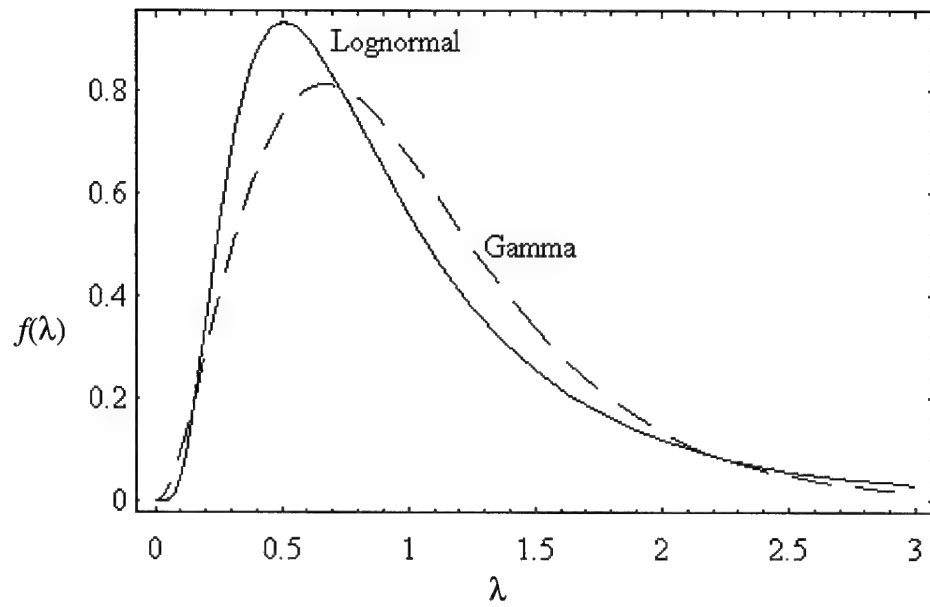
Figure 3.1 Lognormal and Gamma Distributions,
Each $\mu=1$ and $\sigma=(3)^{-\frac{1}{2}}$.
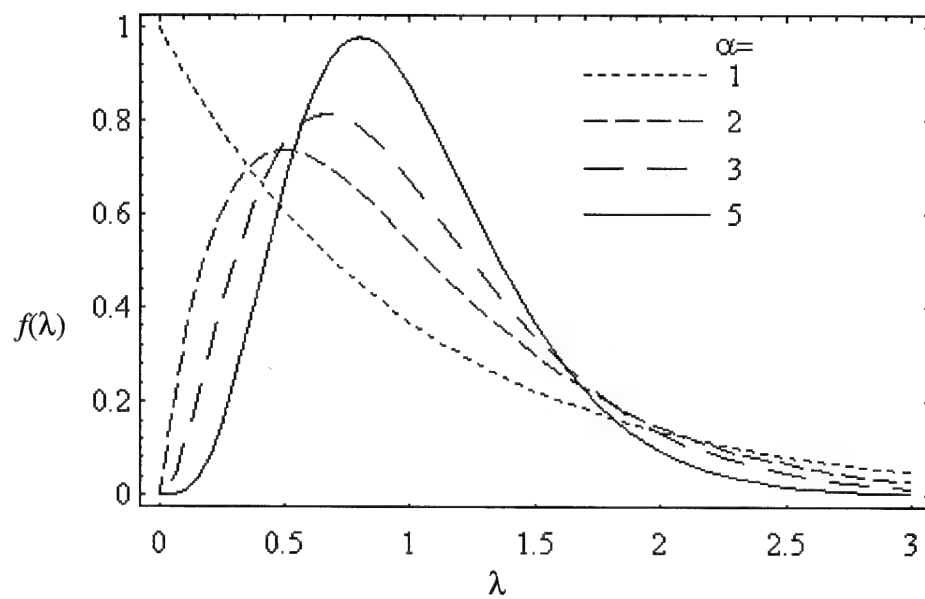
Figure 3.2 Various Possible Shapes of the Gamma Distribution.

3.13

its standard deviation is $\sigma=\beta\sqrt{\alpha}$. Its widely variable shapes are seen in Figure 3.2,

where the mean of each distribution is $\mu=1$.

A Bimodal Distribution Allowed. This case only involves a slight modification to

the variables found in the governing equations. A new variable is needed to specify the

percentage of the total found in each distribution, d_1:

$$f(\lambda) = d_1 f_1(\lambda) + (1-d_1) f_2(\lambda). \qquad (3.25)$$

Here, f_1 and f_2 are Gamma distributions combined in a weighted fashion (according to d_1,

with $0<d_1<1$) to obtain a normalized bimodal distribution. This change retains the same

governing equations and distribution integrability while increasing distribution flexibility.

IV. Solution Approaches

Note that throughout the rest of this work, although the chemical model yielded the same non-dimensional equations, all terms and discussion will favor the mobile/immobile zone conceptualization. The correlation between these two types of models would be useful for all discussions presented here, but time prevented the inclusion of this.

The first step to a solution is to pick a solution approach. An approach that makes sense and is necessary to get to various final forms is to solve the immobile zone governing equation with an integrating factor. The unimodal case will be handled first.

Integrating Factor for Immobile Zones

This technique is summarized with the following four steps:

$$\dot{y}(\lambda,t) = \lambda\big[x(t) - y(\lambda,t)\big],$$

$$\frac{\partial y(\lambda,t)}{\partial t} + y(\lambda,t)\lambda = x(t)\lambda,$$

$$\frac{\partial}{\partial t}\big[y(\lambda,t)e^{\lambda t}\big] = x(t)\lambda e^{\lambda t}, \tag{4.1}$$

$$y(\lambda,t)e^{\lambda t} - y(\lambda,0) = \int_0^t x(s)\lambda e^{\lambda s}ds,$$

$$y(\lambda,t) = y(\lambda,0)e^{-\lambda t} + \int_0^t x(s)\lambda e^{-\lambda(t-s)}ds. \tag{4.2}$$

First, Equation 3.12 is substituted into Equation 3.13, then the above solution will be inserted to yield the following integro-differential equation:

4.1

$$\dot{x}(t) = -p(t)x(t) - \nu \int_0^\infty f(\lambda)\lambda \left[x(t) - y(\lambda,0)e^{-\lambda t} - \int_0^t x(s)\lambda\, e^{-\lambda[t-s]}ds \right] d\lambda \quad .(4.3)$$

If the order of integration is switched, and we define the following terms:

$$\begin{aligned}
\mu &= \int_0^\infty f(\lambda)\lambda d\lambda, \\
q(t) &= p(t) + \nu\mu, \\
w(t) &= \nu \int_0^\infty f(\lambda)\lambda y(\lambda,0)e^{-\lambda t}\, d\lambda, \\
j(t-s) &= \nu \int_0^\infty f(\lambda)\lambda^2 e^{-\lambda[t-s]}d\lambda,
\end{aligned} \qquad (4.4)$$

our integro-differential equation becomes:

$$\dot{x}(t) = -q(t)x(t) + w(t) + \int_0^t x(s)j(t-s)ds. \qquad (4.5)$$

With the three-parameter Gamma distribution defined earlier, and an initial condition of $y(\lambda,0)=y_0$ the integrals become:

$$\begin{aligned}
\mu &= \int_0^\infty f(\lambda)\lambda d\lambda = \alpha\beta + \gamma, \\
w(t) &= \nu \int_0^\infty f(\lambda)\lambda y_0\, e^{-\lambda t}\, d\lambda = \nu\, y_0 \frac{(\mu + \beta\gamma t)e^{-\gamma t}}{(1+\beta t)^{\alpha+1}}, \\
j(\tau) &= \nu \int_0^\infty f(\lambda)\lambda^2 e^{-\lambda\tau}\, d\lambda, \\
&= \frac{\nu\left[\mu^2 + \alpha\beta^2(1+2\gamma\tau) + \gamma^2\tau^2\left(2\beta + \beta^2\right)\right]e^{-\gamma\tau}}{\left[1+\beta\tau\right]^{\alpha+2}}.
\end{aligned} \qquad (4.6)$$

Recall that the distribution is defined to be zero for $0 < \lambda < \gamma$. Mathematica was used to

obtain these closed-form integrals, using the change of variable: $z=\lambda-\gamma$ (see Appendix A).

The bimodal case requires several different variable definitions:

$$\mu_1 = \int_0^\infty f_1(\lambda)\lambda d\lambda,$$

$$\mu_2 = \int_0^\infty f_2(\lambda)\lambda d\lambda,$$

$$\mu = d_1\mu_1 + (1-d_1)\mu_2,$$

$$w_1(t) = v\int_0^\infty f_1(\lambda)\lambda y(\lambda,0)e^{-\lambda t}d\lambda,$$

$$w_2(t) = v\int_0^\infty f_2(\lambda)\lambda y(\lambda,0)e^{-\lambda t}d\lambda, \qquad (4.7)$$

$$w(t) = d_1 w_1(t) + (1-d_1)w_2(t),$$

$$j_1(\tau) = v\int_0^\infty f_1(\lambda)\lambda^2 e^{-\lambda\tau}d\lambda,$$

$$j_2(\tau) = v\int_0^\infty f_2(\lambda)\lambda^2 e^{-\lambda\tau}d\lambda,$$

$$j(\tau) = d_1 j_1(\tau) + (1-d_1)j_2(\tau).$$

Other than these definitions, the bimodal case is equivalent to the unimodal case.

Integrating Factor for Mobile Zone

Generally, the integrating factor is:

$$IntegratingFactor = e^{\int q(t)dt}, \qquad (4.8)$$

but if q is assumed constant with time, the integrating factor, with the definition of W is:

$$IntegratingFactor = e^{qt},$$

$$W(t) = \int_0^t w(s)e^{qs}ds. \qquad (4.9)$$

This integrating factor yields:

$$x(t) = e^{-qt}\{x(0) + W(t)\} + \int_0^t\left[e^{-q(t-s)}\int_0^s x(s')j(s-s')ds'\right]ds. \qquad (4.10)$$

Reversing the order of integration and defining new terms yields:

$$\tau' = t - s,$$
$$\tau = t - s', \tag{4.11}$$
$$J(\tau) = \int_0^\tau j(\tau - \tau')e^{-q\tau'}d\tau',$$

$$x(t) = e^{-qt}\{x(0) + W(t)\} + \int_0^t x(s')J(t - s')ds'. \tag{4.12}$$

This form could easily be altered to match the general form of a linear Volterra integral equation of the second kind, and it also includes a difference kernel. The importance of this is discussed in the solution uniqueness section. Allowing p to change with time makes calculating both proper forms of W and J a numerical endeavor instead of closed-form integrals.

Analytic Solution for One-Parameter Model

The one-parameter case, Equations 3.14 and 3.15, has an analytic solution given by (see Appendix B for the details):

$$z = \sqrt{(\mu - p)^2 + \mu\nu(2\mu + 2p + \mu\nu)},$$
$$c_1 = \frac{1}{2z}\left[x_0(-\mu + p + \mu\nu + z) - 2y_0\mu\nu\right],$$
$$c_2 = \frac{1}{2z}\left[x_0(\mu - p - \mu\nu + z) + 2y_0\mu\nu\right],$$
$$c_3 = \frac{1}{2z}\left[y_0(\mu - p - \mu\nu + z) - 2x_0\mu\right], \tag{4.13}$$
$$c_4 = \frac{1}{2z}\left[y_0(-\mu + p + \mu\nu + z) + 2x_0\mu\right],$$
$$x(t) = c_1\exp\left[\frac{-(\mu + p + \mu\nu + z)t}{2}\right] + c_2\exp\left[\frac{-(\mu + p + \mu\nu - z)t}{2}\right],$$
$$y(t) = c_3\exp\left[\frac{-(\mu + p + \mu\nu + z)t}{2}\right] + c_4\exp\left[\frac{-(\mu + p + \mu\nu - z)t}{2}\right],$$

where μ is defined in Equation 4.4. It must be remembered at this time that if μ is a function of time, (as some researchers claim: Brusseau and Rao, 1989:56; Rao et al,1980a; Cussler, 1984), this approach would have to be modified by changing the integrating factor to:

$$IntegratingFactor = e^{\int \mu(t')dt'} . \tag{4.14}$$

Initial conditions must be reset anytime p is to be changed to a new constant value. This solution was computed in the main code (Appendix G), and is algebraically arranged this way to minimize calculations within an iterative loop. The constants and even the coefficient of t in each exponential could be calculated outside the loop, and would only have to be recalculated at pump changing times.

Clean Flow Approximation

Another solution approach chosen assumed the pump rate was high enough to ensure that $x \ll y$ for at least some amount of time. This physically means that clean water is assumed to be passing all immobile zones to determine mass-transfer rates (the best possible mass transfer rate from immobile zones). Under these assumptions, the governing equations and corresponding solutions are (assuming constant pump rate):

$$\dot{y}(\lambda,t) \approx -\lambda y(\lambda,t),$$
$$\dot{x}(t) \approx -px(t) - v\int_0^\infty f(\lambda)\{-\lambda y(\lambda,t)\}d\lambda, \tag{4.15}$$
$$y(\lambda,t) \approx y(\lambda,0)e^{-\lambda t},$$

$$x(t) \approx e^{-pt}\left[x(0) + \int_0^t w(s)e^{ps}ds\right]. \tag{4.16}$$

Here, w is the function defined earlier in Equation 4.4. Equation 3.23 defines α to be positive, and if it is an integer, this integral can be evaluated by recursive integration by parts, using the relation:

$$\int \frac{e^{ax}}{x^m} dx = \frac{-1}{m-1} \frac{e^{ax}}{x^{m-1}} + \frac{a}{m-1} \int \frac{e^{ax}}{x^{m-1}} dx,$$ (4.17)

until the final integral is of the form:

$$EI(z) = \int_{-z}^{\infty} \frac{e^{-s}}{s} ds.$$ (4.18)

Mathematica was unable to accomplish this process, so it was completed by hand and a Mathematica module was written to accomplish it (using the built-in ExpIntegralEi[z], see Appendix C for the details on this module and the function defining the clean flow approximation). Non-integer values for α are assumed to yield a final integral that requires numerical approximation (just as EI does, though a built-in Mathematica function would be unavailable).

Pump Rate Changes/Soaking

Here, problems associated with pump rate changes and soaking, specific to solution approaches will be discussed. Problems specific to numerical methods will be discussed in the Numerical Methods section.

The General Integrating Factor for the Mobile Region. The soaking phase is a definite requirement in this work to show rebound differences between different models, and it had to immediately follow a given period of pumping (requiring a mid-experiment change in pump rate). It was also a requirement to demonstrate pulsed pumping

4.6

concepts. As was mentioned previously in this section, any solution utilizing an integrating factor for the mobile region, (solution approaches yielding the Volterra integral equation and limiting pump-rate solution) assumed a constant pump rate. Clearly, a soaking phase is incompatible with the clean flow approximation. (A pump rate of zero is clearly below the threshold value for a valid clean flow approximation!)

It was briefly pointed out that a different integrating factor than was used would be required if pump rate was a function of time. If this general form for the integrating factor (Equation 4.8) was used to accommodate pump-rate changes, closed-form integrations would be impossible for these solution approaches, leaving only numerical options for these integrations. Avoiding numerical approximations enhances accuracy and usually reduces computation cost. Therefore, close-form integrations are sought when possible.

The One-Parameter Analytic Solution. This solution also assumed a constant pump rate, so pump rate changes had to be dealt with as initial conditions. The solution was valid until the pump change time, then the pumps were assumed to change instantaneously. The x and y values at pump change time were then used as initial conditions to a new solution, with a new "constant" pump rate. This process of starting with new initial conditions is termed *reinitialization*. There are problems associated with this process for numerical methods, to be discussed in that section.

Solution Uniqueness

To investigate solution uniqueness, the solution approach involving an integrating factor for the mobile region will be examined. This approach led to equations 4.12 and 4.16, which are easily manipulated into the general form of a linear Volterra integral equation (second kind). In Yosida's notation (1991:145), the general form is:

$$f(s) = \varphi(s) - \lambda \int_a^s K(s,t)\varphi(t)dt, \qquad (4.19)$$

where λ is a constant and not the rate parameter, f is a known function, and φ is the function to be found. Yosida and others have proven that this general form has "essentially only one solution" and that solution, when examined based upon a series of iterated kernels is "almost uniformly convergent." (Tricomi, 1985:10-15; Yosida, 1991:145-147; Linz, 1985:29-35) The fact that ours also includes a difference kernel also contributes to uniqueness. Essentially, this form gives a great deal of assurance to the existence of a unique, bounded, non-zero solution. This assurance is applicable to any forms preceding it (i.e. other approaches to the same system of differential equations).

V. Numerical Methods

Integro-Differential Equation

The first numerical method attempted was applied to the Volterra integro-differential equation, Equation 4.5. A short experiment was conducted with forward and backward Euler methods in order to facilitate the construction of a trapezoid integration method. The program built using this method became the workhorse for much of the analysis.

Trapezoid Method. This implicit method is best summarized by the following sequence, which transforms the integro-differential equation into simply an integral equation (not using the integrating factor):

$$q = p + \nu\mu,$$
$$z(t) = \int_0^t x(s)K(s,t)ds,$$
$$H\{t,x(t),z(t)\} = -qx(t) + w(t) + z(t),$$
$$\dot{x}(t) = H\{t,x(t),z(t)\}.$$

(5.1)

First, h will be defined as a non-dimensional time step, and Z and X will be defined as approximations of z and x. After integrating over one time step, t_{n-1} to t_n, we obtain:

$$x(t_n) = x(t_{n-1}) + \int_{t_{n-1}}^{t_n} H\{s,x(s),z(s)\}ds.$$

(5.2)

With initial conditions of $Z_0=0$ and $X_0=x_0$, both z and the integral in Equation 5.2 may be replaced by a trapezoid approximation:

$$Z_n = \frac{h}{2} x(t_0) K(t_0, t_n) + h \sum_{i=1}^{n-1} x(t_i) K(t_i, t_n) + \frac{h}{2} x(t_n) K(t_n, t_n),$$

$$X_n = X_{n-1} + \frac{h}{2} \left\{ H(t_{n-1}, X_{n-1}, Z_{n-1}) + H(t_n, X_n, Z_n) \right\} \tag{5.3}$$

$$n = 1, 2, \ldots,$$

(Linz, 1985:178). This is easily seen to be two equations in two unknowns, (Z_n and X_n) with an implicit, algebraic solution. Although this technique has third-order local truncation error on one step, Z's composite format yields a second-order global truncation error (Isaacson and Keller, 1994:316; Burden and Faires, 1985:164). This was proven for the one-parameter case: error was proportional to h^2 (see Appendix D for details of this). It was demonstrated for the unimodal case using uncertainty estimation in the same appendix.

Multistep Methods. Multistep methods follow the previous general procedure, but use higher order, interpolatory integration schemes to approximate both integrals (Linz, 1985:178). Multiple starting values are required for these methods, and numerical instability is possible (Linz, 1985:178). Though this technique was attempted using starting values for both the one-parameter and one-distribution cases from the analytic one-parameter case solution, no working code was finished.

Block-By-Block Methods. This technique involves initially the same procedure as multistep methods, including the usage of higher order integration schemes. However, it uses intermediate points (between nh and $(n+1)h$) and some form of interpolation to generate multiple equations and multiple unknowns. These unknowns are typically found in a block of several by solving the equations simultaneously, hence the name.

An example of this method would be to use Simpson's rule and quadratic interpolation to generate two equations in two unknowns. Linz (1985:186) claimed that this was easily proven to be a fourth-order technique. Fourth order accuracy was obtained with an easy test case having only one integration involved, but the interpolation scheme inserted no error due to the solution being a constant: $f(x)=1$ (Linz, 1985:118-120). Although the integration scheme is locally fifth-order, and globally fourth in its composite format, the quadratic interpolation is only third-order (see Appendix E for this proof). I claim that the technique is globally second-order due to the usage of the quadratic interpolation formula twice on each step. This was demonstrated with a simple test case, and not the actual model (see Appendix F). A higher order method could no doubt be designed, but the accuracy was not necessary. Because the efforts involving quadratic interpolation only gave promise of second-order accuracy, the same order available already in the previously coded trapezoid scheme, these efforts were abandoned before ever achieving higher order accuracy with a more involved scheme.

Pump Rate Changes/Soaking/Reinitialization. In solving the integro-differential equation, the only reinitialization required was with the analytic solution of the one-parameter case. The accuracy of this process was quite important as it was being compared to the same case being solved numerically to closely monitor error growth. For output purposes only, $y(\lambda,t)$ was found at discrete λ's. This gave important information about the soak phase redistribution of contaminant.

Volterra Integral Equation (Second Kind)

This approach has promise of better accuracy for a given step-size because it appears to involve the numeric approximation of only one integral instead of two. Although the integrals associated with it (when the Gamma distribution is used) are a bit more cumbersome, computationally, and involve approximation of exponential integrals, the method, without other complications, could still be expected to yield better accuracy per step. This method is made much more tractable by choosing α (Gamma distribution shape factor) to be an integer, but this is of minimal consequence; non-integer values were not really necessary for this work.

The main disadvantages of this method, associated mostly with pump changes, have been alluded to in the previous section. It was previously pointed out that any method using the general form of integrating factor for the mobile zone (Equation 4.8) required the numerical evaluation of all integrations otherwise feasible in closed-form. This is only one possible solution to pump changes for this method. Another way to accommodate pump changes is to reinitialize each time the pump is to be changed, as was discussed for the one-parameter case. Unfortunately, this too forces numerical evaluation of otherwise closed-form integrations, unless an integrable (closed-form) interpolating function could be found for $y(\lambda,0)$ at each reinitialization. I claim that these problems associated with pump changes would minimize accuracy benefits of this method. In fact, total error could be worse, because more actual integral approximations would be required than for the integro-differential equation, after a pump change.

Because the general approach to integral equations is nearly identical to integro-differential equations, the applicable numerical methods fall into the same categories: trapezoid, multistep, and block-by-block methods. Although none of these methods were ultimately applied to the Volterra equation, some of the complexity was faced in obtaining the clean flow approximation. The same integral was accomplished there.

Justification for Choice of Method

As was previously mentioned, pump rate changes had to be dealt with carefully. Any method attempted was faced with a jump discontinuity. The trapezoid method as applied to the integro-differential equation maintained stability as long as the pump rate was constant on a given step. This involved the assumption that the rate change was instantaneous at the end of a step such that the old value for the next step was just the previous value, but the pump rates (old and new values for the new step) were now at the new value. This was clearly the easiest method to deal with pump rate changes.

Because soaking after a pumping phase involved a pump rate change (from non-zero to zero), soaking was clearly easier with the aforementioned trapezoid method. The clean flow approximation was clearly invalid for a soaking phase, because a pump rate of less than 10 was found to invalidate it, and pump rate was assumed constant for it (as previously mentioned). It was therefore useless for pulsed pumping also. Although dealing with the Volterra held initial promise of better accuracy per step, the complexity was a hindrance. Ultimately, due to time constraints and previously stated reasons, the trapezoid method was applied to the integro-differential equation as the overall method of

choice. However, much was learned and demonstrated with the clean flow approximation. If accuracy ever became more critically important, a higher order method would probably be applied to the integro-differential equation. In that case, solving the complications associated with pump rate changes would be challenging.

Error Estimation

There are two approaches typically used to estimate or bound error values, and a third was devised for this work. The first is the rigorous theoretical approach which delves into the heart of numerical method design and carries every possible source of error to the final result. Such an approach is intractable for our system. The second is simply to compute the same sequence of values using a sufficiently smaller step size, and observe the change in the solution. This makes sense because it is a very safe assumption that the error for the first computation is going to be orders of magnitude larger than the second. This is what defines a sufficiently smaller step size. This equates to the assumption that the difference between the two computations very well approximates the true error of the first computation. This method was applied in this work.

It was also noted in the model development section that the one-parameter case, although it had an analytic solution, could be solved numerically by the same methods applied to the one-distribution and bimodal cases. As a third approach, I hypothesize that the exact error in the one-parameter case, which can be easily calculated, is a good benchmark test of error growth for two basic reasons. First, round-off errors and integral approximation errors are very nearly identical in theory, since all the cases when solved

5.6

numerically involve the same numerical method with only minor differences in their defining functions. Second, at least for the earlier time frames, all cases yield very similar numerical results.

Even though this technique involved nearly doubling the numerical computations, it fit very efficiently into the algorithm and proved a very useful addition to the program. Throughout the applications section, error estimates will be referenced as originating with this technique or the second mentioned above. The second method mentioned (using a significantly reduced step-size to estimate uncertainty) is probably better at absolute error estimation than the third (assuming error in one-parameter case approximates error in distributed cases), so it will be used as much as possible.

Uncertainty of Numerical Solutions Displayed

All numerical solutions displayed have a standard criterion applied to them concerning uncertainty. Unless otherwise noted, step size was chosen to render estimated uncertainty negligible (five orders of magnitude smaller than the solution itself in most cases). This estimate was obtained by the numerical solution of the one-parameter case, for which exact error was calculated. Typically, $h=0.01$ was sufficient to accomplish this uncertainty order of magnitude goal, so deviations from this step size will be noted. On several occasions, this estimate of uncertainty was tested with the smaller step size run to estimate the decimal place of change (hence the estimated decimal place of uncertainty, as previously discussed also).

Usage of x_0, y_0, Distributions, and Distribution Mean, μ

In this work, x_0, y_0, and μ were kept at unity for solution purposes. Reference values may be chosen in order to scale the solutions to a wide range of dimensional, field and laboratory scenarios. Also, x and y represent fractions of the reference concentration. The solutions investigated assume equilibrium has been established between x and y before the simulations begin (they are equal at unity). The model could have easily been used to investigate soaking adsorption (or storage in immobile regions) by starting y at zero, or to investigate time required during soaking for equilibrium to be established by

starting x at zero and y at unity. No contaminated fluid was allowed to enter the region of interest from surrounding regions, but retaining this possibility in this model is quite simple.

Since λ was defined during non-dimensionalization by Equation 3.11 as a ratio of the actual rate parameter to a reference value, a unity value of μ was used throughout this work. In summary, for all solutions displayed, the initial conditions were $x=1$ and $y=1$ and a distribution mean of $\mu=1$ was used.

Since the three-parameter Gamma distribution, with parameters of:

$$\begin{aligned} \alpha &= 3, \\ \beta &= 1/3, \\ \gamma &= 0, \\ \mu &= \alpha\beta + \gamma = 1, \end{aligned}$$ (6.1)

produced a distribution quite similar to the lognormal distribution, these were used, unless otherwise noted.

Variations in ν and p

The first observation to be made about these two adjustable parameters is that they have similar effects upon the solution after rate-limited transport begins to dominate (after the break in logarithmic slope): that is, increased pump rates do something similar to decreased ν 's as illustrated in Figure 6.1. Ultimately, neither seems to affect the logarithmic slope after rate-limited transport begins to dominate, but both affect the concentration at which this rate-limited transport domination begins to occur. Pump rate

6.2
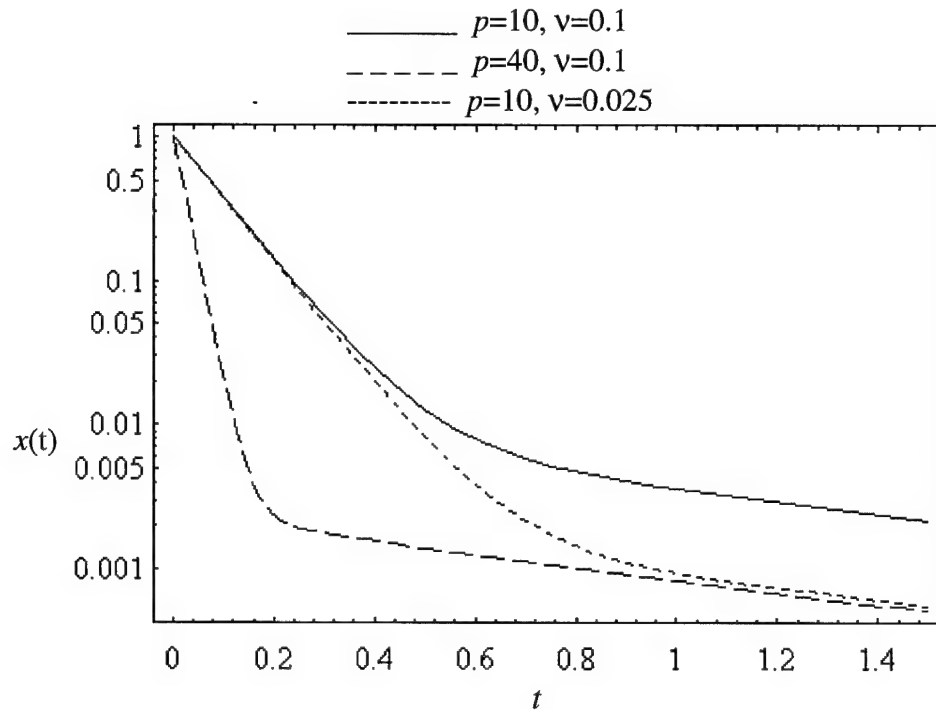
Figure 6.1. Effects of Changes in ν and p (One Parameter Solution)

increases cause rate-limited transport domination earlier and at lower concentrations, and

an obviously increased logarithmic slope during advection domination. This last

observation is true even when there are no immobile regions because advection is really

only causing dilution due to perfect mixing, as mentioned earlier. Decreases in ν cause x

to follow the same dilution slope during advection domination (due exclusively to pump

rate), but follow it longer to a lower concentration.

In summary, advection (dilution) is dominated by rate-limited transport at the

level-off point, the time and concentration for this point being affected both by p and ν.

The logarithmic slope after rate-limited transport domination begins is constant for this

one-parameter case. But, as we will see later with more clarity, this is only true for the

6.3

one-parameter case and possibly a certain class of distributions to be investigated (with

non-zero γ). In any case, at least the starting logarithmic slope seems to be primarily a

function of the distribution case, somewhat independent of p and v.

After examining both field and laboratory data, and conferring with an expert in

the field of groundwater hydrogeology, (Heyse, 1995), I observed that most BTC's have

starting regions where advection dominates. Therefore, very few solutions were

investigated for pump rates and v 's for which there is no advection domination period.

The trapezoidal code in Appendix G calculates this period for the analytic solution so that

the output scheme can sufficiently follow the curvature at this point. The point was

simply calculated by setting both exponential terms in Equation 4.13 equal to each other,

and solving for the time which makes the equality valid. A negative value output

signifies that advection never dominates.

These observations determined the minimum pump rate to be investigated. As

mentioned previously, a period of advection domination is common, so the pump rate at

Table 6.1. Non-Dimensional Pump Rates, p, and v Combinations
for No Advection Domination

Water Content Ratio, v	Non-Dimensional pump rate, p
1.0	2.0
0.5	1.5
0.1	1.1
0.01	1.01
0.001	1.001

which this period became minimal was used as the minimum pump rate. Table 6.1 gives selected values of p and v for which there is no advection domination. It appears from this table that an approximate rule of thumb for no advection domination (using the given initial conditions and distribution) is: $p \le 1 + v$.

If it is known that advection does not initially dominate for a given scenario, smaller pump rates should be investigated. Heyse (1995) estimated that a typical value for v is 0.1. Ball and Roberts (1991:1241) have estimated from 0.004 to 0.2 for a similar constant. For this work, unless otherwise noted, a v of 0.1 will be used.

Because the clean flow approximation was easy to determine, its use will be maximized. This equates to using it at all pump rates greater than that for which it is deemed adequate. Because the above analysis suggests that v affects the value for which the clean flow approximation is adequate, using a value of v different from 0.1 would require a repeat of the adequacy analysis. For the numerical solution, a lower bound for p was set at 1.0 and an upper bound set as per the following analysis.

Pump Rates for an Adequate Clean Flow Approximation

The first step in making the clean flow approximation useful is the determination of a rate for which it becomes adequate. Ultimately, this solution can always be used as a lower bound to y for any non-zero pump rate, but it's illustrative usefulness for x is not realized unless the pump rate is raised sufficiently high. Figure 6.2 shows a pump rate which makes the clean flow approximation of x poor, while Figure 6.3 illustrates a pump rate yielding a better approximation, deemed adequate. Because this solution over-
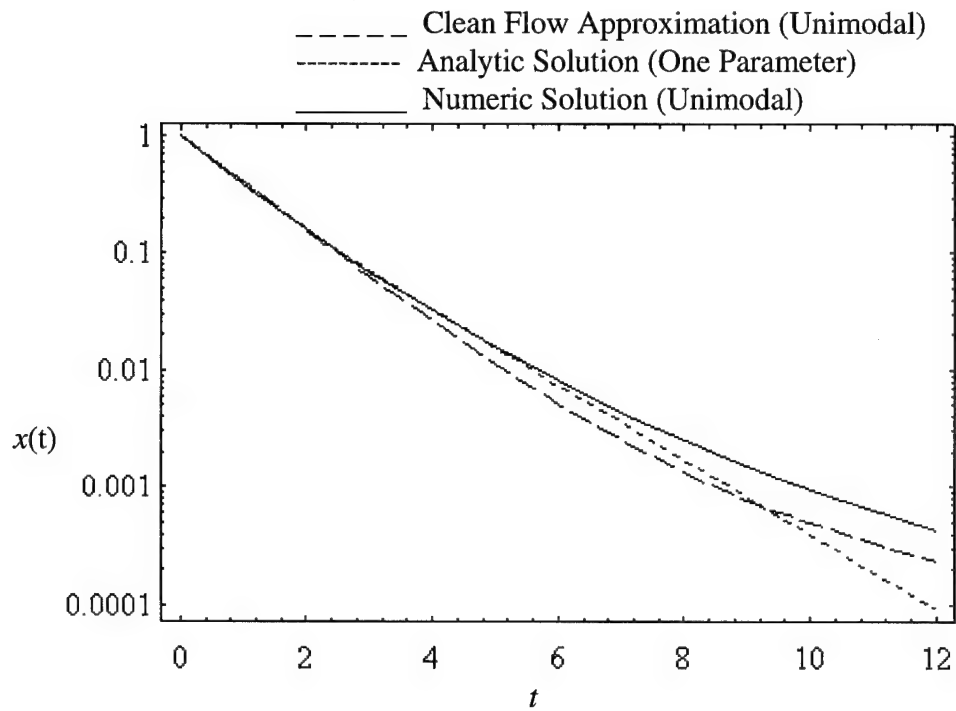
Figure 6.2 Pump Rate (p=1) Yielding a Poor Clean Flow Approximation
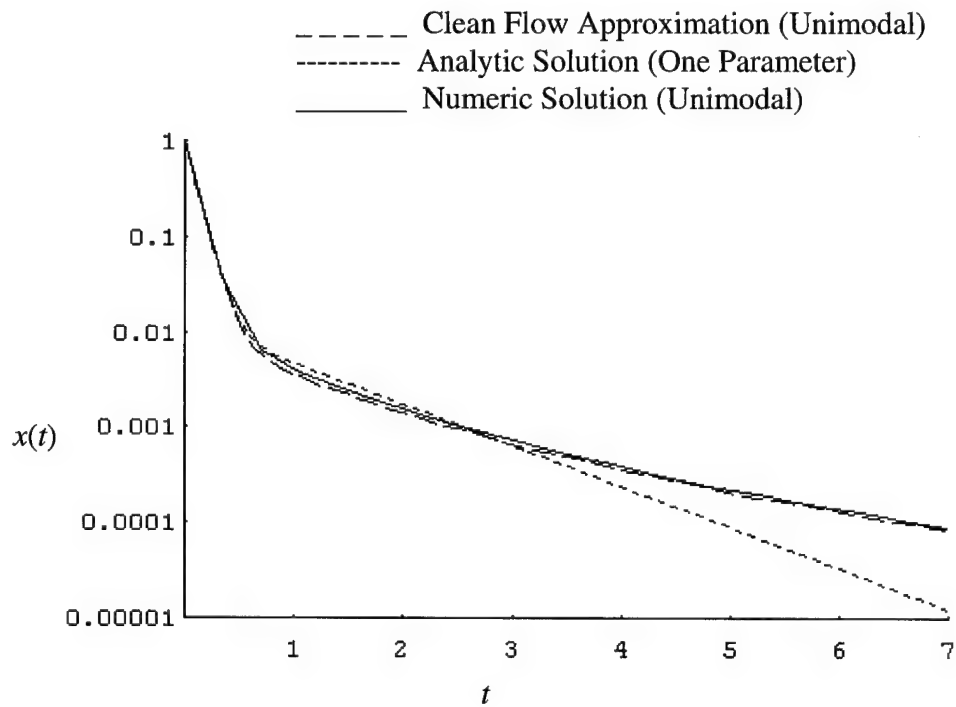
Figure 6.3: Pump Rate (p=10) Yielding an Adequate Clean Flow Approximation

6.6

estimates the transfer from y to x, x will be high early on and low for the rest of the time. The criterion for this determination of adequacy was that they were visibly similar through the advection domination stage and until the unimodal case diverges from the one-parameter case.

Comparison of x and y for Unimodal Case vs One-parameter Case

Mobile Region Concentration. The fact that the unimodal case diverges from the one-parameter case is a major observation. In Figure 6.3, the pump is run long enough to clean up a major portion of the fast and median sites associated with the unimodal case and a major portion of the contaminant in the one-parameter case. Figure 6.4 illustrates the same scenario, but the pumps ran twice as long. Pump rate was 10 unless otherwise
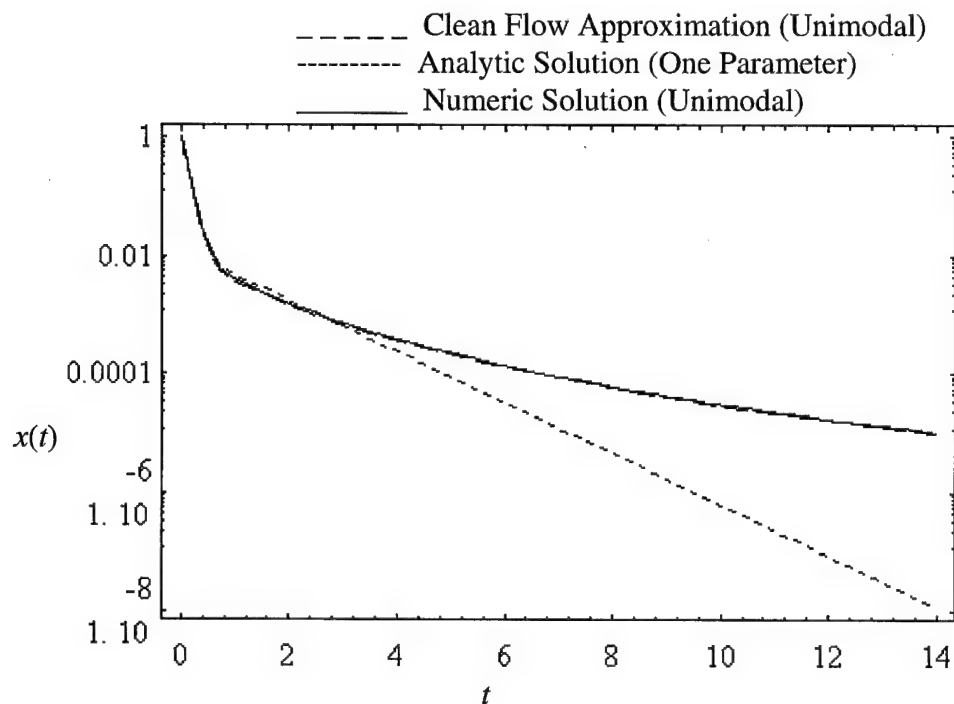
Figure 6.4: Longer Run (p=10) For Clean Flow Approximation

6.7

specified in this entire section. The divergence begins to occur at time, $t=3$, as slow sites associated with the unimodal case continue their slow cleanup. Note that for this given distribution, nearly three orders of magnitude difference is seen between the two cases by $t=14$.

The exact point of this divergence varies greatly, and the parameters affecting this point are of great importance. This point ultimately determines when consideration of a range of rate parameters, if actually present, is worth the effort. If divergence does not occur until safe concentrations are reached with no possibility of rebound, then multi-parameter rate-limited transport models are not worth the added complexity and computing time. On the other hand, if this point is reached not long after breakthrough in a long-term cleanup operation, multi-parameter rate-limited transport models of this sort would be needed. Also, even if safe concentrations were reached before this point, the possibility of rebound must be thoroughly investigated before this sort of rigorous (although first-order) rate-limited transport modeling is deemed unnecessary.

Immobile Region Concentration. Even though x is typically what is predicted by models and observed in the field and laboratories, the more important variable is y. In this formulation, it represents contaminant that is still stored in the ground and in need of removal. Only when contaminant redistribution is examined later, will $y(\lambda,t)$ be examined directly. The average immobile region concentration is defined as:

$$\bar{y}(t) = \int_0^\infty f(\lambda)y(\lambda,t)d\lambda .$$ (6.2)

It is this quantity, when multiplied by total immobile zone water content, $(\theta_{im})_{\text{total}}$, that quantifies total aqueous contaminant still in immobile regions. Based upon the known

6.8

standard deviation of the Gamma distribution, $\beta\alpha^{\frac{1}{2}}$, the code in Appendix G discretizes λ based upon a selected number of bins, with the upper bound being three standard deviations above the greater of the two means of the bimodal distribution. The composite midpoint numerical quadrature approximation to Equation 6.2 is:

$$\bar{y}(t) \approx \sum_{i=1}^{b} f(\lambda_i) y(\lambda_i, t)(\Delta\lambda_i), \tag{6.3}$$

where b is the number of bins and $\Delta\lambda_i$ is the bin width. The following similar technique was used to approximate $y(\lambda, t)$:

$$y(\lambda, t) = y(\lambda, 0)e^{-\lambda t} + \int_0^t x(s)\lambda e^{-\lambda(t-s)}ds,$$

$$y(\lambda_i, t_n) \approx y(\lambda_i, 0)e^{-\lambda_i t_n} + \sum_{m=1}^{n} w_m h x_m \lambda_i e^{-\lambda_i(t_n - t_m)}, \tag{6.4}$$

where w_m is the composite trapezoid weights ($\frac{1}{2}, 1, ..., 1, \frac{1}{2}$). In this work, twenty-four bins were used.

Figure 6.5 illustrates the behavior of $\bar{y}(t)$ for the same scenario as Figure 6.3. Note that the divergence of the unimodal case from the one-parameter case occurs earlier for $\bar{y}(t)$ than for x. Once $\bar{y}(t)$ begins to diverge, it takes a while for x to react. Note also that the further out in time you go, the better the limiting pump-rate solution gets.

Change in Average Effective Rate Parameter with Time

One very important process that is occurring for the unimodal case that has not been examined yet, is a change in the effective mean rate parameter with time. The
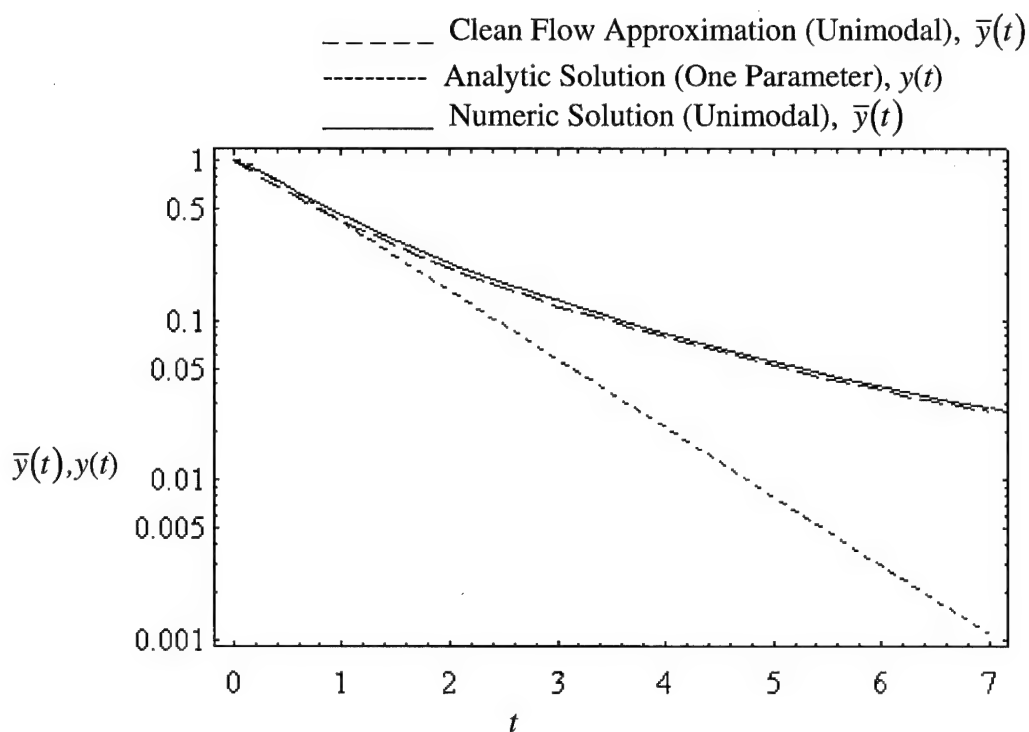
Figure 6.5. Behavior of $y(t)$ and $\bar{y}(t)$ for One-Parameter and Unimodal Cases

expression defining this parameter is:

$$\bar{\lambda}(t) = \frac{\int_0^\infty f(\lambda)\lambda y(\lambda,t)d\lambda}{\bar{y}(t)}.$$ (6.5)

The integral in the numerator was approximated for the numerical solution found by the

code in Appendix G using the same basic technique described by Equation 6.4. The

analytical values of the integrals for the clean flow approximation were found using

techniques described in Appendix C. Figure 6.6 illustrates $\bar{\lambda}(t)$.

If Equation 6.5 could be used to obtain a simple expression for single rate

parameter variation with time for certain general classes of contaminants, this could be
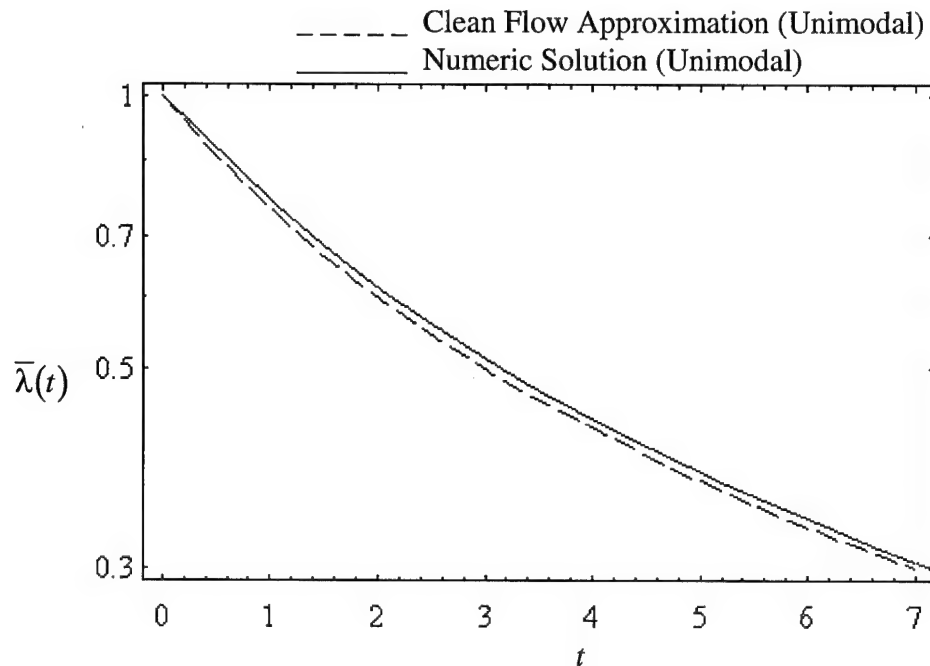
Figure 6.6. $\overline{\lambda}(t)$ vs Time.

very useful to present modelers. Their numerical solution techniques might allow the

simple insertion of this function in place of their single rate-parameter. I anticipate that if

the expression derived for this function was inserted into the one-parameter case

governing equations, a numerical solution of them would closely approximate the derived

limiting rate solution. A thorough test of this hypothesis is warranted before using this

expression (or a suitably derived approximation to it) in more complex governing

equations. Of course, the form of the theoretical distribution (continuous or discrete)

determines the complexity of the resulting function. With this apparent change in

effective mean rate parameter in view, we will now examine the soak phase in detail.

<u>Tailing and Rebound of Unimodal Case vs One-Parameter Case: The Soak Phase</u>

<u>Short Pump, Short Soak</u>. Here, short is determined in relation to the size of the

inverse mean rate parameter of the unchanging distribution, $1/\mu$ (not the effective mean

rate parameter previously described). Figure 6.7 illustrates a relatively short pump cycle

with an equal soaking period. Due to the presence of some faster sites in the unimodal

case than the one parameter case's sites, the unimodal case cleans up faster in this time

Figure 6.7. Behavior of x for Short Pump, Short Soak.

frame and appears to rebound quite similarly. But because the differences are quite small,

we will move on to a mid-range pumping period.

6.12

Short Pump, Mid-Range Soak. Mid-range here is defined as approximately ten inverse mean rates, $10/\mu$. Figure 6.8 illustrates a parallel sequence of plots of x, $\bar{y}(t)$, and $\bar{\lambda}(t)$ for a one time-unit pump period followed by a thirteen time unit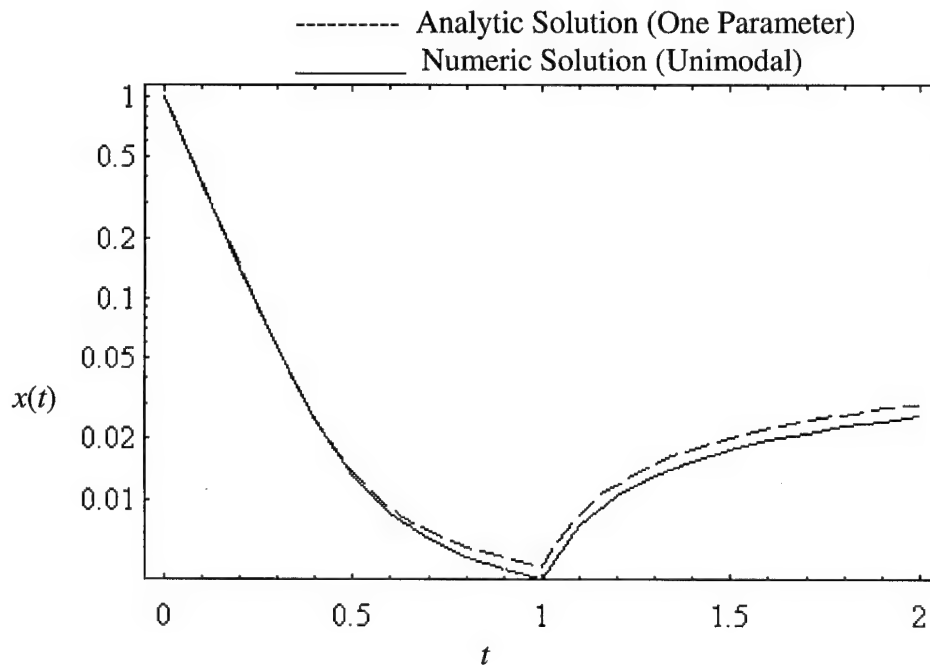 soak period. Remember that the analytic solution for $\bar{\lambda}(t)$ is only valid for the initial pump period (with sufficiently high pump rates). Here we see x for the unimodal case starting below x for the one-parameter case, yet rebounding above it and continuing to rebound beyond the time frame shown. From Figures 6.8b and 6.8c, we can see that $\bar{y}(t)$ will clearly drive x to a higher final (asymptotic) value for the unimodal case and will take much longer to approximately equilibrate. The one-parameter case has visibly equilibrated by six time units, and the unimodal case is visibly very close to it by fourteen time units.

Even though x for these two cases is still visibly quite similar, Figure 6.8c gives a very important insight. Note that for over three time units after pump shutoff, the effective mean rate parameter continues to decrease. This is because all of the y's above x continue to decrease, and for this short time, dominate contaminant redistribution of contaminant back into faster sites that begins at pump shutoff. Even after fourteen time units, the effective rate has not reattained unity (all y's have not sufficiently approached x yet). This is a simple, but important point that x and y asymptotically approach each other during the soak phase. Finally, note that even though the fastest pump rate, if used continuously, provides the fastest cleanup, the necessity of treating renders soaking beneficial (if the time can be afforded). Slow sites continue to be reduced in

6.13
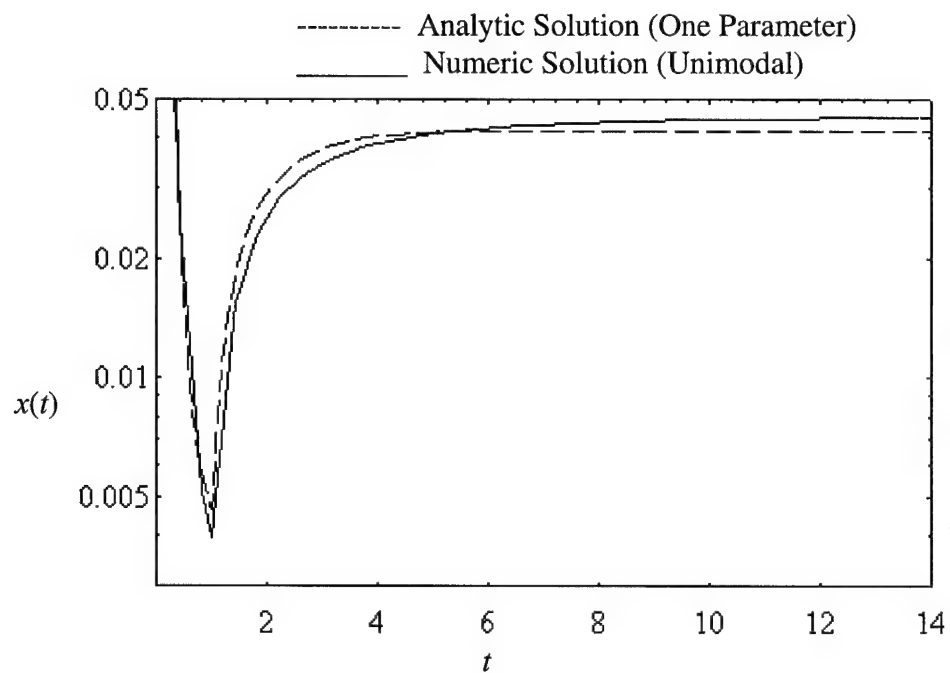
Figure 6.8a. Behavior of x for Short Pump, Mid-Range Soak.
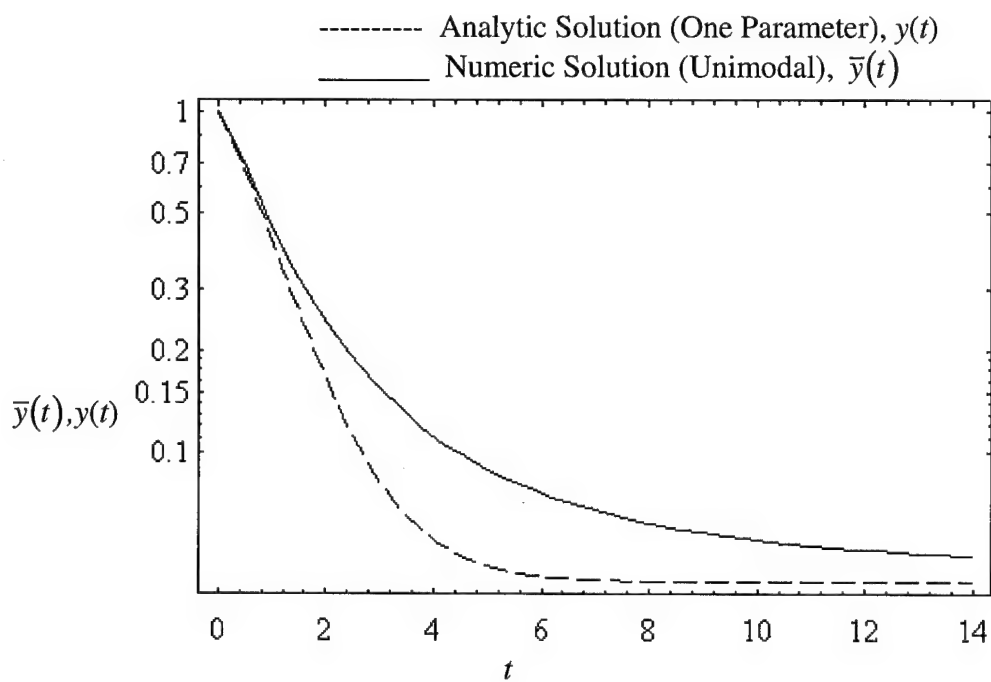
Figure 6.8b. Behavior of $y(t)$ and $\bar{y}(t)$ for Short Pump, Mid-Range Soak.

6.14
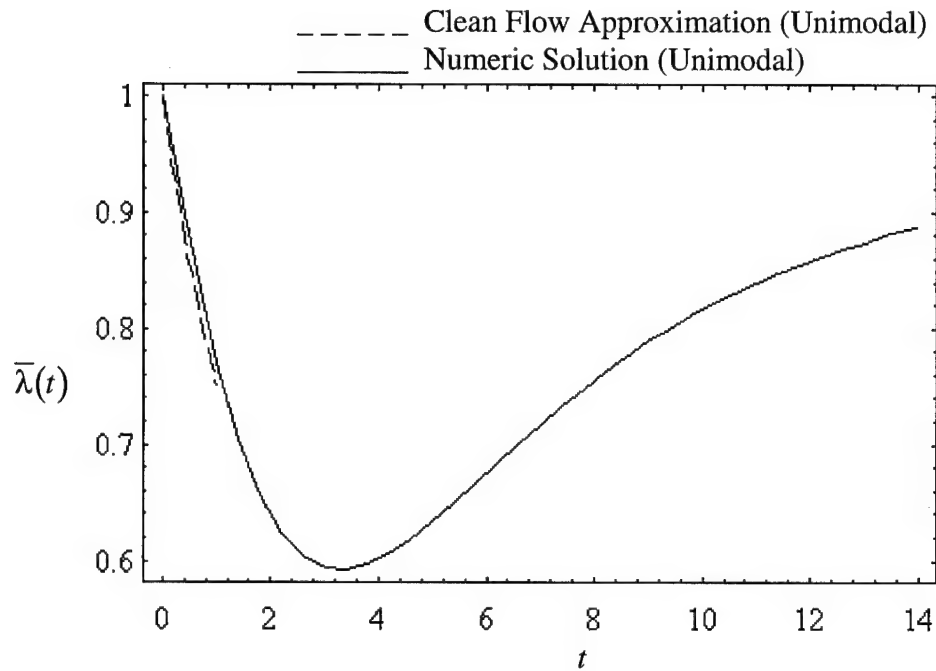
Figure 6.8c. Behavior of $\bar{\lambda}(t)$ for Short Pump, Mid-Range Soak.

concentration by contaminant movement to both the mobile region and faster sites. We will see more of this later.

Mid-Range Pump and Soak. Figure 6.9 illustrates this sequence of a fourteen time unit pump and an equal soak time. The longer and harder one pumps, the larger these two cases diverge: over two orders of magnitude in this sequence. Note that the effective mean rate gets quite small. In fact, this mean rate is so small that a finer discretization of λ in the code would probably be necessary if greater accuracy was desired. Nevertheless, a continued decrease in this mean rate is observed, and its log-curvature appears to be decreasing. Theory demands that as time approaches infinity, this

6.15

Figure 6.9a. Behavior of x for Mid-Range Pump and Soak.
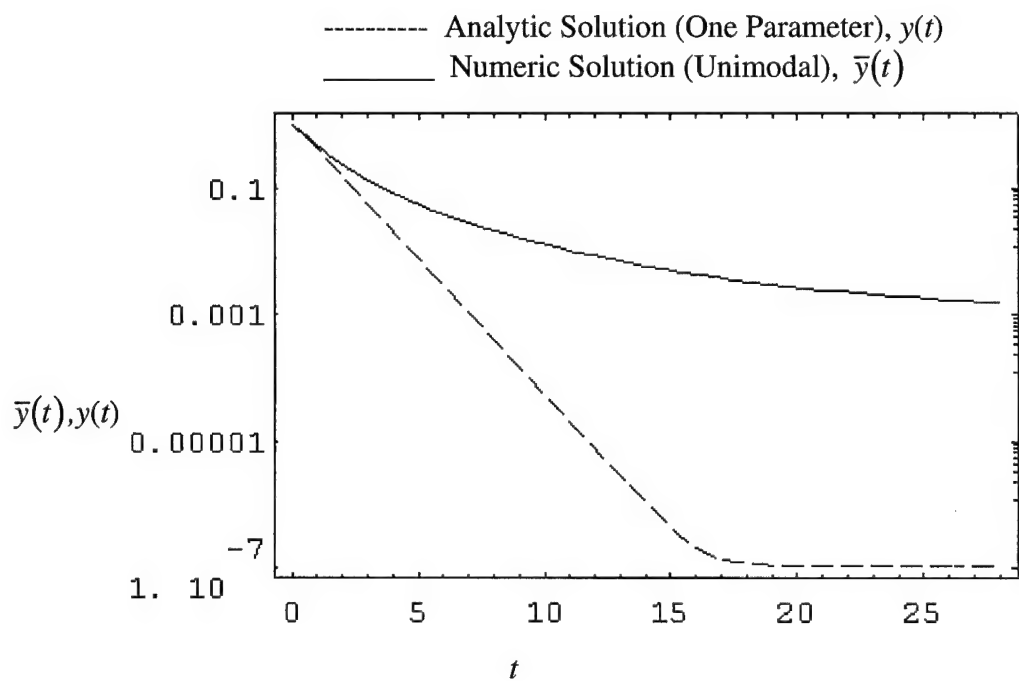
Figure 6.9b. Behavior of $y(t)$ and $\bar{y}(t)$ for Mid-Range Pump and Soak.

6.16

Figure 6.9c. Behavior of $\overline{\lambda}(t)$ for Mid-Range Pump and Soak.

mean rate becomes infinitely small, because contaminant would then only be present at these sites with an infinitely small rate parameter.

Note also that equilibration time remains about three time units for the one-rate case while equilibration continues well beyond fourteen soaking time units for the unimodal case. The rebound of the effective mean rate is slower in this sequence because slower sites have now been somewhat emptied, requiring longer time periods for equilibration, and hence longer periods for rebound of this rate.

Mid-Range Pump and Long Soak. Figure 6.10 illustrates this sequence in which the soak period clearly allows x and $\overline{y}(t)$ for the unimodal case to nearly equilibrate. The apparent slope discontinuities are merely due to a numerical output that was too coarse (although step size remained at 0.01). Figure 6.10c indeed shows that our $\overline{\lambda}(t)$ has nearly

6.17

$$1$$

$$0.01$$

$$0.0001$$

$x(t)$

$$-6$$
$$1.\ 10$$

$$-8$$
$$1.\ 10$$

$$0 \quad 20 \quad 40 \quad 60 \quad 80 \quad 100$$

t
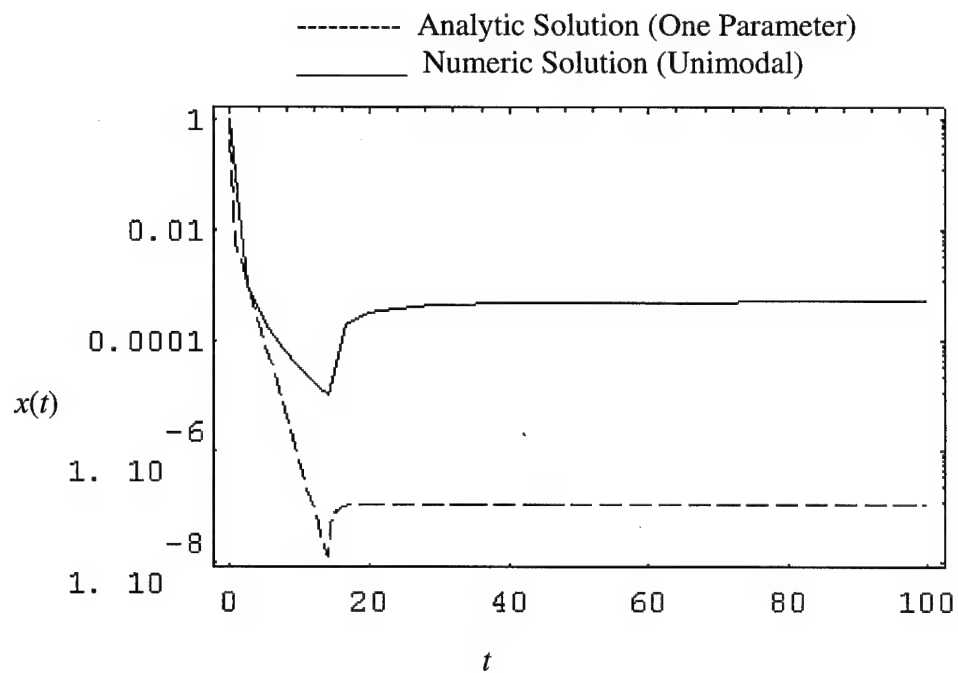
Figure 6.10a. Behavior of x for Mid-Range Pump, Long Soak.

---------- Analytic Solution (One Parameter), $y(t)$
_____ Numeric Solution (Unimodal), $\bar{y}(t)$

$$0.1$$

$$0.001$$

$\bar{y}(t), y(t)$ $\quad 0.00001$

$$-7$$
$$1.\ 10$$

$$0 \quad 20 \quad 40 \quad 60 \quad 80 \quad 100$$

t
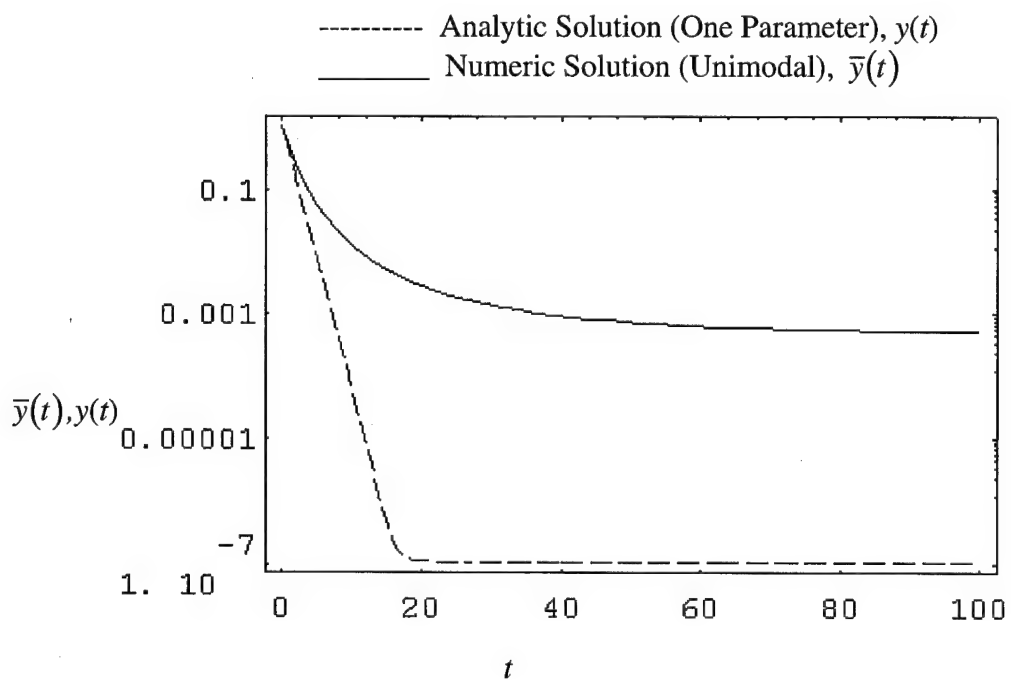
Figure 6.10b. Behavior of $y(t)$ and $\bar{y}(t)$ for Mid-Range Pump, Long Soak.

6.18

$\overline{\lambda}(t)$
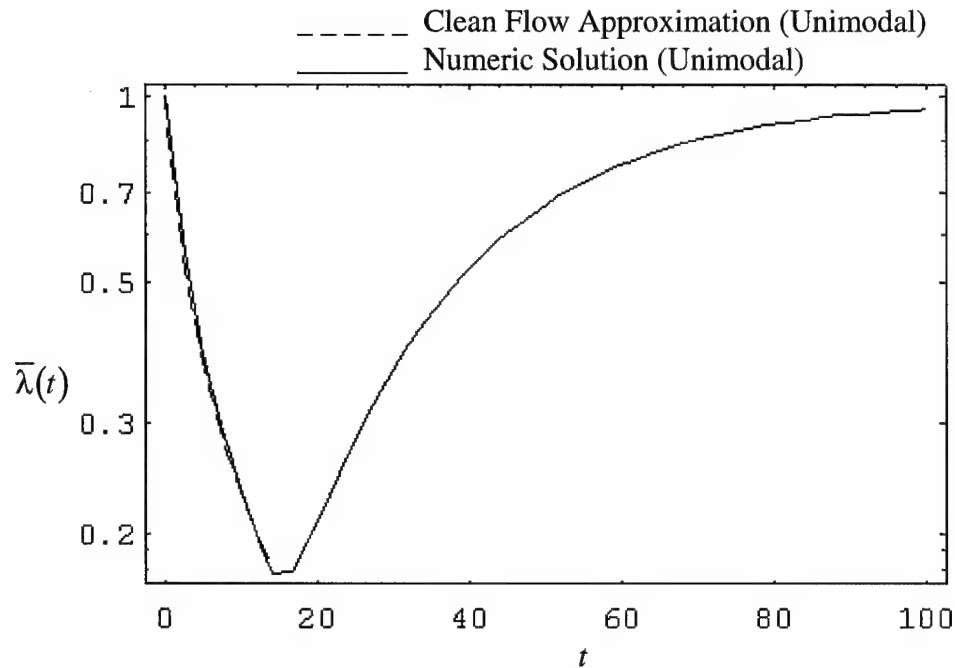
Figure 6.10c. Behavior of $\overline{\lambda}(t)$ for Mid-range Pump, Long Soak.

reattained unity (the clearest sign of equilibration). Although longer-term sequences were investigated, no further insights were gained.

A Lower Pump Rate ($p=1$) for Mid-range Pump and Soak. The sequence shown in Figure 6.11 was produced in a fashion similar to Figure 6.9 to illustrate the effects of a lower pump rate. Note that the divergence between the two cases is slightly reduced (from over two orders of magnitude in x to less than two). Rebound and equilibration time both are greatly reduced for both cases because a slower pump rate allows slower sites to equilibrate with pumps running, such that there is less equilibration necessary upon turning the pumps off. Note that the limiting rate solution's effective mean rate is
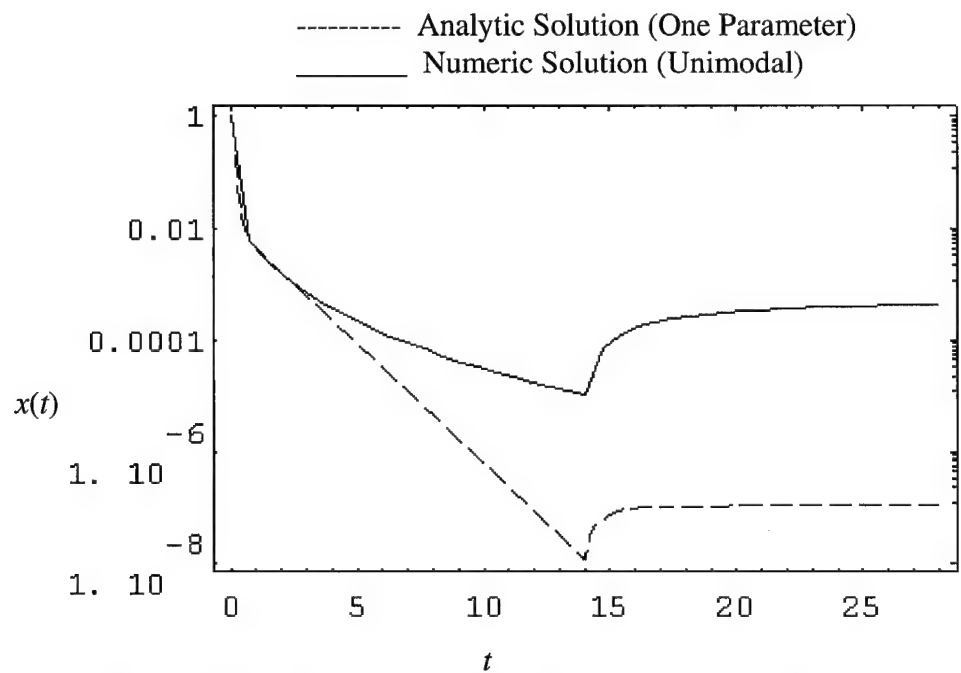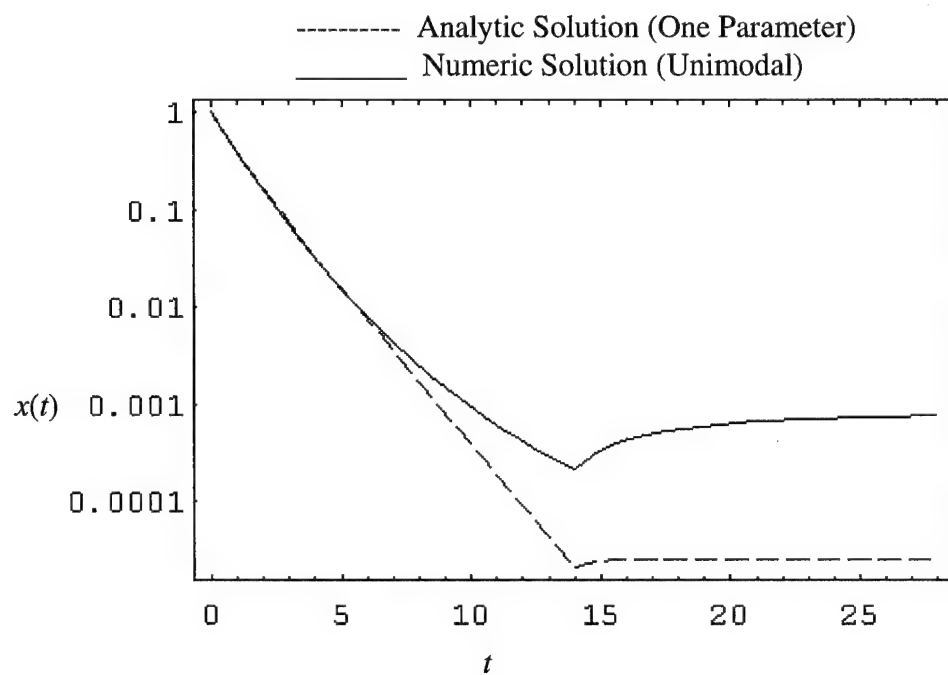
Figure 6.11a. Behavior of x for $p=1$, Mid-range Pump and Soak.
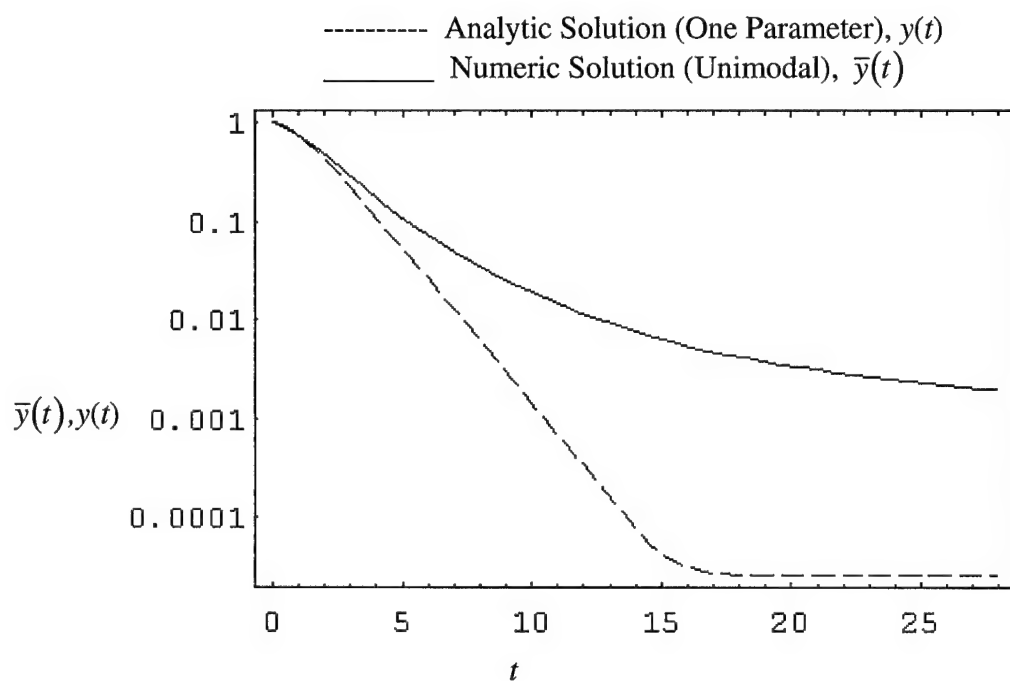
Figure 6.11b. Behavior of $y(t)$ and $\bar{y}(t)$ for $p=1$, Mid-range Pump and Soak.
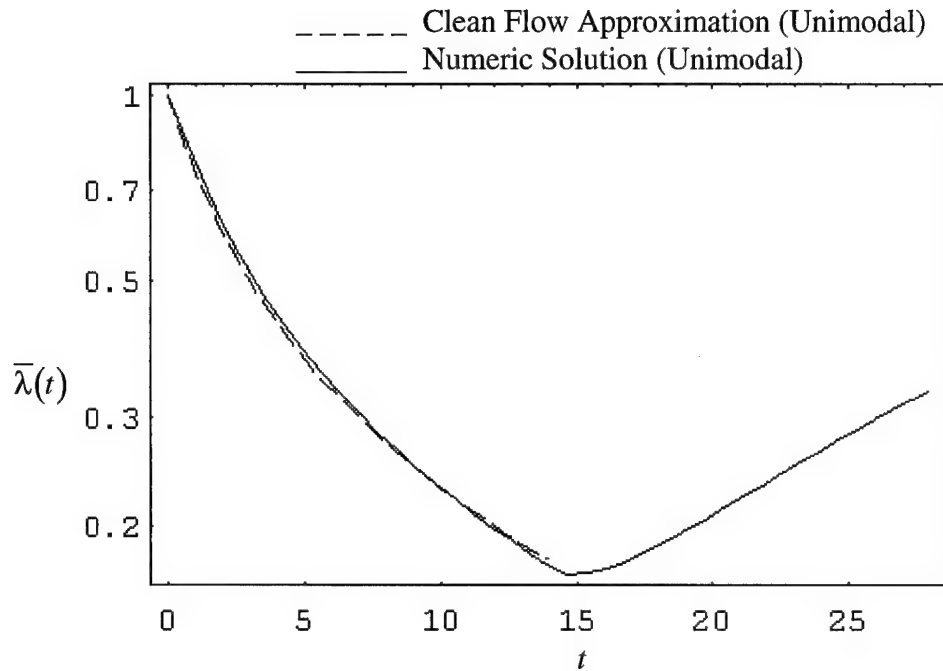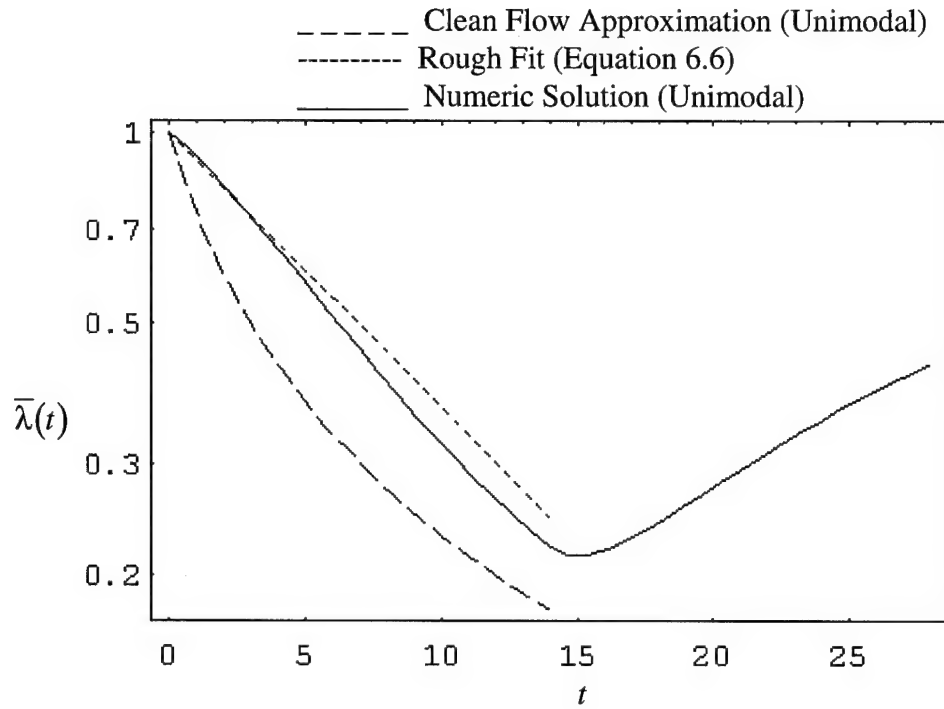
Figure 6.11c. Behavior of $\overline{\lambda}(t)$ for $p=1$, Mid-range Pump and Soak.

much lower than the numerical, further demonstrating that this pump rate makes the clean flow approximation inadequate.

An Approximation to the Effective Mean Rate Parameter. As a final note in this soak phase investigation, Figure 6.11c has the following decreasing exponential plotted in the pumping region:

$$\overline{\lambda}(t) = a\,e^{-bt}, \qquad (6.6)$$

where a and b are constants to be found based upon a hypothesized distribution present in any given situation. Approximating the rising rate parameter during soaking would require more investigation. This is suggested as a possible rough approximation to the

shape of this effective mean rate's change with time. Other distributions would probably require different forms.

Invalid Predictions Using Short-Term Data: the Bimodal vs Unimodal Case

In this section we will investigate the effects of errors in assumed distributions present in the soil. We continue to include the one-parameter case also. If, for example, the distribution shown as a solid line in Figure 6.12 is the actual distribution present, what are the effects of presuming the presence of the other three distributions shown in the figure (each has a mean of unity)? Figure 6.13 illustrates that each distribution yields a very similar solution up to four time units. At this point the unimodal and bimodal cases diverge from the one rate case. Note that the sharper peaked distribution (the lesser amount of slow sites) diverges the least from the one-parameter case. The unimodal standard and our actual distribution continue to be similar all the way until eight time units (twice as long as it took to diverge from the one rate case).

Let us assume that the soil's rate-limited transport characteristics are to be determined in a laboratory experiment that is to last only seven time units (a decrease in concentration at the well head by a factor of 10^{-4}). Clearly, the presence of the sharp peak of slow sites would go unnoticed in the lab and cause unexpected tailing and rebound in the field. The lab work might still reveal the presence of a distribution, but unless the work was done over a long enough period of time, long term rate-limited transport behavior would still be unpredictable without knowledge of these slow sites. I will suggest an approach that could reduce the necessary lab time later.

6.22
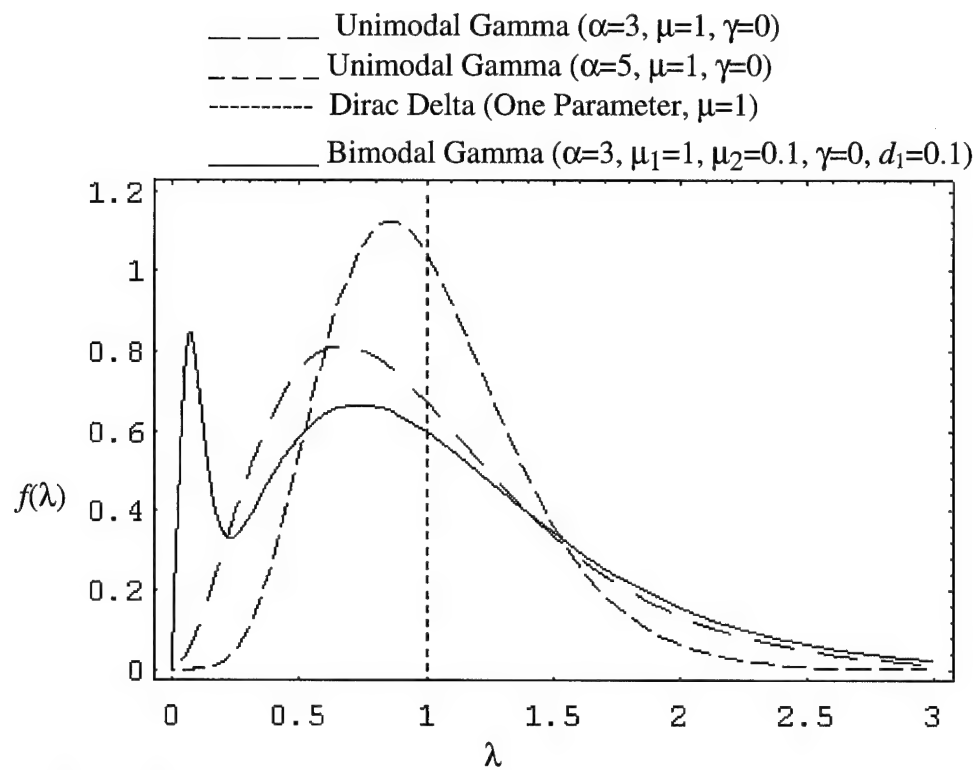
Figure 6.12. Distributions for Short-term vs Long-term Comparison.

Key Same as Figure 6.12.
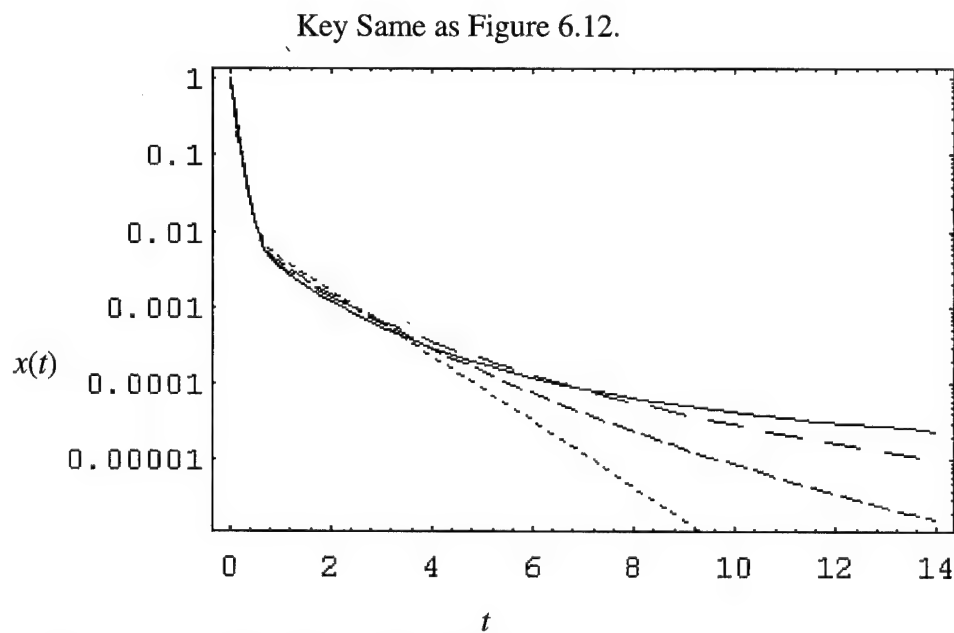
Figure 6.13. Behavior of x for Short-term vs Long-term Comparison.

6.23

Remember that the Gamma distribution was chosen for its flexibility as well as its integrability. It allows for an assumed non-zero, minimum value for the rate. Figure 6.14 illustrates minimum values of 0.25, 0.5, and 0.75 while keeping a unity mean. Figure 6.15 shows solutions for each of these distributions with some interesting insights. Previously we noted that the one parameter case yielded a log-linear slope in x after rate-limited transport domination. We also noted that certain non-zero minimum rate parameter values (non-zero γ's) could allow x to reach a log-linear slope in a given time period. Figure 6.15 demonstrates this. Nevertheless, note that the logarithmic slope is still less and concentrations are still higher when this log-linearity begins. If there is a maximum aggregate size or a maximum tortuous pore length into which contaminant can diffuse, this would set a theoretical minimum mass transfer rate. I therefore suggest using an estimated or experimentally derived minimum rate in this case. I do not understand the chemical conceptualization well enough to discuss the merit of a minimum rate for that model.

<u>Redistribution of Contaminant During Soak Phase</u>

In the soak phase section, redistribution was mentioned often but never really illustrated. Figure 6.16 actually shows this redistribution. The horizontal lines are the presumed single immobile concentration driven by a single rate (a line instead of a point at $\lambda=1$ for illustrative purposes), while the curves represent y for each discretized rate and for a few selected times. A discretized rate here is referring to the number of discrete values of λ used to produce these plots (24). A fourteen time unit pump and a fourteen

_ _ _ Unimodal Gamma (α=3, μ=1, γ=0.25)
_ _ _ _ _ Unimodal Gamma (α=3, μ=1, γ=0.5)
---------- Unimodal Gamma (α=3, μ=1, γ=0.75)
_____ Unimodal Gamma (α=3, μ=1, γ=1)
.... Dirac Delta (One Parameter, μ=1)
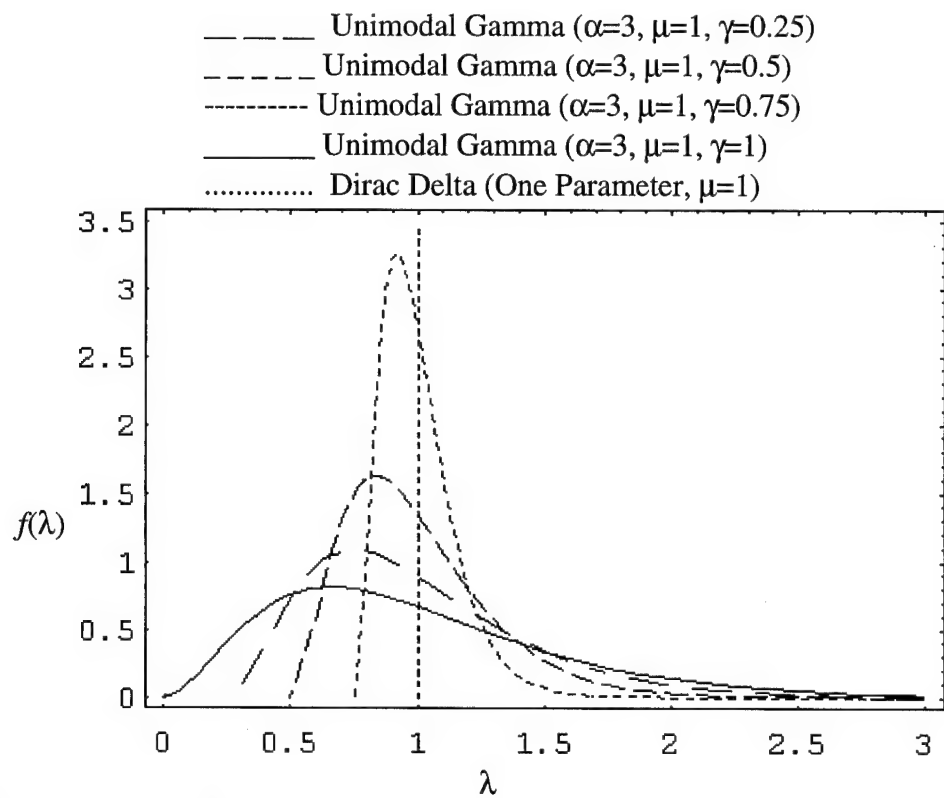
Figure 6.14. One Parameter and Gamma Distributions with γ=0, 0.25, 0.5, 0.75.

Same Key as Figure 6.14.
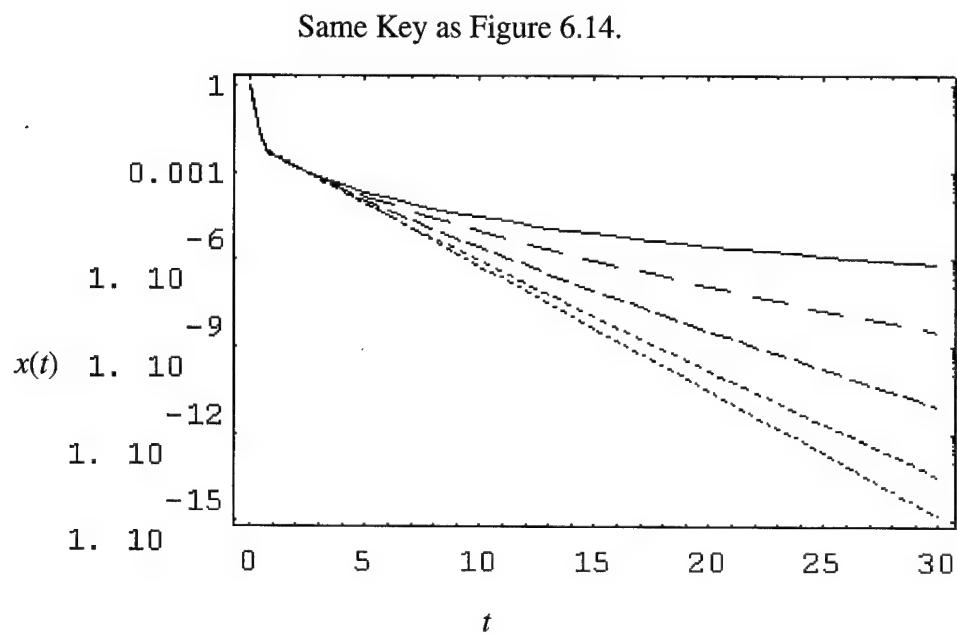
Figure 6.15. Behavior of x for One Parameter and γ=0, 0.25, 0.5, 0.75.

6.25
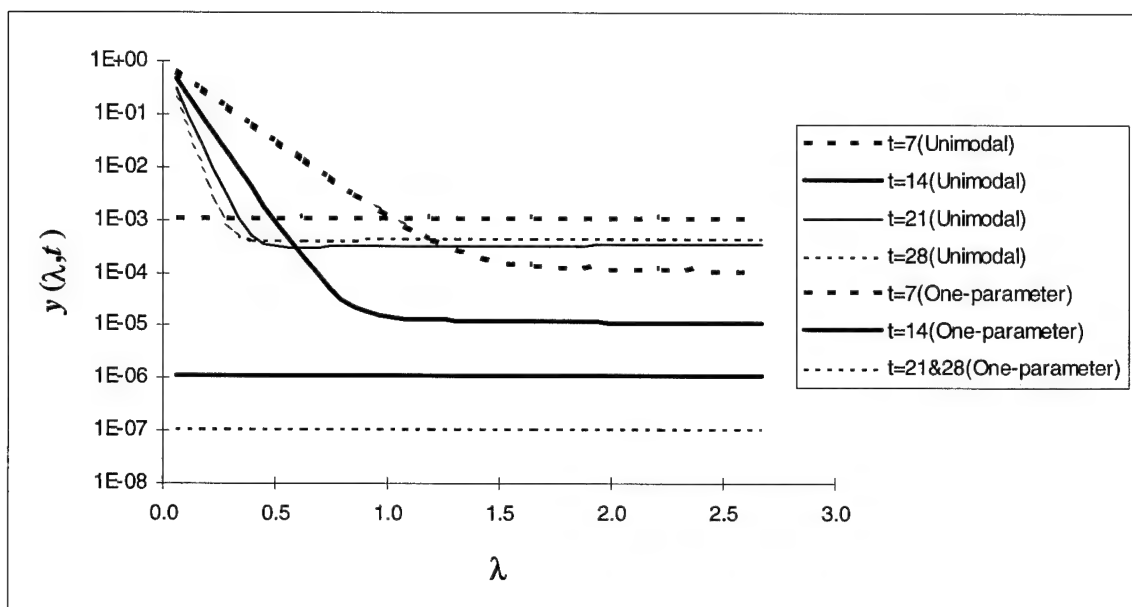
Figure 6.16. Contaminant Redistribution.

time unit soak was used for this figure, and snapshots of y are shown at t=7,14,21 and 28. Remember that y is unity initially for all rates.

The sharp elbow in each curve represents the break point between rates for which the LEA would be valid and those for which it would not be valid. The sites for which the LEA would not be valid are the ones that cause the non-loglinear (decreasing logarithmic) slope in x. Although this curvature will be present out to infinity (for distributions with γ=0), it will become negligible eventually due to the small water content fractions of such small rates (according to the distribution). The curvature will be absent eventually for non-zero values of γ, as was previously shown. For t=7, rates above approximately 1.7 appear to have their respective y values equal to x, while rates above 1.0 (the distribution mean) appear to have this condition for t=14. This demonstrates for

6.26

this distribution that well before fast sites (above the mean) reach a level validating the LEA, unimodal solutions have already greatly diverged from the one rate case.

Note primarily the clear movement of slow site contaminant to fast sites during the soaking phase from t=14 to 21 to 28. Total contaminant present in any given range of sites is determined by Equation 6.2, with bounds of integration appropriate to the site range of interest. The observed rates of redistribution start out quite fast, but quickly slow as contaminant is drawn from slower and slower sites.

Pulsed Pumping Concepts

Now we seek a clearer picture of soak benefits. For this example, we will consider only our standard unimodal case and our one rate case. Figure 6.17 illustrates two sequences: a seven time unit pump and soak double cycle versus a fourteen time unit pump and soak single cycle. Note that total pumping and soaking time is identical.

First of all, a reduced final concentration is attained by two cycles instead of one for either contaminant distribution case. The concentration difference is most pronounced for the one-parameter case because equilibration time is so much shorter. In order for similar differences to appear for the unimodal case, soaking times must be long enough to allow more total equilibration. In any event, a benefit is still illustrated for the unimodal case. Although y shows very little difference, x shows a significant difference and the effective mean rate plot shows a marked difference. The higher effective ending rate for the one cycle case indicates that less slow contaminant was cleaned up than for the two cycle case.

6.27
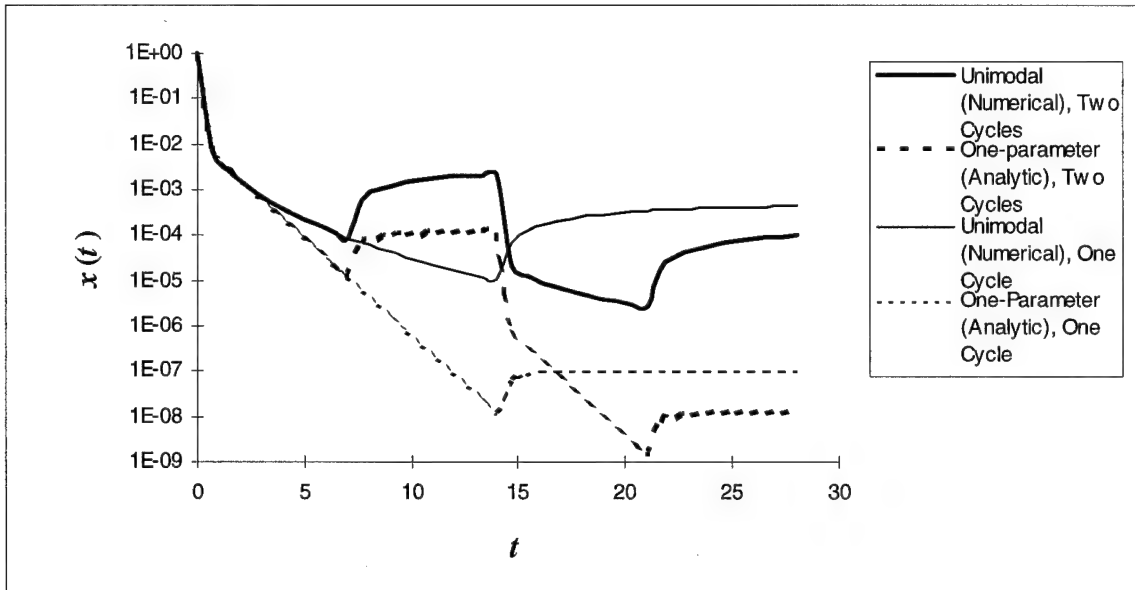
Figure 6.17a. Behavior of x for Pulsed Pumping.
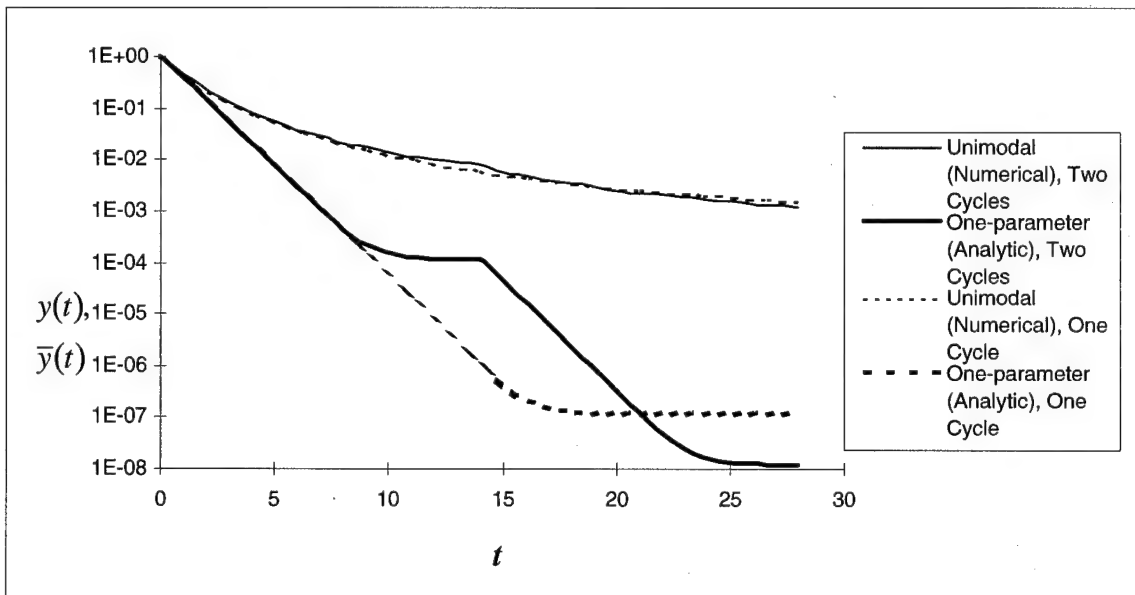
Figure 6.17b. Behavior of $y(t)$ and $\bar{y}(t)$ for Pulsed Pumping
(Note: $y(t)$ for One-Parameter and $\bar{y}(t)$ for Unimodal).

6.28
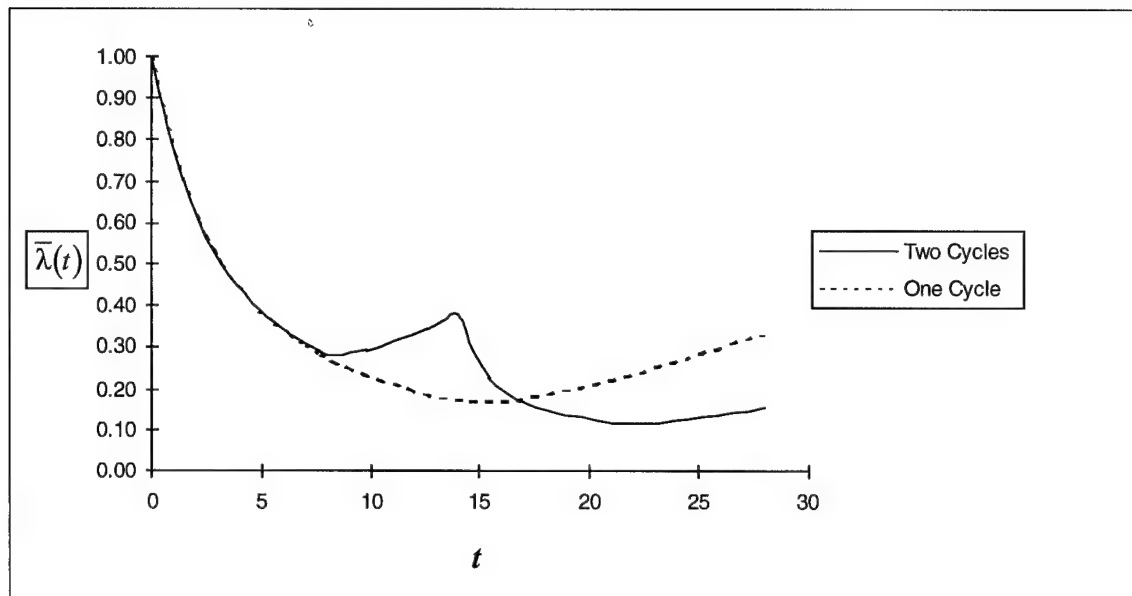
Figure 6.17c. Behavior of $\overline{\lambda}(t)$ for Pulsed Pumping.

Finally, although it is not easily seen in Figure 6.17b, the two cycle case has slightly higher average concentrations over the entire pumping regions than the one cycle case. This would benefit any necessary treating operations.

A Continuous Distribution of Rate Parameters Models Tailing, Rebound and the Time and Pump Rate Dependence of a Single Effective Rate Parameter Well

Rate limited transport due to a range of mass transfer rates, if present instead of a single rate, is a very plausible explanation for many unpredictable behaviors. The existence of a distribution of mass transfer rates would explain tailing and rebound above most rate-limited transport model predictions. More importantly, the time and pump-rate dependence of the single "representative" rate used by most present modelers is implicit in this model.

The solutions to the developed model clearly demonstrate tailing and rebound above the one-parameter case, and a time and pump rate dependent effective single rate parameter. If rate-limited transport is indeed the cause of many instances of unpredictable behavior, a more accurate way of modeling it might be needed. When more than one rate-limiting process is present, this work's method is offered as a more realistic (based on theory) and probably more accurate means of modeling rate-limited transport than most common methods.

Explicit Knowledge of Slow Sites Present and Deposition History are Essential to Accurate, Predictive Modeling

Assuming the coexistence of multiple mass-transfer rates, accurate, long-term field and laboratory predictions require detailed knowledge of existing slow mass transfer

rates and deposition history. It was clearly seen that y coupled with the distribution determined x, and if the starting values of y are not well known (from deposition history), then the model is without initial conditions. Further, (even with accurate initial conditions), accurate long-term predictions are impossible without knowledge of the mass transfer rates in the slow site regime (i.e. with only short term data).

It is also clearly seen in the literature that three dimensional models are inherently challenging. Before the challenge can adequately be met, at the very least, reasonably good initial conditions and good long-term soil sorption/transport characteristics must be known. Soil sorption/transport characteristics often realistically involve multiple mass transfer rates. It is clear that if the range of rates is wide enough, they are best modeled by either a discrete or continuous distribution of rate parameters instead of just one "representative" rate parameter. This work gave some insight into how wide is wide enough. It appears that unless the minimum mass transfer rate present is very near the representative rate, significant predictive errors are likely in the long-term (see Figures 6.14 and 6.15).

Gaining This Knowledge Probably Requires Long-Term Laboratory Experiments

As we examined the bimodal and varied unimodal cases for a hypothetical scenario, it was clear that predictions based upon short term experiments are only worth making for short term field situations. Slow sites that are yet unobserved in the lab could easily be present in the field. Also, because deposition history in the field is at best only vaguely known, very good sampling techniques and tricky laboratory work indeed are

necessary to obtain both soil sorption/transport characteristics and initial conditions simultaneously.

One suggested means of minimizing lab time necessary to discover long-term soil sorption/transport characteristics is the discovery of a predictable general shape of the distribution for classes of contaminants and soils. If the shape was known, the faster sites discovered by short-term experiments could be used to estimate the slower sites using the general shape mentioned above. Also, models which inherently have the ability to estimate parameters from first principles (such as diffusion-based models), rather than repeated curvefitting, are probably closest to the goal of accurate predictions. These types of models have the immense benefit of foregoing long-term laboratory work for long-term cleanups (assuming initial contaminant presence is known).

Pulsed Pumping Generally Appears to Benefit

This work did minimal investigation of pulsed pumping. It was generally found to benefit when the treatment process was a limiting cost consideration. This conclusion is only true from the perspective of rate-limited transport, since other transport processes were generally ignored. Soak time must clearly be available for pulsed pumping to even be considered. In other words, cleanup will always go more slowly using pulsed pumping, and unless this longer cleanup time is acceptable, the efficiency benefits are out of reach. This technique generally caused higher average concentrations while the pumps were running, yielding a more efficient treatment process. The efficiency of a given treatment process is maximized normally with maximum contaminant concentrations

being extracted from the wells. Also, the pumping efficiency is increased as well because

contaminant extracted per pumping unit time is increased.

Suggestions for Further Research

First of all, a wider variation in input parameters p and v is very much in order.

Exploring every conceivable possibility in the field would likely give more insight into

exactly when such a model is necessary. Comparing laboratory and field data to this

model could give insights both into the accuracy of its sorption/transport modeling ability

as well as what process causes what effect in BTC's.

Another beneficial addition to this work would be to allow contaminanted water

to flow into the region of interest, the typical laboratory procedure for generating BTC's.

This would make the above suggestion feasible. Deposition modeling is equally

important.

Actually, this model without modification could be used to analyze stagnant

deposition. A few computer runs with this initial condition were done, but again, a much

more thorough investigation is called for. As with cleanup, a thorough investigation of a

wide range of possible input parameter values and initial conditions would allow the

application of many conclusions made in this work to any given field situation. It would

also lead to more insight into when such a model is indeed necessary.

Recall that Equation 3.7 gives a standard form of the three-parameter Gamma

Distribution:

$$f(\lambda) = \frac{1}{\beta\Gamma(\alpha)}\left(\frac{\lambda-\gamma}{\beta}\right)^{\alpha-1}\exp\left[\frac{-(\lambda-\gamma)}{\beta}\right],$$ (3.7)

$$-\infty < \gamma < \infty, \quad \lambda > \gamma, \quad \alpha > 0, \quad \beta > 0,$$

$$\Gamma(\alpha) = \int_0^\infty \varphi^{\alpha-1} e^{-\varphi} d\varphi.$$

For this work, γ must always be greater than zero (rate constants are always positive),

which is why z is greater than zero also. The distribution in this form could not be

integrated by Mathematica, but with the following coordinate transformation, it became

integrable:

$$f(z) = \frac{1}{\beta\Gamma(\alpha)}\left(\frac{z}{\beta}\right)^{\alpha-1}\exp\left[\frac{-(z)}{\beta}\right].$$ (A.1)

$$0 < z < \infty, \quad \alpha > 0, \quad \beta > 0, \quad dz = d\lambda$$

The following Mathematica sequence shows how analytic forms for μ, σ, j, and w were

obtained (note that $\alpha=a$, $\beta=b$, and $\gamma=g$):

f1[a_,b_,z_]:=(1/(b*Gamma[a]))*(z/b)^(a-1)*Exp[-z/b]

Integrate[f1[a,b,z],{z,0,Infinity}] (*Normalized Probability Distribution Proven*)

1

Integrate[f1[a,b,z]*(z+g),{z,0,Infinity}] (*λ=z+g, Proven Distribution Mean*)

a b + g

Sqrt[Integrate[f1[a,b,z]*(z-a*b)^2,{z,0,Infinity}]] (*Proven Standard Deviation*)

(a*b^2)^(1/2)

Integrate[f1[a,b,z]*(z+g)^2*Exp[-t(z+g)],{z,0,Infinity}] (*

((b^(-1))^a*(a*b^2 + a^2*b^2 + 2*a*b*g + g^2 + 2*a*b^2*g*t + 2*b*g^2*t +

  b^2*g^2*t^2))/(E^(g*t)*(b^(-1) + t)^a*(1 + b*t)^2)

Integrate[f1[a,b,z]*(z+g)*Exp[-t(z+g)],{z,0,Infinity}]

((b^(-1))^a*(a*b + g + b*g*t))/(E^(g*t)*(b^(-1) + t)^a*(1 + b*t))

Appendix B: Mathematica Analytic Solution of One-Parameter Case

In this appendix, the Mathematica sequence used to obtain the analytic solution of the one rate case is described. Also included is the module built to allow pump cycling with this solution. Although the output was a bit messy and the simplification process was a little tedious, Mathematica definitely made the overall task easy:

eqns={x'[t]+p*x[t]==v*k*(y[t]-x[t]), y'[t]==k*(x[t]-y[t]),y[0]==y0,x[0]==x0};

Simplify[DSolve[eqns,{x,y},t]]

Without the simplify command, five pages of solution was output. With it, the solution was a page long, with the rest of the simplifying done by hand. All hand simplifying was tested against plots of a function built from the actual output of this sequence. Also, the solutions calculated by the code in Appendix G were tested against these forms also. The following is the form of the functions used for this solution:

xa[u_,p_,v_,x0_,y0_,t_]:=

  (1/(2*(Sqrt[(u-p)^2+u*v*(2*u+2*p+u*v)])))*

        (x0*(-u+p+u*v+(Sqrt[(u-p)^2+u*v*(2*u+2*p+u*v)])) -

        2*y0*u*v)*Exp[-(u+p+u*v+(Sqrt[(u-p)^2+u*v*(2*u+2*p+u*v)]))*t/2] +

  (1/(2*(Sqrt[(u-p)^2+u*v*(2*u+2*p+u*v)])))*

        (x0*(u-p-u*v+(Sqrt[(u-p)^2+u*v*(2*u+2*p+u*v)])) +

        2*y0*u*v)*Exp[-(u+p+u*v-(Sqrt[(u-p)^2+u*v*(2*u+2*p+u*v)]))*t/2];

ya[u_,p_,v_,x0_,y0_,t_]:=

  (1/(2*(Sqrt[(u-p)^2+u*v*(2*u+2*p+u*v)])))*

        (-2*x0*u + y0*(u-p-u*v+(Sqrt[(u-p)^2+u*v*(2*u+2*p+u*v)])))*

              Exp[-(u+p+u*v+(Sqrt[(u-p)^2+u*v*(2*u+2*p+u*v)]))*t/2] +

  (1/(2*(Sqrt[(u-p)^2+u*v*(2*u+2*p+u*v)])))*

        (2*x0*u + y0*(-u+p+u*v+(Sqrt[(u-p)^2+u*v*(2*u+2*p+u*v)])))*

              Exp[-(u+p+u*v-(Sqrt[(u-p)^2+u*v*(2*u+2*p+u*v)]))*t/2];

It was also necessary, at times, to use this function for a pump and soak sequence. This was made possible by the following function, which essentially reinitializes the solution at soaking time:

xcyc[u_,p_,tp_,v_,x0_,y0_,t_]:=Which[t<=tp,xa[u,p,v,x0,y0,t],

        t>tp,xa[u,0,v,xa[u,p,v,x0,y0,tp],ya[u,p,v,x0,y0,tp],t-tp]]

ycyc[u_,p_,tp_,v_,x0_,y0_,t_]:=Which[t<=tp,ya[u,p,v,x0,y0,t],

        t>tp,ya[u,0,v,xa[u,p,v,x0,y0,tp],ya[u,p,v,x0,y0,tp],t-tp]]

B.2

Appendix C: Module for Exponential Integral Form and Clean Flow Approximation

In the Solution section, Equations 4.15 and 4.16 defined the task at hand:

$$\int \frac{e^{ax}}{x^m}dx = \frac{-1}{m-1}\frac{e^{ax}}{x^{m-1}} + \frac{a}{m-1}\int \frac{e^{ax}}{x^{m-1}}dx, \qquad (4.15)$$

$$EI(z) = \int_{-z}^{\infty}\frac{e^{-s}}{s}ds. \qquad (4.16)$$

The following module, *ixm* was built to do Equation 4.15's integration by parts, utilizing

Mathematica's built-in function to evaluate Equation 4.16 for the last integration by parts:

ixm[g_,h_,av_,mv_]:=Module[{cum,i},

    (*this finds: Integrate[Exp[a*x]/x^m,{x,g,h}]*)

    (*g & h must be positive, and mv must be an integer>0*)

    cum=ExpIntegralEi[av*h]-ExpIntegralEi[av*g];

    Which[mv>2,Do[cum=(-1/(i-1))*(Exp[av*h]/h^(i-1) -

        Exp[av*g]/g^(i-1))+av*cum/(i-1),{i,2,mv}],

    mv==2,cum=-Exp[av*h]/h + Exp[av*g]/g + av*cum];

    N[cum]]

The following modules were used to actually plot *x(t)*, $\bar{y}(t)$, and $\bar{\lambda}(t)$:

```
xlim[t_,p_,v_,d1_,a1_,b1_,g1_,a2_,b2_,g2_,x0_,y0_]:=Module[{w1i,w2i,d2=1-d1},

        w1i=y0*Exp[(g1-p)/b1]*(a1*ixm[1,1+b1*t,(p-g1)/b1,a1+1] +

                        (g1/b1)*ixm[1,1+b1*t,(p-g1)/b1,a1]);

        w2i=y0*Exp[(g2-p)/b2]*(a2*ixm[1,1+b2*t,(p-g2)/b2,a2+1] +

                        (g2/b2)*ixm[1,1+b2*t,(p-g2)/b2,a2]);

        N[Exp[-p*t]*(x0 + v*d1*w1i + v*d2*w2i)]];

yave[t_,d1_,a1_,b1_,g1_,a2_,b2_,g2_,y0_]:=

        d1*((b1^(-1))^a1*y0)/(E^(g1*t)*(b1^(-1) + t)^a1)+

        (1-d1)*((b2^(-1))^a2*y0)/(E^(g2*t)*(b2^(-1) + t)^a2);

muave[t_,a_,b_,g_,y0_]:=((b^(-1))^a*(a*b + g + b*g*t)*y0)/         .

        (E^(g*t)*(b^(-1) + t)^a*(1 + b*t));

lambar[t_,d1_,a1_,b1_,g1_,a2_,b2_,g2_,y0_]:=

        (d1*muave[t,a1,b1,g1,y0] + (1-d1)*muave[t,a2,b2,g2,y0])/

        yave[t,d1,a1,b1,g1,a2,b2,g2,y0]
```

These proved quite useful in the quick examination of a multitude of solution behaviors.

This appendix will demonstrate the second order convergence of this implementation of the composite trapezoidal method and summarize the uncertainty monitoring principles for this work. Figure D.1 is a pump and soak solution (short term) for which uncertainty and convergence is to be analyzed.
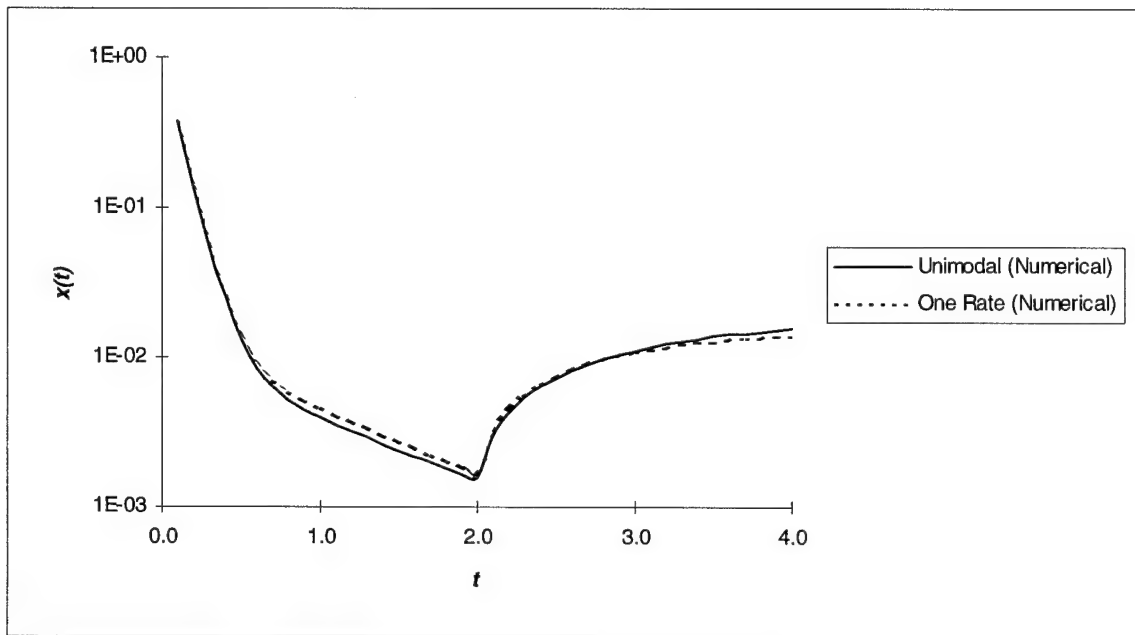
Figure D.1. Short Term Pump and Soak Solution (h=0.001).

Figure D.2 clearly demonstrates the second order convergence of the method since errors shrunk by a factor of 100 when h was shrunk by a factor of 10.
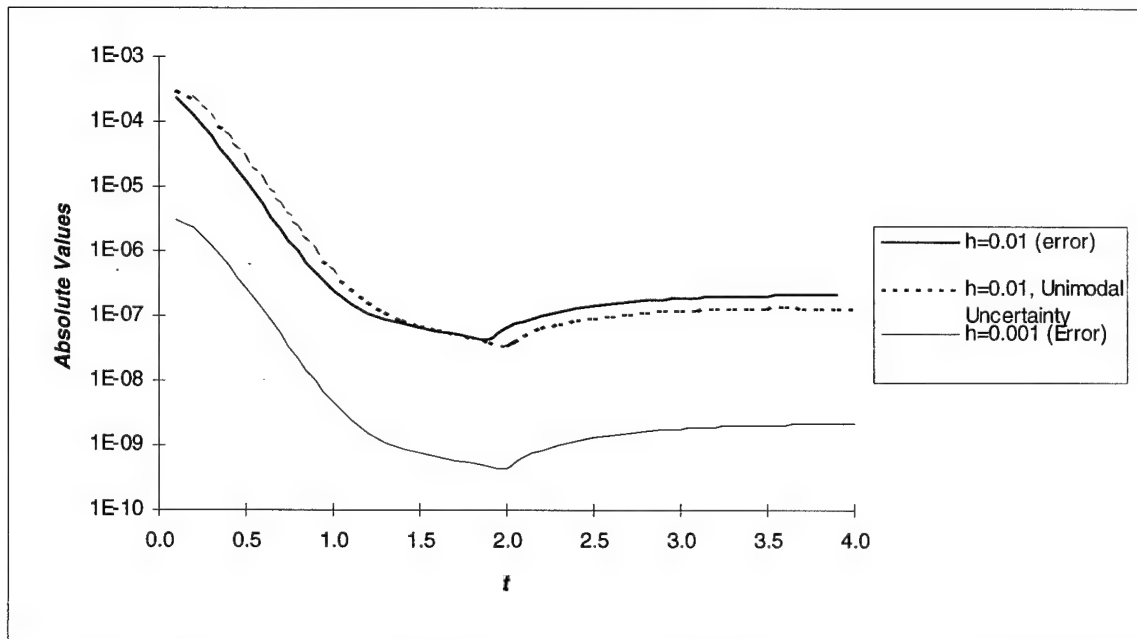
Figure D.2. Change in Error for Change in h from 0.01 to 0.001.

Note that uncertainty denotes a simple difference between the h=0.01 and 0.001 solutions (the second common uncertainty monitoring method mentioned in the Numerical Methods section). Notice also from Figure D.2 that error and estimated uncertainty follow each other. For a more important uncertainty reference, % differences are plotted in Figure D.3.

D.2
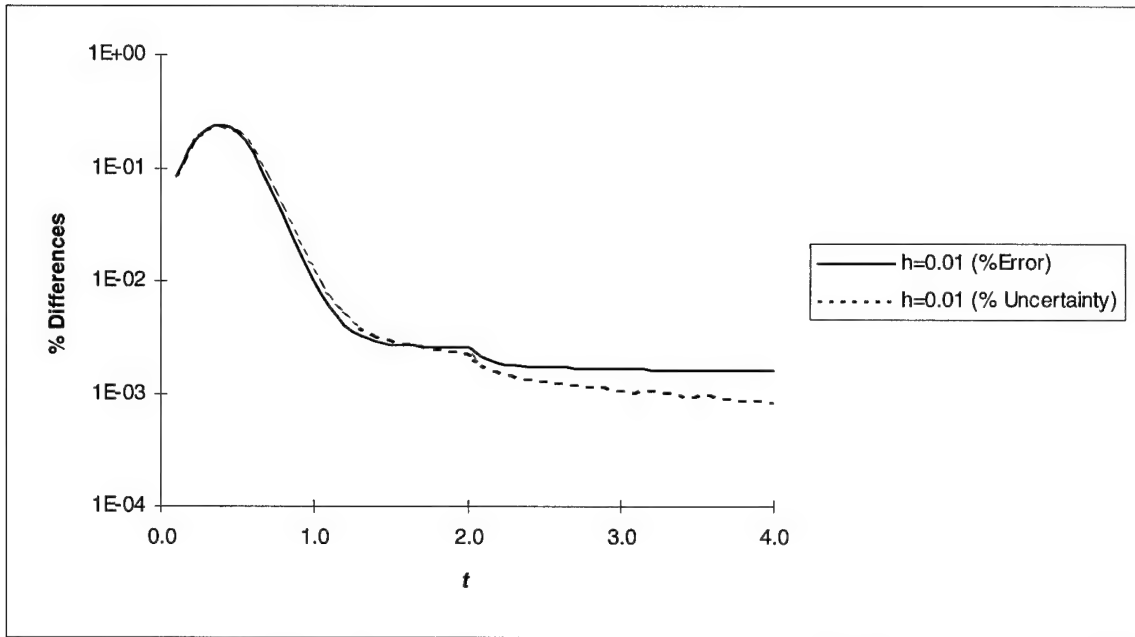
Figure D.3. Percent Uncertainty and Error for h=0.01.

From a percentage reference, there is actually divergence observed, but notice how small relative error actually is to begin with for h=0.01: nearly one thousandth of a percent. Notice also that it does not ever grow after the short initial hump.

Appendix E: Third-order Error of Quadratic Interpolation

This appendix will summarize the proof that quadratic interpolation involves third order error before it is employed in any composite fashion. Quadratic interpolation is accomplished by the following:

$$f_{1/2} = \frac{3}{8} f_0 + \frac{3}{4} f_1 - \frac{1}{8} f_2 \,.$$

(E.1)

To start, the function to be interpolated must be expanded in a Taylor's series about the halfway point for each point to be used in the approximation:

$$f_0 = f_{1/2} + \frac{\left(\frac{-h}{2}\right)}{1!} f'_{1/2} + \frac{\left(\frac{-h}{2}\right)^2}{2!} f''_{1/2} + \frac{\left(\frac{-h}{2}\right)^3}{3!} f'''_{1/2} + \ldots \quad,$$

$$f_1 = f_{1/2} + \frac{\left(\frac{h}{2}\right)}{1!} f'_{1/2} + \frac{\left(\frac{h}{2}\right)^2}{2!} f''_{1/2} + \frac{\left(\frac{h}{2}\right)^3}{3!} f'''_{1/2} + \ldots \quad,$$

(E.2)

$$f_2 = f_{1/2} + \frac{\left(\frac{3h}{2}\right)}{1!} f'_{1/2} + \frac{\left(\frac{3h}{2}\right)^2}{2!} f''_{1/2} + \frac{\left(\frac{3h}{2}\right)^3}{3!} f'''_{1/2} + \ldots \quad.$$

Now, if these are substituted into our quadratic interpolation formula, E.1 and coeficients of the various orders of derivatives are found, this yields:

$$\tilde{f}_{1/2} = f_{1/2} + \frac{h^3}{16} f'''_{1/2} + \ldots$$

(E.3)

Notice that the third order term is the first non-zero contribution to errors in Taylor series truncation, thus making the technique third order in a single application.

Appendix F: Second-order Convergence of Linz's Stated Fourth-order Block-By-Block

Method

In the previous appendix, we saw that Linz's example block-by-block technique was clearly only at most third order when applied to an example function that is not constant. This author believes based upon theory and the following example program, that because quadratic interpolation is applied to two integrals per step, and for this work it would be applied in a composite format (for Z), the method reduces to second order (as long as composite integration errors do not overwhelm interpolation errors).

This concept is easily proven for composite integration, as demonstrated by several authors. (Young and Gregory, 1988:373, Hildebrand, 1987:95) Its basis there hints strongly to its reality for quadratic interpolation, since Newton-Cotes type integration approximation schemes are interpolatory by nature. But to further substantiate the hypothesis, without delving into a messy proof, we will simply code this method.

The following code was used to generate the following tables' values.

```
       PROGRAM BTest

       IMPLICIT DOUBLE PRECISION (A-H, O-Z)
       DOUBLE PRECISION    f[ALLOCATABLE](:)
       INTEGER*4           m,kp,j,n,n1,n2
       CHARACTER*7         fname
10     FORMAT (E11.4E2,',',E22.16E2,',',E22.16E2,',',E22.16E2)

20     t=0D0
       f0=1D0
       WRITE(*,*)'Input h,m,kp'
       READ(*,*) h,m,kp
c
c      Allocate necessary array sizes
c
       ALLOCATE    (f(0:m))
c
```

```
c       Reads in output filename
c
        WRITE(*,*) 'Output to file? (1=yes,anything else=no)'
        READ(*,*) jf
        IF (jf.EQ.1) THEN
            WRITE(*,*)'Enter 7-char output file([appos]filenam[appos]):'
            READ(*,*) fname
c
c       File for data to be written to
c
            OPEN (1,FILE=fname//'.out',STATUS='UNKNOWN',
     +          ACCESS='SEQUENTIAL',FORM='FORMATTED')
            WRITE (1,*) 'f0,h='
            WRITE (1,*) f0,h
            WRITE (1,*)
            WRITE(1,*)'t ',fname,'.num ',fname,'.ana '
            WRITE (1,10) t,f0,f0,t
        END IF
        WRITE (*,*)
        WRITE (*,10) t,f0,f0,t
c
c       Initializing variables
c
        f(0)=f0
c
c       Start loop
c
100     DO 1000 n=0,m-2,2
            n1=n+1
            n2=n+2
c
c       Step times
c
            t=n*h
            th=(n + 0.5D0)*h
            t1=n1*h
            t2=n2*h
c
c       Summations
c
            s1=0D0
            IF (n.NE.0) THEN
                DO 200 j=0,n
                    IF ((j.EQ.0).OR.(j.EQ.n)) THEN
                        wt=1D0
                    ELSE IF (MOD(j,2).EQ.0) THEN
                        wt=2D0
                    ELSE
                        wt=4D0
                    END IF
                    s1=s1 + wt*f(j)
200             CONTINUE
            END IF
            f(n1)=((f(n) + (h/6D0)*(-15D0*f(n)-20D0*s1*(h/3D0)-32D0*
     +      ((h/3D0)*s1 + h*f(n)*5D0/12D0)+4D0*(h/3D0)*(s1 + f(n)))) +
     +      ((h/6D0)*(3D0 - 32D0*(-h/12D0) + 4D0*h/3D0))*
     +      (f(n)+ (h/3D0)*(-6D0*f(n)-8D0*s1*(h/3D0)-32D0*
     +      ((h/3D0)*s1 + h*f(n)*5D0/12D0)-8D0*(h/3D0)*(s1 + f(n))))/
     +      (1D0-(h/3D0)*(-32D0*(-h/12D0) - 6D0 - 8D0*h/3D0)))/
     +      (1D0 - (h/6D0)*(-24D0 - 24D0*2D0*h/3D0 + 4D0*4D0*h/3D0) -
     +      ((h/6D0)*(3D0 - 32D0*(-h/12D0) + 4D0*h/3D0))*
     +      ((h/3D0)*( -24D0 - 32D0*2D0*h/3D0 - 8D0*4D0*h/3D0 ))/
     +      (1D0-(h/3D0)*(-32D0*(-h/12D0) - 6D0 - 8D0*h/3D0)))
            f(n2)=((f(n)+ (h/3D0)*(-6D0*f(n)-8D0*s1*(h/3D0)-32D0*
```

```
     +      ((h/3D0)*s1 + h*f(n)*5D0/12D0)-8D0*(h/3D0)*(s1 + f(n)))) +
     +      ((h/3D0)*( -24D0 - 32D0*2D0*h/3D0 - 8D0*4D0*h/3D0 ))*f(n1))/
     +      (1D0-(h/3D0)*(-32D0*(-h/12D0) - 6D0 - 8D0*h/3D0))
c
c      Calculate fan
c
            fan2=2D0*DEXP(-4D0*t2) - DEXP(-2D0*t2)
            diff2=fan2-f(n2)
c
c      Output to screen and file values for f each kp_th step
c
            IF (kp.EQ.1) THEN
                fan1=2D0*DEXP(-4D0*t1) - DEXP(-2D0*t1)
                diff1=fan1-f(n1)
                WRITE (*,10) t1,f(n1),fan1,diff1
                WRITE (*,10) t2,f(n2),fan2,diff2
                IF (jf.EQ.1) THEN
                    WRITE (1,10) t1,f(n1),fan1,diff1
                    WRITE (1,10) t2,f(n2),fan2,diff2
                END IF
            ELSE IF (MOD(n2,kp).EQ.0) THEN
                WRITE (*,10) t2,f(n2),fan2,diff2
                IF (jf.EQ.1) THEN
                    WRITE (1,10) t2,f(n2),fan2,diff2
                END IF
            END IF
1000  CONTINUE
      IF (MOD(n2,kp).NE.0) THEN
          WRITE (*,10) t2,f(n2),fan2,diff2
          IF (jf.EQ.1) THEN
              WRITE (1,10) t2,f(n2),fan2,diff2
          END IF
      END IF

      DEALLOCATE  (f)
c
c      Allow another run
c
      WRITE (*,*) 'Another run? (1=yes,anything else=no)'
      READ (*,*) mo
      IF (mo.EQ.1) GOTO 20
      END
```

Table F.1. Error for Block-by-block Technique, Non-constant Example (function location: Linz, 1985:187)

h=	0.1	0.01	0.001
t=0.1	2.03E-3	2.05E-5	2.05E-7
t=0.2	1.98E-3	2.25E-5	2.25E-7

This technique is clearly proven to be only second order for this example.

*Appendix G: Composite Trapezoidal Code for Integro-differential Equation, With
Bimodal Case Allowed, Three Different Pump Changing Schemes, Flexible Output of X
and Y, and Calculation of Mean Y and Effective Mean λ*

```
c       This program solves for the mobile water concentration, X, in a
c       fixed volume, V, of constant saturation soil.  A single volumetric flow
c       parameter, Q, is used to extract solvent that has solute(s)
c       dissolved in it.  Clean solvent is assumed to be flowing through the
c       outer boundaries of V as the pump runs.  The soil is modeled
c       as a continuum of immobile regions through which no solvent is flowing.
c       No solute(s) are assumed sorbed within these regions, and solutes have
c       only a diffusive path to follow in order to reach the mobile zone.
c       Whether due to different sorption site characteristics or different
c       geometries of immobile regions, solute moves from immobile to mobile
c       regions based upon a distribution of rate parameters, lam (lambda),
c       having a probability density function, f(lam).  Two cases are allowed
c       for (initially):  2 average lam's, u1 and u2 (with d1% in u1 and
c       d2% in u2, and a corresponding average immobile concentration, Y),
c       and a bimodal Gamma distribution of lam's (with d1% in f1(lam) and d2% in
c       f2(lam), and a corresponding continuum of immobile regions with
c       concentrations, Y(lam,t).  A first order rate model is used for the
c       non-equilibrium transfer of solute to the mobile region, and X and Y
c       both are modeled as volume-averaged concentrations.  A ratio of immobile
c       to mobile solvent content in the soil, v, is also used.
c
c       The governing two differential equations (with these assumptions) are:
c
c       1. Ydot=lam*[X(t)-Y(lam,t)]
c
c       2. Xdot+p*X=v*Integral from 0->infinity[f(lam)*lam*[Y(lam,t)-X(t)]]dlam
c
c          p=Q/(V*kr), where kr is a reference rate constant used to
c                          non-dimensionalize everything
c          Dot implies the partial derivative with respect to time
c
c       The first equation is solved by an integrating factor to obtain:
c
c       Y(lam,t)=Y(lam,0)*Exp[-k*t]+
c                   Integral from 0->t[lam*X(t")*Exp[-lam*(t-t")]]dt"
c
c       This is plugged into equation #2 and manipulated algebraically to
c       obtain the form which is solved numerically.
c
c       Xdot is dealt with by integration then trapezoid rule, and
c       the integral from 0->t is dealt with using composite trapezoid rule.
c
c       The Gamma distributions used have parameters alpha, beta, and gamma
c       (a,b,g).  Their form is:
c
c       f(lam)=(1/(b*GAMMA[a]))*(((lam-g)/b)^(a-1))*Exp[-(lam-g)/b]
c       Integrals involving this were analytically found and entered into the
c       code in appropriate places.  u=mean of each distribution=a*b + g, and
c       the standard deviation of each distribution is b*Sqrt(a)
c
        PROGRAM TRAP8
c
c       Variable Definitions
c
c       General:
c           to=previous time
```

```fortran
c          t=present time
c          m=total # of time steps to be taken
c          h=time step size
c          no=previous time step
c          n=present time step
c          q=p+v*u (p,u defined above,po->qo from previous time step)
c          lam(j),y(j)=j bins of discretized lambda's/y's,j=1...# of bins
c          y0=starting concentration in each immobile region
c          y0a=present y0 for analytic solution
c          x=concentration in mobile region
c          x(1,i)=trapezoid @ ith step
c          x(2,i)=trapezoid @ ith step using average model
c          w=function of t (different when average lam is used, called wa)
c          wf(t)=v*Integral from 0->Infinity
c                    [f(lam)*lam*y0(lam)*Exp[-lam*t]]dlam
c          wfa(t)=v*u*y0*Exp[-u*t]
c          wo=wf(previous time)...woa=wfa(previous time)
c          tau=t-t'
c          k(i)=kf(tau), function of tau (different for average lam, ka(i))
c          kf(tau)=v*Integral from 0->infinity[f(lam)*lam^2*Exp[-lam*tau]]dlam
c          kfa(tau)=v*u^2 * Exp[-u*tau]
c          x0=starting value of x
c          x0a=present initial value of x for analytic solution
c          npx=number of steps between output of x
c          npy=number of steps between output of y
c          nps=number of steps taken at last pump rate change
c          npc=number of steps to be taken before next pump change
c          nc=number of pump and soak cycles to be taken
c          jox,joy=# of outputs of x and y per pump on cycle
c          jfx,jfy=# of outputs of x and y per pump off cycle
c          c1-4f(p),cm1f,cm2f=constants for analytic solution evaluation
c          c1-4n,cm1,cm2=present values for constants in analytic solution
c
c     Minimal variable declarations (remember:  allocatable isn't F-77)
c
      IMPLICIT DOUBLE PRECISION (A-H, O-Z)
      DOUBLE PRECISION    x[ALLOCATABLE](:,:)
      DOUBLE PRECISION    k[ALLOCATABLE](:)
      DOUBLE PRECISION    ka[ALLOCATABLE](:)
      DOUBLE PRECISION    kf,kfa,lamb,lamv
      DOUBLE PRECISION    y[ALLOCATABLE](:)
      DOUBLE PRECISION    lam[ALLOCATABLE](:)
      DOUBLE PRECISION    f[ALLOCATABLE](:)
      INTEGER*4           m,j,ns,n,npc,npo,npf,nc,gam1,gam2,gamv
      INTEGER*4           jox,joy,jfx,jfy,npx,npy
      INTEGER*1           na1,na2,nav
      CHARACTER*7         fname
c
c     Functions
c
      wf(tv,uv,vv,nav,bv,gv,y0v)=(uv + bv*gv*tv)*y0v*vv/
     +           (DEXP(gv*tv)*((1D0 + bv*tv)**(nav + 1D0)))
      wfa(tv,uv,vv,y0v)=uv*vv*y0v*DEXP(-uv*tv)
      kf(tau,uv,vv,nav,bv,gv)=vv*(
     +      (uv**2D0) + (nav*(bv**2D0)*(1D0 + 2D0*gv*tau)) +
     +      ((gv**2D0)*(tau**2D0)*(2D0*bv + (bv**2D0))))*DEXP(-gv*tau)/
     +       ((1D0 + bv*tau)**(nav + 2D0))
      kfa(tau,uv,vv)=(uv**2D0)*vv*DEXP(-uv*tau)
      zf(pv,uv,vv)=SQRT((uv-pv)**2D0 + uv*vv*(2D0*(uv+pv) + uv*vv))
      cm1f(pv,uv,vv)=(-pv - uv - zf(pv,uv,vv) - uv*vv)/2D0
      cm2f(pv,uv,vv)=(-pv - uv + zf(pv,uv,vv) - uv*vv)/2D0
      c1f(pv,uv,vv,x0v,y0v)=(1D0/(2D0*zf(pv,uv,vv)))*
     +    (x0v*(pv - uv + zf(pv,uv,vv) + uv*vv) - 2D0*y0v*uv*vv)
      c2f(pv,uv,vv,x0v,y0v)=(1D0/(2D0*zf(pv,uv,vv)))*
     +    (x0v*(-pv + uv + zf(pv,uv,vv) - uv*vv) + 2D0*y0v*uv*vv)
```

G.2

```
      c3f(pv,uv,vv,x0v,y0v)=(1D0/(2D0*zf(pv,uv,vv)))*
     +     (y0v*(-pv + uv + zf(pv,uv,vv) - uv*vv) - 2D0*x0v*uv)
      c4f(pv,uv,vv,x0v,y0v)=(1D0/(2D0*zf(pv,uv,vv)))*
     +     (y0v*(pv - uv + zf(pv,uv,vv) + uv*vv) + 2D0*x0v*uv)
      gamf(nav,bv,gv,gamv,lamv)=(1D0/(gamv*bv))*
     +     (((lamv-gv)/bv)**(nav-1D0))*DEXP((gv-lamv)/bv)
c
c     Formats
c
c     File x's
10    FORMAT(',',E11.4E2,',',E22.16E2,',',E22.16E2,',',E22.16E2)
c     Pump on x's
12    FORMAT ('pon,',E11.4E2,',',E22.16E2,',',E22.16E2,',',E22.16E2)
c     Pump off x's
14    FORMAT ('poff,',E11.4E2,',',E22.16E2,',',E22.16E2,',',E22.16E2)
15    FORMAT (E10.4E2,E13.7E2,E10.4E2,E13.7E2,E10.4E2,E10.4E2,E10.4E2)
c     Input, header info
16    FORMAT (',',E8.3E2,',',E8.3E2,',',E8.3E2,',',I3,',',I3,
     +         ',',E8.3E2,',',E8.3E2,',',E8.3E2)
c     File lambda,y format
17    FORMAT (E10.4E2,',',E10.4E2)
c
c     Input initial pump rate,pi, distribution parameters for each of two
c     distributions, d1 (% in 1st dist.), na1, na2, u1, u2, (b1, b2 calc.)
c     g1, g2, initial conditions x0, y0, step size, h, # of pump cycles, nc,
c     # of pump steps, npo, # of printouts of x and y per pump cycle,
c     iox, ioy, # of soak steps, npf, # of printouts of x and y per soak
c     cycle, ifx, ify.
c
20    CONTINUE
      WRITE(*,*)'Default distribution?((d1,a,u,g)=(.5,3,1,0))(1=yes)'
      READ (*,*) ndef
      IF (ndef.EQ.1) THEN
          d1=1D0
          na1=3
          na2=na1
          u1=1D0
          u2=u1
          g1=0D0
          g2=g1
      ELSE
          WRITE (*,*) 'Input d1,na1,na2,u1,u2,g1,g2'
          READ (*,*) d1,na1,na2,u1,u2,g1,g2
      END IF
      d2=1D0-d1
      u=d1*u1 + d2*u2
25    WRITE (*,*) 'Input pi,v,x0,y0,h,jox,joy,jfx,jfy,la'
      READ (*,*) pi,v,x0,y0,h,jox,joy,jfx,jfy,la
      WRITE (*,*) 'Set cycle times(=0), thresholds(=1), or %chng(=2)?'
      READ (*,*) ncyc
      IF (ncyc.EQ.0) THEN
          WRITE (*,*) 'Input nc,npo,npf'
          READ (*,*) nc,npo,npf
          m=(npo+npf)*nc
          npc=npo
      ELSE IF (ncyc.EQ.1) THEN
          WRITE (*,*) 'Input m,pft,pot'
          READ (*,*) m,pft,pot
          npc=0
      ELSE
          WRITE (*,*) 'Input m,po'
          READ (*,*) m,po
          npc=0
      END IF
      p=pi
```

G.3

```fortran
        c1n=c1f(p,u,v,x0,y0)
        c2n=c2f(p,u,v,x0,y0)
        tb=(LOG(c1n)-LOG(c2n))/zf(p,u,v)
        WRITE (*,*) 'tb=',tb,', restart? (1=yes)'
        READ (*,*) st
        IF (st.EQ.1) GOTO 20
        c3n=c3f(p,u,v,x0,y0)
        c4n=c4f(p,u,v,x0,y0)
        cm1=cm1f(p,u,v)
        cm2=cm2f(p,u,v)
        npx=jox
        npy=joy
c
c       Initial conditions applied to anaytic solution
c
        y0a=y0
        yd=y0
        x0a=x0
c
c       Initial time set to 0
c
        t=0D0
        ta=t
c
c       Allocate necessary array sizes
c
        ALLOCATE      (x(1:2,0:m))
        ALLOCATE      (k(0:m))
        ALLOCATE      (ka(0:m))
        ALLOCATE      (y(1:la))
        ALLOCATE      (lam(1:la))
        ALLOCATE      (f(1:la))
c
c       Reads in output filename
c
        diff=0D0
        WRITE(*,*) 'Output to file? (1=yes,anything else=no)'
        READ(*,*) jf
        IF (jf.EQ.1) THEN
            WRITE(*,*)'Enter 7-char output file([appos]filenam[appos]):'
            READ(*,*) fname
c
c       File for x data to be written to with header info and initial conditions
c
            OPEN (1,FILE=fname//'.exx',STATUS='UNKNOWN',
     +          ACCESS='SEQUENTIAL',FORM='FORMATTED')
            WRITE (1,*) 'pi,v,d1,na1,na2,u1,u2,g1,g2,x0,y0,h='
            WRITE (1,*) pi,v,d1,na1,na2,u1,u2,g1,g2,x0,y0,h
            WRITE (1,*)
            WRITE(1,*)'t*Kr ',fname,'.dis ',fname,'.err ',fname,'.ave ='
            WRITE (1,10) t,x0,diff,x0
c
c       File for y data to be written to with header info
c
            OPEN (2,FILE=fname//'.why',STATUS='UNKNOWN',
     +          ACCESS='SEQUENTIAL',FORM='FORMATTED')
            WRITE (2,*) 'pi,v,d1,na1,na2,u1,u2,g1,g2,x0,y0,h='
            WRITE (2,*) pi,v,d1,na1,na2,u1,u2,g1,g2,x0,y0,h
            WRITE (2,*) 'fname=',fname
            WRITE (2,*)
        END IF
c
c       Header info to screen
c
        WRITE (*,*)
```

G.4

```
          WRITE (*,*) fname,', t,xdis,err,xan,ydis,yan,lamb='
          WRITE (*,15) t,x0,diff,x0,yd,y0,u
c
c         Initializing several variables
c
          b1=(u1-g1)/na1
          b2=(u2-g2)/na2
          q=p+v*u
          k(0)=d1*kf(t,u1,v,na1,b1,g1) + d2*kf(t,u2,v,na2,b2,g2)
          ka(0)=kfa(t,u,v)
          x(1,0)=x0
          x(2,0)=x0
          xan=x0
          CALL gam (na1,gam1)
          CALL gam (na2,gam2)
          bs=((u2+3D0*b2*SQRT(na2))-g1)/la
          DO 50 j=1,la
               lam(j)=g1 + (2*j - 1)*bs/2
               f(j)=d1*gamf(na1,b1,g1,gam1,lam(j)) +
     +            d2*gamf(na2,b2,g2,gam2,lam(j))
50        CONTINUE
c
c         Present values for w, wa, and constants for analytic solution
c
          w=d1*wf(t,u1,v,na1,b1,g1,y0) + d2*wf(t,u2,v,na2,b2,g2,y0)
          wa=wfa(t,u,v,y0)
          ns=0
c
c         This ensures no integral contributions/summations on the first step
c
          jd=0
c
c         Constants to minimize calculations in the loop
c
          c1=h/2D0
          c2=c1**2
c
c         Start loop
c
          DO 1000 n=1,m
c
c         Step time
c
               no=n-1
               t=n*h
c
c         Sets previous "new" values for w equal to the one time step old ones
c
               wo=w
               woa=wa
c
c         New values for w and wa
c
               w=d1*wf(t,u1,v,na1,b1,g1,y0) + d2*wf(t,u2,v,na2,b2,g2,y0)
               wa=wfa(t,u,v,y0)
c
c         Present values for k and ka
c
               k(n)=d1*kf(t,u1,v,na1,b1,g1) + d2*kf(t,u2,v,na2,b2,g2)
               ka(n)=kfa(t,u,v)
c
c         Summations
c
               stf=0D0
```

G.5

```fortran
            stb=0D0
            stfa=0D0
            stba=0D0
            IF (n.GT.2) THEN
                DO 200 j=1,n-2
                    stf=stf + x(1,j)*k(no-j)
                    stb=stb + x(1,j)*k(n-j)
                    stfa=stfa + x(2,j)*ka(no-j)
                    stba=stba + x(2,j)*ka(n-j)
200             CONTINUE
            END IF
            stb=stb + jd*x(1,no)*k(1)
            stba=stba + jd*x(2,no)*ka(1)
c
c      Trapezoid steps
c
            x(1,n)=(x(1,no) + c1*(w + wo - q*x(1,no) +
     +         jd*c1*(x(1,0)*k(no) + x(1,no)*k(0) + 2D0*stf) +
     +         c1*(x(1,0)*k(n) + 2D0*stb)))/
     +         (1D0 + c1*q - k(0)*c2)
            x(2,n)=(x(2,no) + c1*(wa+ woa- q*x(2,no) +
     +         jd*c1*(x(2,0)*ka(no)+ x(2,no)*ka(0)+ 2D0*stfa)+
     +         c1*(x(2,0)*ka(n)+ 2D0*stba)))/
     +         (1D0 + c1*q - ka(0)*c2)
c
c      First step complete
c
            jd=1
c
c      Calculate xan
c
            ta=(n-ns)*h
            xan=c1n*DEXP(cm1*ta) + c2n*DEXP(cm2*ta)
c
c      Pump changing scheme
c
            IF (ncyc.EQ.1) THEN
                IF ((p.EQ.0D0).AND.(x(1,n).GT.pot)) npc=n-ns
                IF ((p.EQ.pi).AND.(x(1,n).LT.pft)) npc=n-ns
            ELSE IF (ncyc.EQ.2) THEN
                pd=100D0*ABS(x(1,no) - x(1,n))/xan
                IF (pd.LT.po) npc=n-ns
            END IF
            IF ((n-ns).EQ.npc) THEN
                diff=xan-x(2,n)
                y0b=c3n*DEXP(cm1*ta) + c4n*DEXP(cm2*ta)
c      Calculate y(lam,t) for output time and specified discrete lam's
                yd=0
                temp=0
                DO 400 j=1,la
                    sy=0
                    DO 300 j1=1,n-1
                        sy=sy + x(1,j1)*DEXP(h*lam(j)*(j1-n))
300                 CONTINUE
                    y(j)=(y0 + lam(j)*h*x0/2)*DEXP(-lam(j)*t) +
     +                    lam(j)*h*(sy + x(1,n)/2D0)
                    yd=yd + f(j)*y(j)*bs
                    temp=temp + f(j)*y(j)*bs*lam(j)
400             CONTINUE
                lamb=temp/yd
                npc=0
                ns=n
c      Reset analytic solution IC's
                y0a=c3n*DEXP(cm1*ta) + c4n*DEXP(cm2*ta)
                x0a=xan
```

G.6

```
c       Reset jp, npc, and nlp is set to ensure proper output; also,
c       output has pump on or pump off anotation next to it.
                IF (p.EQ.0D0) THEN
                    p=pi
                    IF (ncyc.EQ.0) npc=npo
                    npx=jox
                    npy=joy
                    WRITE (*,15) t,x(1,n),diff,xan,yd,y0b,lamb
                    IF (jf.EQ.1) WRITE (1,12) t,x(1,n),xan,diff
                ELSE
                    p=0D0
                    IF (ncyc.EQ.0) npc=npf
                    npx=jfx
                    npy=jfy
                    WRITE (*,15) t,x(1,n),diff,xan,yd,y0b,lamb
                    IF (jf.EQ.1) WRITE (1,14) t,x(1,n),xan,diff
                END IF
c       Reset p, q and analytic solution constants for pump change
                c1n=c1f(p,u,v,x0a,y0a)
                c2n=c2f(p,u,v,x0a,y0a)
                c3n=c3f(p,u,v,x0a,y0a)
                c4n=c4f(p,u,v,x0a,y0a)
                cm1=cm1f(p,u,v)
                cm2=cm2f(p,u,v)
c       Time shift for analytic solution
                q=p+v*u
            END IF
            IF ((MOD(n-ns,npx).EQ.0).AND.(ns.NE.n)) THEN
                diff=xan-x(2,n)
                y0b=c3n*DEXP(cm1*ta) + c4n*DEXP(cm2*ta)
c       Calculate y(lam,t) for output time and specified discrete lam's
                yd=0
                temp=0
                DO 460 j=1,la
                    sy=0
                    DO 430 j1=1,n-1
                        sy=sy + x(1,j1)*DEXP(h*lam(j)*(j1-n))
430                 CONTINUE
                    y(j)=(y0 + lam(j)*h*x0/2)*DEXP(-lam(j)*t) +
     +                      lam(j)*h*(sy + x(1,n)/2D0)
                    yd=yd + f(j)*y(j)*bs
                    temp=temp + f(j)*y(j)*bs*lam(j)
460             CONTINUE
                lamb=temp/yd
                WRITE (*,15) t,x(1,n),diff,xan,yd,y0b,lamb
                IF (jf.EQ.1) WRITE (1,10)   t,x(1,n),xan,diff
            END IF
            IF (MOD(n-ns,npy).EQ.0) THEN
c       Output y
                IF (jf.EQ.1) THEN
                    WRITE (2,*)
                    WRITE (2,*) 'lam(j),y_t=',t
                    DO 500 j=1,la
                        WRITE (2,17) lam(j),y(j)
500                 CONTINUE
                END IF
                IF (jf.EQ.1) THEN
                    WRITE (2,*)'y0b(analytic),yd,lamb=',y0b,yd,lamb
                    WRITE (2,*)
                END IF
            END IF
            IF (n.EQ.ns) WRITE (*,*) 'Pump changed!'
1000 CONTINUE
c
c       Deallocation
```

G.7

```fortran
c
      DEALLOCATE   (x)
      DEALLOCATE   (k)
      DEALLOCATE   (ka)
      DEALLOCATE   (y)
      DEALLOCATE   (lam)
      DEALLOCATE   (f)
c
c     Allow another run
c
      IF (jf.EQ.1) THEN
          CLOSE (1)
          CLOSE (2)
      END IF
      WRITE (*,*) 'Another run? (1=yes,anything else=no)'
      READ (*,*) mo
      IF (mo.EQ.1) GOTO 20
      END

      SUBROUTINE gam (nalf,nans)

      INTEGER*4      nans
      INTEGER*1      nalf,m

      nans=1
      DO 2000 m=2,nalf-1
          nans=nans*m
2000  CONTINUE

      END
```

Bibliography

Adams, Thomas A. and Robert C. Viramontes. <u>Analytical Modeling of Aquifer Decontamination by Pulsed Pumping When Contaminant Transport is Affected by Rate-Limited Sorption and Desorption</u>. MS Thesis, AFIT/GEE/ENG/93-S1. School of Engineering, Air Force Institute of Technology (AU), Wright-Patterson AFB, OH, September 1993 (AD-A271 105).

Ball, William P. and Paul V. Roberts. "Long-Term Sorption of Halogenated Organic Chemicals by Aquifer Material. 2. Intraparticle Diffusion," <u>Environmental Science and Technology:</u> 25: 1237-1249 (1991).

Brusseau, Mark L. and P.S.C. Rao. "Sorption Nonideality During Organic Contaminant Transport in Porous Media," <u>Critical Reviews in Environmental Control, 19</u>: 33-99 (1989).

Burden, Richard L. and J. Douglas Faires. <u>Numerical Analysis</u> (Third Edition). Boston: Prindle, Weber and Schmidt Publishers, 1985.

Claborn, Billy J. and Ken A. Rainwater. "Well-Field Management for Energy Efficiency," <u>Journal of Hydraulic Engineering</u>, 117: 1290-1303 (October 1991).

Connaughton, Doreen F. et al. "Description of Time-Varying Desorption Kinetics: Release of Naphthalene From Contaminated Soils," <u>Environmental Science and Technology, 27</u>: 2397-2403 (1993).

Cooney, D. O. et al. "Effects of Particle Size Distribution on Adsorption Kinetics in Stirred Batch Systems," <u>Chemical Engineering Science, 38</u>: 1535 (1983).

Cussler, E. L. <u>Diffusion: Mass Transfer in Fluid Systems</u>. New York: Cambridge University Press, 1984.

Domenico, Patrick A. and Franklin W. Schwartz. <u>Physical and Chemical Hydrogeology</u>. New York: John Wiley and Sons, Inc., 1990.

Gilbert, Richard O. <u>Statistical Methods for Environmental Pollution Monitoring</u>. New York: Van Nostrand Reinhold, 1987.

Hartman, Richard T. Optimal Pulsed Pumping for Aquifer Remediation When Contaminant Transport is Affected by Rate-Limited Sorption: A Calculus of Variation Approach. MS Thesis, AFIT/GEE/ENC/94S-2. School of Engineering, Air Force Institute of Technology (AU), Wright-Patterson AFB, OH, September 1994 (AD-A284 700).

Heyse, Edward. Mass Transfer Between Organic and Aqueous Phases: Investigations Using A Continuously Stirred Flow Cell. DP Dissertation, University of Florida, December 1994.

Heyse, Edward. Faculty, Department of Engineering and Environmental Management, Air Force Institute of Technology, Wright-Patterson AFB, OH, Telephone and Personal Interview, Summer 1995.

Hildebrand, F. B. Introduction to Numerical Analysis (Second Edition). New York: Dover Publications, Inc., 1987.

Isaacson, Eugene and Herbert Bishop Keller. Analysis of Numerical Methods. New York: Dover Publications, Inc., 1994.

Linz, Peter. Analytical and Numerical Methods for Volterra Equations. Philadelphia: Siam, 1985.

Masters, Gilbert M. Introduction to Environmental Engineering and Science. Englewood Cliffs, NJ: Prentice Hall, 1991.

Microsoft FORTRAN PowerStation: Professional Development System Version 1.0 for MS-DOS and Windows Operating Systems. Computer Software. Microsoft Corporation, 1993.

Nkedi-Kizza, et al. "Ion Exchange and Diffusive Mass Transfer During Miscible Displacement Through an Aggregated Oxisol," Soil Science Society of America Journal, 46: 471-476 (1982).

-----. "On the Equivalence of Two Conceptual Models for Describing Ion Exchange During Transport Through an Aggregated Oxisol," Water Resources Research, 20(8): 1123-1130 (1984).

Olsen, Roger L. and Michael C. Kavanaugh. "Can Groundwater Restoration Be Achieved," Water Environment and Technology, 5: 42-47 (1993).

Rao, P. S. C. et al. "Experimental and Mathematical Description of Nonadsorbed Solute Transfer by Diffusion in Spherical Aggregates," Soil Science Society of America Journal, 44: 684-688 (1980).

Travis, Curtis C. and Carolyn B. Doty. "Can Contaminated Aquifers at Superfund Sites be Remediated?," Environmental Science Technology, 24: 1464-1466 (1990).

Treybal, Robert E. Mass Transfer Operations (Third Edition), New York: McGraw-Hill Book Company, 1980.

Tricomi, F. G. Integral Equations. New York: Dover Publications, Inc., 1985.

Valocchi, A. J. "Effect of Radial Flow on Deviations from Local Equilibrium During Sorbing Solute Transport Through Homogeneous Soils," Water Resources Research, 22(12): 1693-1701 (1986)

Vest, Gary D., Deputy Assistant Secretary of the Air Force for Environmental Safety and Occupational Health. Address to Air Force Institute of Technology students and faculty. Air Force Institute of Technology, Wright-Patterson AFB, OH, 23 July 1992.

Villermaux, Jacques. "Deformation of Chromatographic Peaks Under the Influence of Mass Transfer Phenomena," Journal of Chromatographic Science: 12: 822-831 (1974).

Weber, Walter J. et al. "A Distributed Reactivity Model for Sorption by Soils and Sediments. 1. Conceptual Basis and Equilibrium Assessments," Environmental Science and Technology, 26: 1955-1962 (1992).

-----. "Review Paper: Sorption Phenomena in Subsurface Systems: Concepts, Models and Effects on Contaminant Fate and Transport," Water Res., 25(5): 499-528 (1991).

Wolfram, Stephen. Mathematica: A System for Doing Mathematics by Computer (Second Edition). Reading, MA: Addison-Wesley Publishing Company, 1991.

Wu, Shian-chee and Philip M. Gschwend. "Sorption Kinetics of Hydrophobic Organic Compounds to Natural Sediments and Soils," Environmental Science and Technology, 20: 717-725 (1986).

Yosida, Kosaku. Lectures on Differential and Integral Equations. New York: Dover Publications, Inc., 1991.

Young, David M. and Robert Todd Gregory. <u>A Survey of Numerical Mathematics</u>. New York: Dover Publications, Inc., 1988.

Vita

Capt Jon E. Hodge was born on 9 August 1963 in Kansas City, Missouri. He graduated from the last graduating class of Olathe High School in 1981, and entered the Air Force Academy. He there recieved a Bachelor of Science degree in Physics with two tracks: Optics and Aeronautical Engineering, Propulsion. Upon graduation in May 1985, he entered Undergraduate Pilot Training at Vance AFB, Oklahoma. Graduating a year later, he underwent six months of weapons system specific training in the B-52G at Castle AFB, California. His first assignment was Blytheville AFB, Arkansas, soon to be Eaker AFB, and five years later to be closed. While stationed there, he flew six combat missions from the island of Diego Garcia during Desert Storm. He then began to pursue graduate education at the Air Force Institute of Technology (AFIT). After two years more flying in the B-52H at Minot AFB, North Dakota, including a demanding flight scheduler's position, he entered AFIT's School of Engineering in May 1994.

Permanent Address: 19615 K-68 Hwy
                      Paola, KS 66071

REPORT DOCUMENTATION PAGE

Form Approved
OMB No. 0704-0188

1. AGENCY USE ONLY *(Leave blank)*	2. REPORT DATE December 1995	3. REPORT TYPE AND DATES COVERED Master's Thesis

4. TITLE AND SUBTITLE
A POINT MODEL OF AQUIFER CLEANUP WITH A DISTRIBUTION OF FIRST-ORDER RATE PARAMETERS

5. FUNDING NUMBERS

6. AUTHOR(S)

Jon E. Hodge, Capt, USAF

7. PERFORMING ORGANIZATION NAME(S) AND ADDRESS(ES)

Air Force Institute of Technology,
WPAFB OH 45433-6583

8. PERFORMING ORGANIZATION REPORT NUMBER

AFIT/ENP/GAP/95D-08

9. SPONSORING/MONITORING AGENCY NAME(S) AND ADDRESS(ES)

10. SPONSORING/MONITORING AGENCY REPORT NUMBER

11. SUPPLEMENTARY NOTES

12a. DISTRIBUTION/AVAILABILITY STATEMENT

Approved for public release; distribution unlimited

12b. DISTRIBUTION CODE

13. ABSTRACT *(Maximum 200 words)*

Many try modeling groundwater contaminant transport to predict it. Is this possible with rate-limited processes, and under what conditions? On occasion, cleanups go slower than predicted (tailing) and hazardous concentrations reappear after cleanup is thought complete (rebound). Rate-limited transport is blamed by many. When immobile water is present, diffusion from varied sizes and shapes of immobile regions can cause varied rate limitations (due to varied diffusion path lengths). Although known, most modelers represent these varied rate-limiting processes with a single "representative" rate-parameter. This can yield poor predictions for long-term experiments, and the parameter is generally time and pump-rate dependent. This model employs a distribution of first-order rate parameters to investigate the effects of using a single rate-parameter. Spatial effects are ignored by using volume-averaged concentrations (a point, well-mixed model) and dilutive pumping and rate-limited transport are modeled to isolate rate-limited transport for study. A three-parameter Gamma distribution defines the rate parameter continuum. A clean flow approximation is used extensively, and pulsed pumping is examined briefly. An effective time and pump-rate dependence is seen in the average rate. Long-term soil and contaminant transport characteristics along with uptake history or good experimentally-derived initial contaminant presence are concluded as necessary for accurate predictions.

14. SUBJECT TERMS
Distributed Model, Gamma Model, Rate-limited Sorption, ,Tailing, Rebound, Groundwater Contaminant Transport, Aquifer Decontamination, Groundwater Cleanup

15. NUMBER OF PAGES
123

16. PRICE CODE

17. SECURITY CLASSIFICATION OF REPORT	18. SECURITY CLASSIFICATION OF THIS PAGE	19. SECURITY CLASSIFICATION OF ABSTRACT	20. LIMITATION OF ABSTRACT
Unclassified	Unclassified	Unclassified	UL

GENERAL INSTRUCTIONS FOR COMPLETING SF 298

The Report Documentation Page (RDP) is used in announcing and cataloging reports. It is important that this information be consistent with the rest of the report, particularly the cover and title page. Instructions for filling in each block of the form follow. It is important to *stay within the lines* to meet *optical scanning requirements*.

Block 1. Agency Use Only *(Leave blank)*.

Block 2. Report Date. Full publication date including day, month, and year, if available (e.g. 1 Jan 88). Must cite at least the year.

Block 3. Type of Report and Dates Covered. State whether report is interim, final, etc. If applicable, enter inclusive report dates (e.g. 10 Jun 87 - 30 Jun 88).

Block 4. Title and Subtitle. A title is taken from the part of the report that provides the most meaningful and complete information. When a report is prepared in more than one volume, repeat the primary title, add volume number, and include subtitle for the specific volume. On classified documents enter the title classification in parentheses.

Block 5. Funding Numbers. To include contract and grant numbers; may include program element number(s), project number(s), task number(s), and work unit number(s). Use the following labels:

C	-	Contract	**PR** -	Project
G	-	Grant	**TA** -	Task
PE	-	Program Element	**WU** -	Work Unit Accession No.

Block 6. Author(s). Name(s) of person(s) responsible for writing the report, performing the research, or credited with the content of the report. If editor or compiler, this should follow the name(s).

Block 7. Performing Organization Name(s) and Address(es). Self-explanatory.

Block 8. Performing Organization Report Number. Enter the unique alphanumeric report number(s) assigned by the organization performing the report.

Block 9. Sponsoring/Monitoring Agency Name(s) and Address(es). Self-explanatory.

Block 10. Sponsoring/Monitoring Agency Report Number. *(If known)*

Block 11. Supplementary Notes. Enter information not included elsewhere such as: Prepared in cooperation with...; Trans. of...; To be published in.... When a report is revised, include a statement whether the new report supersedes or supplements the older report.

Block 12a. Distribution/Availability Statement. Denotes public availability or limitations. Cite any availability to the public. Enter additional limitations or special markings in all capitals (e.g. NOFORN, REL, ITAR).

DOD	-	See DoDD 5230.24, "Distribution Statements on Technical Documents."
DOE	-	See authorities.
NASA	-	See Handbook NHB 2200.2.
NTIS	-	Leave blank.

Block 12b. Distribution Code.

DOD	-	Leave blank.
DOE	-	Enter DOE distribution categories from the Standard Distribution for Unclassified Scientific and Technical Reports.
NASA	-	Leave blank.
NTIS	-	Leave blank.

Block 13. Abstract. Include a brief *(Maximum 200 words)* factual summary of the most significant information contained in the report.

Block 14. Subject Terms. Keywords or phrases identifying major subjects in the report.

Block 15. Number of Pages. Enter the total number of pages.

Block 16. Price Code. Enter appropriate price code *(NTIS only)*.

Blocks 17. - 19. Security Classifications. Self-explanatory. Enter U.S. Security Classification in accordance with U.S. Security Regulations (i.e., UNCLASSIFIED). If form contains classified information, stamp classification on the top and bottom of the page.

Block 20. Limitation of Abstract. This block must be completed to assign a limitation to the abstract. Enter either UL (unlimited) or SAR (same as report). An entry in this block is necessary if the abstract is to be limited. If blank, the abstract is assumed to be unlimited.